Nanobodies as novel tools to study morphogen function *in vivo*

Part I

Nanobody-mediated morphogen trapping: Patterning and growth control in the absence of morphogen spreading

Part II

Dissection of Decapentaplegic gradient formation along the apicobasal axis using scaffold-bound nanobodies

Inauguraldissertation

zur

Erlangung der Würde eines Doktors der Philosophie

vorgelegt der

Philosophisch-Naturwissenschaftlichen Fakultät der Universität Basel

von

Stefan Harmansa

aus Rheinfelden, Deutschland

Basel, 2016

Genehmigt von der Philosophisch-Naturwissenschaftlichen Fakultät auf Antrag von

Prof. Dr. Markus Affolter	Prof. Dr. Konrad Basler
(Fakultätsverantwortlicher)	(Korreferent)

Basel, den 23. Februar 2016

Prof. Dr. Jörg Schibler

Dekan der Philosophisch-Naturwissenschaftliche Fakultät

Summary

Nanobodies are small, monomeric antibody mimetic proteins produced by members of the camelid family (camels and llamas), that can be engineered by fusion to proteins carrying a specific function. These "functionalized" protein binders emerge as novel tools for protein manipulation *in vivo*. During my PhD studies I have generated scaffold-bound nanobodies (SBNs) specific to EGFP in order to interfere with gradient formation of a EGFP-tagged version of the Decapentaplegic (EGFP::Dpp) morphogen. Morphogens are secreted signaling molecules forming concentration gradients and controlling organ patterning and growth during animal development. *Drosophila* Decapentaplegic (Dpp) is one of the best studied morphogens, but it remains unclear how its concentration gradient is established and how it and controls patterning and growth of the *Drosophila* wing imaginal disc. In this PhD Thesis I summarize the development and characterization of SBNs and their applications in studying the fomation and function of the Decapentaplegic morphogen gradient in the *Drosophila melanogaster* wing imaginal disc.

In the first part of this Thesis, I will discuss how SBNs allowed us to investigate the importance of the Dpp gradient on proliferation and growth control of the wing imaginal disc. Using morphotrap, a SBN that localizes to the outer cell surface, we could completely block gradient formation and study the effect of a loss of the Dpp gradient on patterning and growth. We find that induction of Dpp target genes, and hence patterning, directly depends on the spreading of Dpp. Furthermore, we show that the Dpp gradient is crucial for growth and size control of the medial wing disc region. Moreover, we find that the Dpp gradient is not necessary for proliferation and size control of the lateral region of the wing disc. This data challenges previously published growth models, in which growth control solely depends on the signaling dynamics of Dpp.

In the second part of this Thesis I investigate the mechanism of Dpp gradient formation in the wing disc. The wing disc is a complex three-dimensional structure, consisting of two contiguous epithelial layers. How the long-range Dpp gradient is established in the wing disc remains controversial. I have created different SBNs that localize to specific subcellular regions along the apicobasal axis. These SBNs allow us to reduce or block the dispersal of specific gradient subfractions and assess their contribution to wing development. We find that EGFP::Dpp disperses along three main routes: within the epithelial plane of the wing disc, in the luminal cavity between the two epithelial layers and along the basal lamina. Preliminary results suggest that these subfractions encode for different functions of Dpp. While we find that the patterning function of Dpp is encoded by the basolateral subfractions, the growth function of Dpp seems to be influenced by all three subfraction. Further experiments will investigate how target cells perceive and integrate Dpp input from these different subfractions.

Acknowledgements

First of all, I would like to thank Prof. Markus Affolter for letting me stay in his lab for all this years and for all his advice. His seemingly endless enthusiasm and numerous long discussions about how morphogens might or might not control growth of embryonic primordia were a great support and made me push myself and my research. Furthermore, his elegant ways of simplifying scientific concepts, when planning experiments or while preparing presentations strongly influenced my own style of approaching scientific questions.

Another great source of knowledge and support during my PhD was Dr. Emmanuel Caussinus. He not only introduced me to the mysteries of molecular cloning but also helped to shape all my major research projects. His extremely efficient and uncomplicated nature made our collaboration a real pleasure, and many things would not have been possible without him. Thanks a lot for this Emmanuel! At this point I also want to deeply thank Fisun Hamaratoglu. Fisun was the person introducing me to the secrets of fly genetics; she taught me how to perform beautiful immunostainings and guided me during my master studies. From this time on, she became a valuable source of support, help and inspiration, strongly impacting my development as a scientist.

I also want to thank Prof. Konrad Basler and Prof. Giorgos Pyrowolakis for volunteering to join my thesis committee and for all their input on my projects. Moreover, I would like to thank my dear friend and fellow Dpp researcher Ilaria Alborelli for a thousand and one discussions about Dpp signalling, wing disc development, apical-basal polarity and the sense of life. It was a great pleasure and a lot of fun having you in the lab! Many thanks to Shinya Matsuda for discussions and fruitful collaborations. Thanks to Henry Belting for many entertaining, sometimes scientific but mostly cycling related discussions. Moreover, special thanks to the whole Affolter lab for a great lab atmosphere. And not to forget, many thanks to Anna Baron from the Nigg Lab for scientific support and being a good friend.

However, most thanks deserve my girlfriend Andrea and my parents for their endless support during my studies. They had to endure my moaning when experiments did not work out, but always managed to cheer me up again. This Thesis would not have been written without their mental support. Special thanks to Andrea for sharing so many aspects of our lives, enduring my quirks, being my dearest friend and an awesome climbing partner!

Contents

1 General Introduction

How a single fertilized cell develops into a complex, multicellular organism has been an outstanding and fascinating question for generations of developmental biologists. Two key processes that need tight control during development are cell proliferation and cell differentiation. More than 100 years ago, experiments performed by the German biologist Hans Driesch provided evidence that these two key processes are interlinked and controlled at the level of the whole organism. When Driesch separated the two blastomeres of a sea urchin embryo at the two cell stage, the separated blastomeres were able to self-regulate and gave rise to two complete, yet half-sized, blastulae [1, 2]. Similar experiments were performed by Hans Spemann, subdividing the cleaving salamander egg into two halves, resulted in two well shaped tadpoles [3]. These results suggested that cells contain the capacity to develop potentially independent (self-regulation) but that cells function together as a collective to give rise to the whole organism.

In the 1920s, in the lab of later Nobel laureate Hans Spemann, Hilde Mangold performed grafting experiments in the salamander that were instrumental for understanding the concept of self-regulation and what might control and orchestrate the cells of a developing embryo. Mangold grafted the dorsal-lip of a strongly pigmented salamander embryo to the ventral side of a low pigmented embryo. Strikingly, the dorsal-lip graft was able to change the cell fate of neighbouring host cells such that a Siamese twin was formed [4]. The grafted region, the dorsal-lip, became known as the Spemann's organizer and provided the basis for the present view that animal development depends on cell-cell induction, where groups of cells (so called "organizers") induce the differentiation of their neighbours [2][5]. What factors might emerge from such organizing centres and instruct surrounding cells remained unclear.

In 1952, Alan Turing provided the theoretical framework that secreted substances, which he termed morphogens ("form producers"), could instruct the self-organization of spatial patterns [6]. Starting from a homogeneous distribution, two morphogens with slightly different diffusion properties can create spatial patterns by a so called reaction-diffusion system. Turing's *reaction-diffusion* formalism gained increasing interest and was used as a model for various animal pigmentation patterns, such as the pattern of the leopard [7, 8, 9] or more recently the pattern of the zebra fish [10, 11] and also for modelling digit patterning in the developing limb [12]. While Turing suggested a mechanism by which uniform production (in all cells) of the morphogen can lead to spacial patterns, the idea of morphogens released from localized sources (organizing-centres à la Spemann organizer) was still developing.

In 1938, Albert Dalcq and Jean Pasteels introduced the concept of thresholds in morphogenesis, suggesting that a certain cellular response requires signalling input above a certain level or "threshold" [13, 14]. Based on the idea that a cellular response can be induced above a defined threshold and not below, Lewis Wolpert formulated the French flag model of morphogen-controlled positional information in 1969 [15, 16]. He suggested that a morphogen secreted from localized source cells can instruct cell fate and positional information in the surrounding target tissue, called the "morphogenic

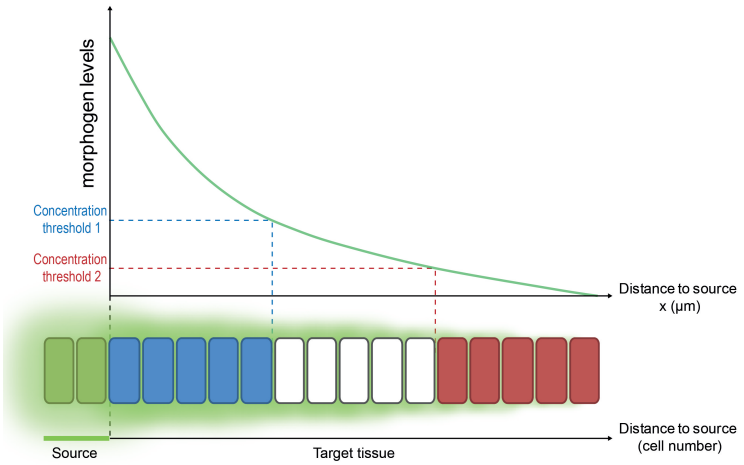

Figure 1: Morphogens pattern tissues in a concentration-dependent manner From the producing cells (left), the morphogen (green) forms a concentration gradient into the adjacent target tissue. Cells in the target tissue can sense the morphogen levels and adopt distinct cell fates in a threshold response. With increasing distance to the source cells, morphogen levels are decreasing. According to Wolpert's French flag analogy, cells sensing high morphogen levels (above a certain "threshold") adopt a blue fate, while cells sensing medium morphogen levels adopt a white and cells sensing low morphogen levels adopt a red fate. Figure adapted from [14].

field". According to Wolpert's French flag model, morphogen are secreted from a group of source cells and form concentration gradients into the adjacent target tissue. Cells in the target tissue sense the morphogen concentration and activate target genes above distinct concentration thresholds, such that different distances to the source cells result in distinct target gene expression profiles, and hence spatial patterned gene expression (Fig.1). Hence, the non-uniform distribution of a single molecular species can specify several distinct cell fates and thereby pattern tissues in a series of structures aligned in a given order.

At the time Wolpert published the French flag model, the morphogen concept was purely conceptual, no molecules have been described that fulfil the requirements of a true morphogen. Despite this lack of proof of existence, mathematical models were developed to explain how diffusible molecules could form stable gradients [17, 7]. In 1970, a "source-sink" model was suggested by Francis Crick [18]. Crick proposed that cells at the distal edge of the target tissue act as a "morphogen sink". Morphogen diffusion and destruction by "sink" cells a the edge of the morphogenetic field theoretically result in the formation of stable, *steady state* concentration gradients, with maximum morphogen concentrations close to the source and lowest concentrations near the distal sink. Despite this theoretical advances, it took another two decades before the discovery and characterization of the first morphogen Bicoid in *Drosophila*.

1.1 Morphogen gradients in development

The discovery of the distribution and function of *Drosophila* Bicoid provided the first connection between a protein gradient and pattern formation. Bicoid is a transcrip-

tion factor, expressed in the anterior region of the early syncytial blastoderm during *Drosophila* embryogenesis. At this stage of development, nuclei divide without separating the cells by a membrane, such that diffusible substances can freely disperse in the cytoplasm between nuclei within the syncytial blastoderm. Bicoid was found to form an anterior to posterior concentration gradient [19] that is required for definition of positional information and development of the anterior parts of the embryo [20, 21]. However, the molecular nature (transcription factor) and the environment of Bicoid gradient formation (syncytium) is clearly distinct from most other morphogens which act as secreted ligands in a cellularized environment.

The first extracellular morphogens discovered belonged to the transforming growth factor β (TGF-β) family. *Drosophila* Decapentaplegic (Dpp), which I will discussed in detail later, is involved in the patterning of several developing tissues, including dorsal-ventral axis formation in the embryo and in wing disc development [22, 23, 24, 25]. Besides the members of the TGF-β family, several other signalling factor families hold members acting as morphogens during development; most prominent examples are members of the Hedgehog, Wingless-related integration site (Wnt), Epidemal growth factor (EGF) and Fibroblast growth factor (FGF) families [26, 27, 28]. The concept of morphogen gradients in development has been studied extensively and morphogens have been shown to act in several developmental processes and species. For example, members of the Nodal family of TGF-β ligands are involved in patterning of the deuterostome sea urchin embryo [29] and in patterning of the germ layers in *Xenopus* and vertebrate embryogenesis [30, 31, 26, 32]. Other intensely studied processes are the patterning of the vertebrate limb [33, 34, 35] and the vertebrate neural tube [36, 37] by Sonic hedgehog and members of the BMP and Wnt family. It seems that the simple theme of morphogen gradient mediated patterning is universal and reappears in the development of most multicellular organisms. In addition to the instruction of position and pattern, morphogen gradients have been implicated in regenerative processes [38] and the control of organ growth and size, as I will discuss below, using the example of the TGF-β family member Dpp in the *Drosophila* wing imaginal disc.

1.2 The TGF-β signalling pathway

The TGF-β superfamily of secreted signalling factors comprises of at least 30 members in mammals, of which many have been identified in frogs, fish and flies. The TGF-β superfamily can be subdivided into two functional and structural related groups: the TGF-β, Activin and Nodal families together with some members of the Growth and Differentiation Factors (GDFs) form the TGF-β-like group; while the group of Bone Morphogenetic Proteins (BMPs) includes the BMPs, Anti-Müllerian Hormone and most GDFs [39, 40]. Members of the TGF-β superfamily play roles in a wide variety of developmental processes, as well as throughout animal lifetime. Key processes regulated by TGF-β superfamily members include the control of self-renewal in embryonic stem cells [41] and the regulation of gastrulation, differentiation and organ morphogenesis. Due to their wide spread action, alteration of TGF-β signalling is

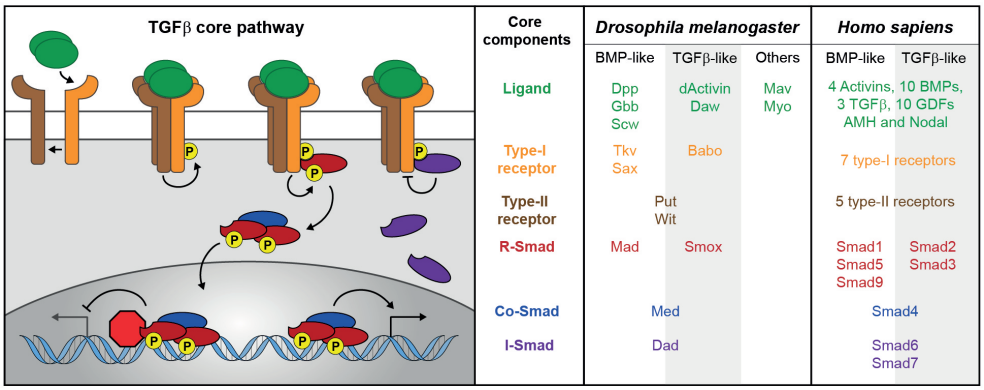

Figure 2: Components of the TGF-β core pathway
left, **middle left**, Binding of TGF-β dimeric ligands (green) to their type-I (orange) and type-II (brown) receptors results in the formation of a tetrameric active receptor complex. Upon receptor complex formation, type-II receptors phosphorylate and thereby activate the type-I receptors kinase domain. R-Smads (red) phosphorylation by the type-I receptor results in heteromeric complex formation between two R-Smads and one Co-Smad, and subsequent relocalization of this complex to the nucleus. The Smad complex co-operates with other DNA-binding proteins and recruit co-activators (nt shown) or co-repressors (red octagon) to either activate or repress target genes. The inhibitors Smads (purple) act as a negative feedback loop, inhibiting type-I receptor kinase activity upon high signalling conditions. **middle right**, **right**, TGF-β pathway components in *Drosophila melanogaster* and *Homo sapiens*. Figure adapted from [39].

linked to several human diseases, including cancer [42, 43, 44], cardiovascular diseases, connective tissue diseases as well as skeletal and muscular disorders [42].

TGF-β superfamily ligands are synthesized as precursor proteins, consisting of a large amino-terminal pro-domain that is required for proper folding of the highly conserved carboxy-terminal region which codes for the mature ligand [45]. Ligands become activated by cleavage of the precursor protein, and form homo- and hetero-dimers which are secreted into the extracellular space. A conserved feature of the TGF-β superfamily ligand is a protein structure termed the cystine knot. The cystine knot structure provides stability and is formed by three disulphide bridges between six highly conserved cysteines. Dimerization of two monomers is mediated by a covalent disulphide bond formed between two conserved cysteine residues [46].

The core components of the TGF-β signalling pathway show a high level of conservation between diverse species from worms to flies and humans. TGF-β signalling is transmitted through heteromeric receptor complexes formed by the type-I and type-II serine/threonine kinase receptors. In general, binding of the dimeric ligands to its type-I and type-II receptors results in the formation of the active receptor complex. In the active receptor complex the type-II receptor, which is constitutively active, phosphorylates the type-I receptor at a GlySer (GS) domain located upstream of the kinase domain, which results in activation of the type-I receptors kinase domain. The active type-I receptor phosphorylates the receptor-Smad (r-Smad) on two C-terminal serine residues located within a (S)SXS motive. Phosphorylated r-Smad forms a heteromeric complex together with the Common-mediator Smad (Co-Smad)

and subsequently accumulates in the nucleus. Nuclear Smad complexes interact with other DNA-binding proteins and recruit co-repressors or co-activators to regulate the levels of target gene expression (Fig.2 left and middle-left). Inhibitory-Smads (I-Smads) are transcriptionally induced by TGF-β signalling and act as inhibitors of the pathway. I-Smads can bind to the type-I receptor but lack the C-terminal (S)SXS phosphorylation site, hence act as inducible negative modulators.

While there is a large number of TGF-β super family ligands in humans, this number is more manageable in *Drosophila melanogaster*, where 7 ligands have been described so far (Fig.2 middle-right and right). Three of them, Decapentaplegic (Dpp) [47], Glas bottom boat (Gbb) [48] and Screw (Scw) [49], belong to the BMP family. While dActivin and Dawdle (Daw) belong to the TGF-β-like family, Maverick (Mav) and Myoglianin (Myo) have not been assigned a family yet.

The *Drosophila* BMP family members are well studied and known to act as extracellular morphogens during fly development. Dpp is the fly homologue of vertebrate BMP2/4, while Gbb and Scw are homologues of the BMP5/6/7/8 subfamily. Dpp has been shown to signal preferentially trough the type-I receptor Thickveins (Tkv) [50], while Gbb preferentially binds to Saxophone (Sax) [51]. Upon Dpp binding, the type-II receptor Punt (Put) [52] can interact with Tkv and activate its kinase domain by phosphorylation. Hereupon, the *Drosophila* R-Smad Mothers against dpp (Mad) [24] is phosphorylated by Tkv. Two phosphorylated Mad (p-Mad) proteins form a trimeric complex together with the *Drosophila* Co-Smad Medea, and this complex then translocates to the nucleus to regulate gene expression. Upon Dpp signalling, expression of the I-Smad Daughters against dpp (Dad) [53, 24] is upregulated; Dad acts as an antagonist of the pathway, reducing Dpp signalling input by competing with Mad for receptor binding and thereby inhibiting its phosphorylation.

1.3 The *Drosophila* wing disc as a model system to study morphogen function

1.3.1 Early wing disc development

A prime model system to study the function of morphogen gradients in patterning and growth control is the *Drosophila* wing imaginal disc, the larval precursor of the fly wing. The 15 imaginal discs of *Drosophila* form the adult appendages and the majority of the fly epidermis of the head and thoracic segments; in contrast, the abdominal segments are formed from clusters of cells called histoblasts. During embryogenesis, imaginal discs become specified and invaginate from the embryonic epidermis to form single layered epithelial sacks. They do not contribute to the larval body plan, but grow and become patterned during the larval stages, to finally form to the fly's adult body during metamorphosis.

The wing imaginal disc is specified from a subset of epithelial cells in the second thoracic segment of the embryo (Fig.3 A), and invaginates at 9-10h AEL (After Egg Laying, at 25°C) [54]. At the stage the discs are defined, all embryonic segments have a clearly defined anterior-posterior (A/P) axis, due to expression of the segment polarity gene *engrailed* (*en*, a homeodomain transcription factor [55, 56]) in the

posterior part of each segment (see Fig.3 A bottom). The cells that give rise to the thoracic imaginal discs, including the wing imaginal disc (from here on wing disc), are specified in the region of the boundary where the anterior En negative and the En positive tissue contacts. Therefore the wing disc directly adopts the A/P axis of the embryonic epidermis, hence the early wing disc already consists of an En negative anterior compartment and an En positive posterior compartment (Fig.3 B). The cells of the anterior and the posterior compartment possess unique properties and do not mix with cells from the other compartment. This behaviour results in a straight interface between the anterior and the posterior cells, called the A/P compartment boundary [57]. During the next 4 to 5 days of larval development the wing disc grows from ~40 cells at the first instar stage [58] to ~60'000 cells at the initiation of pupation [59, 60]. During this time period, the growth of the wing disc needs to be strictly controlled and the tissue needs to be patterned. Growth and patterning are controlled by the Dpp [22, 61, 23] and the Wingless (Wg) [62, 63] morphogens, secreted from organizer regions along the A/P boundary and along the dorsal-ventral (D/V) boundary of the wing disc, respectively (Fig.3 C-D). Both, Dpp and Wg are essential for fly development, and wings fail to form in *dpp* [64, 61] or *wg* mutants [65, 66].

The spatial expression and activity patterns of the two selector genes En [69, 70] and Apterous (Ap) [71] are responsible for the establishment of the A/P and the dorsal-ventral (D/V) compartment boundary, respectively, and the subsequent induction of the corresponding organizer regions. Expression of Dpp in the A/P boundary organizer is controlled by a sequence of signalling events involving En and a third morphogen, Hedgehog (Hh) [72, 73, 74, 75]. En directs the secretion of Hh from posterior cells [76], but at the same time renders posterior cells insensitive to Hh signalling by repression of the Hh signal transducer Cubitus interruptus (Ci) [77]. In contrast, anterior cells express Ci and can properly respond to the short-range Hh gradient which spreads into the anterior compartment (Fig.3 C). The Hh gradient induces *dpp* expression (Hh $\rightarrow$ *dpp*) [61] in a 8-10 cell wide zone in the anterior compartment, but also induces en expression in 3-4 cells wide stripe adjacent to the A/P boundary (only in the late 3rd instar) [78]. The (1) dpp activation by Hh in a wide stripe and (2) dpp repression by En in a narrow stripe results in a dpp expression stripe that is ~5-6 cells wide. From this stripe source, Dpp forms concentration gradients into the anterior and posterior compartment which instruct patterning and growth along the A/P axis [24, 79].

While the A/P boundary is already established when wing disc cells are defined from embryonic epidermal cells, the D/V boundary and also the D/V organizer region is established later, only at the early 2nd instar stage (~48h AEL) [71]. At this stage, *ap* expression is initiated in the prospective dorsal compartment of the wing disc. Subsequently Ap induced Notch signalling between dorsal and ventral cells establishes the D/V boundary and also induce *wg* expression in boundary cells [80, 81]. The Wnt family ligand Wg is secreted from D/V organizer cells and controls the expression domains of the target genes *distal-less* (*dll*) and *vestigal* (*vg*), which are required for wing blade identity, along the D/V axis. Despite the requirement of the *wg* gene for wing development [65, 66], the function of Wg as a classical morphogen was recently

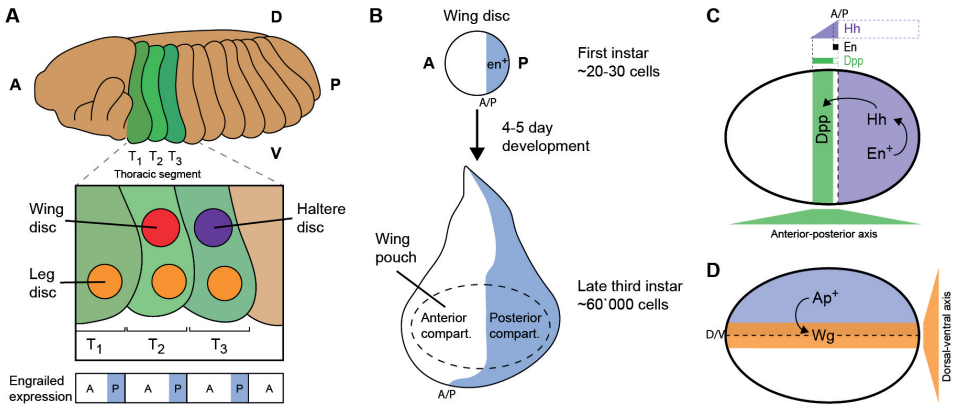

Figure 3: Early wing disc development

A, In the *Drosophila* embryo, the wing disc (red circle) is defined from epidermal cells in the 2nd thoracic segment (T_2). The haltere disc (purple circle) forms in T_3, and all thoracic segments form leg imaginal discs (yellow circles). All embryonic segments are subdivided into anterior (Engrailed negative, white) and posterior (Engrailed positive, blue) domains. A, anterior; P, posterior; D, dorsal; V, ventral. **B**, The wing imaginal disc consists of an anterior and a posterior compartment, which is adopted from the epidermal cells of the 2nd thoracic segment. The early wing disc grows from ~20-30 cells to ~60'00 cells during 4-5 days of larval development. The central region of the wing disc, the wing pouch (marked by a dotted line), is giving rise to the adult wing blade. The growth and pattern of the wing pouch is controlled by morphogen secreted from two organizer regions. **C**, Establishment of the A/P organizer in the wing pouch. In posterior cells Engrailed (En) instructs the expression and secretion of Hedgehog (Hh). Hh signalling induces the expression of *dpp* in a stripe of anterior cells adjacent to the anterior-posterior (A/P) boundary. Dpp is secreted from these cells and forms concentration gradients to both sides of the stripe source. **D**, The dorsal-ventral (D/V) organizer is established by the selector gene *apterous* (*ap*) and secrets Wingless (Wg). The Wg gradients control gene expression along the D/V axis. Figure adapted from [67, 68].

challenged [82], an observation, I will discuss in more detail in section 4.3.

1.3.2 The Dpp morphogen gradient in the wing disc

Decapentaplegic (Dpp), the fly homologue of vertebrate BMP2/4, is essential for the formation of the fly wing. While flies mutant for *dpp* in the wing disc only develop very small wing rudiments [64, 61], ectopic expression of Dpp can result in wing duplications and/or overgrowth [61]. Dpp is expressed in a centrally localized stripe in the wing disc (as discussed above), from where it forms concentration gradients into the anterior and posterior target tissue (Fig.4 left). Due to the lack of a good antibody, scientists have engineered fusion proteins between GFP and Dpp (GFP-Dpp)[83, 84] to visualize Dpp distribution. Expression of GFP-Dpp in the wing disc stripe source using the Gal4/UAS [85] or the LexA/LOP [86] binary expression systems rescues the *dpp* mutant phenotype to a good extend [84, 83]. GFP-Dpp fusion proteins allow direct visualization of Dpp distribution and extraction of gradient shape and range by plotting GFP fluorescence intensity along the A/P axis (Fig.4 middle). Moreover,

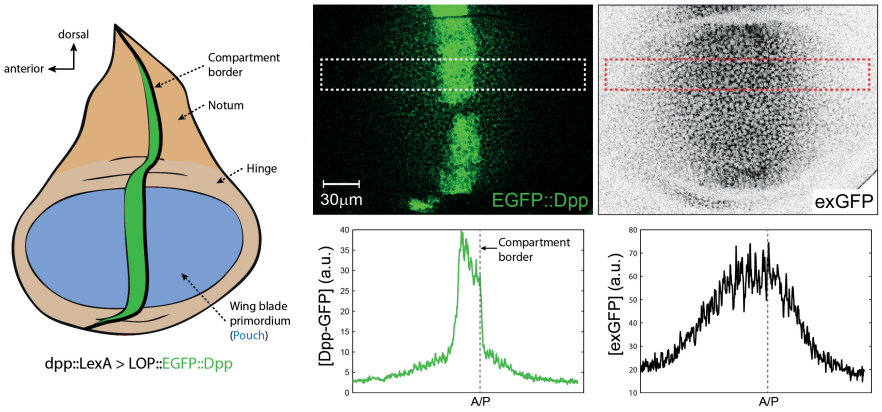

Figure 4: The Dpp morphogen gradient in the *Drosophila* wing imaginal disc
left, Schematic illustration of a wing disc. All wing discs in this thesis are shown with their anterior side facing left and their dorsal side facing up. The wing disc consists of three major regions, the notum (giving rise to the fly's back), the hinge (forming the attachment parts connecting the wing to the fly's body) and the wing pouch (light blue) which will form the actual wing blade. Dpp is expressed in a stripe (green) of anterior cells along the A/P compartment boundary. Below, the genotype of the discs shown to the right is indicated. **middle**, The Dpp gradient can be visualized by expression of a protein fusion between enhanced(E) GFP and Dpp (EGFP::Dpp) in a wild type background. EGFP fluorescence allows direct visualization of the gradient by plotting fluorescence intensities (bottom graph). **right**, In order to visualize the extracellular fraction of EGFP::Dpp only, so called extracellular staining protocols can be used. These protocols allow sensitive visualization of the extracellular Dpp (exGFP) gradient range and shape.

excellent antibodies for the detection of GFP are available, allowing to label the extracellular fraction of EGFP::Dpp only (Fig.4 right). These so called extracellular immunostaining protocols do not use detergents, and therefore do not permeabilize the cell membrane, such that the antibody can only access the extracellular portion of the antigen (explained in detail in 3.2.2). These protocols have been particularly useful to detect the distribution and the subcellular localization of the mature Dpp ligand [87] and other morphogens in the wing disc tissue [88, 89, 90].

In addition to GFP, Dpp has been fused to other fluorophores and tags, such as the photo-convertible fluorescent protein Dendra [91] or the Hemagglutinin (HA) tag [92]. Due to the advantages in visualization and the availability of good antibodies as well as genetically encodable, synthetic GFP binders (see next chapter) I will make use in this thesis work of an EGFP-tagged version of Dpp based on the construct engineered by Teleman *et.al.* [84] (see 3.3.1 for details on the cloning).

1.3.3 Wing disc patterning by the Dpp gradient

Patterning of the wing disc by the Dpp gradient has been studied extensively and is generally well understood and documented ([22, 23, 93], reviewed in [24, 79]). Upon secretion, Dpp forms long range concentration gradients to both sides of its centrally located source. The Dpp concentration gradient is transduced by its receptors Tkv [50] and Punt [52], and translated into an intracellular gradient of p-Mad, which can

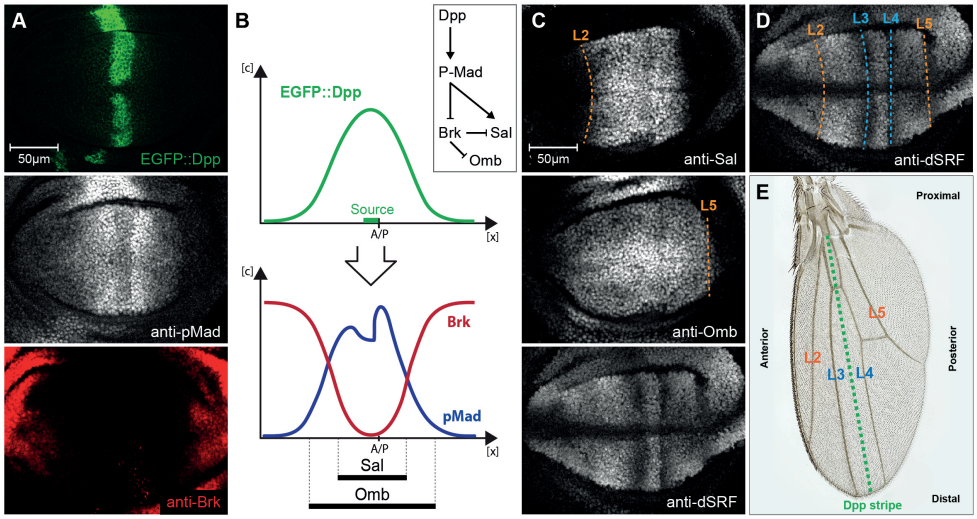

Figure 5: The Dpp signalling gradient patterns the *Drosophila* wing
A, A wild type, third instar wing disc expressing EGFP::Dpp (green) in the stripe domain, stained for p-Mad (grey) and Brk (red). **B**, The Dpp gradient it translated in an intracellular gradient of p-Mad (blue). Since Dpp pathway activity represses the expression of Brk, the Brk gradient profile (red) is inverse to the one of p-Mad. Different sensitivities to Brk repression result in different domain width of Dpp targets like Sal and Omb (black bars). **C**, Third instar wing discs stained for Sal, Omb and the intervein gene dSRF. Prospective positions of wing vein L2 (set by Sal) and L5 (set by Omb) are marked by dotted orange lines. **D**, Wing disc stained for dSRF from (C, bottom). Position of prospective wing veins are marked by dotted lines. Vein L2 and L5 (orange) are positioned by Dpp, while L3 and L4 (blue) are positioned by Hh. **E**, Adult *Drosophila* wing. The region of Dpp production is marked by a dotted green line. Wing veins L2 to L5 are positioned along the anterior-posterior axis.

---

be visualized by an antibody specifically recognizing the phosphorylated form of Mad (Fig.5A, middle). p-Mad levels are slightly reduced in source cells but maximum adjacent to them, and gradually decreasing towards the periphery. Since Tkv is a negatively regulated target of Dpp signalling, source cells express lower levels of Tkv, and hence p-Mad levels are slightly reduced in these cells [94]. As mentioned above, p-Mad forms a complex together with the *Drosophila* Co-Smad Medea and accumulates in the nucleus to regulate Dpp target gene expression. The p-Mad/Medea complex binds to so called silencer elements (SEs) [95, 96] and recruits another transcription factor Schnurri (Shn) [97, 98, 99] to repress the transcription of *brinker* (*brk*) in a concentration-dependent manner. The dose-dependent repression of Brk transcription results in a Brk profile that is inverse to the one of p-Mad (Fig.5 A-B). In summary, p-Mad / Dpp signalling levels are high in the centre and decrease towards the periphery, while Brk levels are high in the periphery and decrease towards the centre of the disc. Brk acts as a general repressor of Dpp target genes [100, 101, 102], therefore the removal of Brk by Dpp in the central region of the disc results in the de-repression and the concurrent activation of several Dpp target genes, such as *daughters against dpp* (*dad*) [103, 104], *spalt* (*sal*) [105] and *optomoter-blind* (*omb*) [106, 107, 108].

While *dad* and *sal* expression is directly activated by Dpp signalling (via binding of the trimeric p-Mad/Medea complex to a so called activator element (AE) [104] in the respective regulatory regions), Omb is activated by yet unknown factors but becomes expressed due to the loss of repression by Brk [102]. Different sensitivities of Dpp target genes to Brk repression result in distinct expression domains that differ in their width. While *omb* is less sensitive to Brk and is expressed in a wide domain, *sal* shows a higher sensitivity to Brk repression resulting in a narrower expression domain (Fig.5B, bottom and C) [22, 24, 109].

Sal and Omb are both transcription factors and are important for wing vein positioning [110, 111]. The *Drosophila* wing features five main longitudinal veins (LVs, named L1-L5), which are positioned in a robust and stereotypic way. L1-L3 are positioned in the anterior compartment of the wing, while L4 and L5 form in the posterior compartment (Fig.5E). The position of prospective wing veins becomes specified already at the larval stage. Vein position of L2-L5 in the wing disc can be visualized by staining for Blistered (Bl, also known as dSRF), a marker expressed in the prospective intervein region (Fig.5C, bottom and D, top). While positioning of L3 and L4 was shown to depend on Hh signalling, veins L2 and L5 are positioned by the Dpp gradient [111]. L2 is specified at the anterior edge of the Sal domain (Fig.5C, top), either directly by low Sal levels [112] or by an unknown secondary signal produced by Sal expressing cells [113, 114]. Positioning of L5 in the lateral posterior compartment is molecularly not fully understood. L5 initiation was shown to depend on Omb and Brk [115] and potentially is repressed by Sal [116]. Therefore, the simplest mechanism would suggest that Sal defines the anterior limit of L5 and the requirement for Omb the posterior limit of L5 (Fig.5C, middle) [111].

1.4 Novel technical approaches to address outstanding questions

While the interpretation of Dpp signalling on the cellular level and the resulting patterning functions are well understood, the mechanism of Dpp gradient formation and the role of the Dpp gradient for proliferation and growth control of the wing primordium is highly debated. A variety of mechanisms have been suggested to explain Dpp gradient formation. These mechanisms range from simple diffusive processes [117, 118, 14, 87, 91] to active ligand transport trough cells by repeated cycles of endo- and exocytosis [83, 119, 120] and along cellular protrusions called cytonemes [121, 122, 123, 124]. Once the gradient has formed, it remains unclear how the Dpp gradient controls the growth and the final size of the wing disc, and hence the fly wing. The proposed models either suggest a direct control of the proliferation rate by Dpp [125, 126] or a permissive range-dependent function of Dpp [127, 128, 109, 129].

A common feature of the approaches taken so far, is that they disturb Dpp distribution by modifying proteins involved in either Dpp dispersal or signalling. Major advantages of these approaches include the fast realization due to the availability of mutants, over-expression constructs or RNAi lines. However, they also bear the danger of indirect effects or effects provoked due to non-physiological conditions (e.g.

due to strong over-expression). In order to circumvent these caveats, I want to introduce in the following section a novel, nanobody-based technique that allows direct modification of EGFP::Dpp protein distribution, leaving other components of the system untouched. Nanobodies are genetically encodable, small protein binders, that allow us to specifically target and modify the Dpp ligand distribution profile. In the following, nanobody-mediated morphogen trapping will allows us to distinguish between some of the proposed mechanisms for gradient formation and growth control. The next section introduces nanobodies as valuable and powerful tools to study developmental processes in multicellular organisms. In the following "Part I" of my thesis, I will summarize how our nanobody-based approaches allowed us to gain a deeper understanding of how the Dpp gradient and Dpp spreading controls the growth of the wing disc. In "Part II", I will present preliminary results on how nanobodies can help to understand how and where Dpp disperses in the wing disc tissue to form a robust concentration gradient.

1.5 Functionalized-nanobodies as novel tools to study morphogen gradients

Classical antibodies (Abs) found in mammalian species consist of two identical heavy and two identical light chains (Fig.6A), which are connected by disulphide bonds. In striking contrast, a considerable fraction of the IgG Abs found in members of the camelid family consist of heavy chains antibodies (HCAbs), lacking the light chains (Fig.6B) [130]. HCAbs consist of only three globular domains, while classical antibodies carry four of these domains. Two of these domains in HCAbs show homology to the second and third constant region of the heavy-chain (CH2, CH3) of classical antibodies. However, the CH1 domain, which connects the heavy with the light chain in classical Abs, is lost in HCAbs. Therefore the antigen-binding region, usually consisting of the variable-domain of the heavy chain (VH) and the light chain (VL), is reduced to a single domain in HCAbs [131]. This single variable domain of heavy chain antibodies was termed VHH or nanobody (© Ablynx). VHHs, similar to VHs, adapt an Ig fold of two β-sheets with three discernible loops that carry the complementary determining regions (CDRs) responsible for antigen recognition (Fig.6C, coloured). The CDR containing loops of the VHH (especially CDR1 and CDR3) are extended compared to the ones of the VHs [132]. Therefore, the extended loops in VHHs can adapt highly versatile, finger-like structures, reaching into pockets (also acting as enzyme inhibitors) and recognizing three dimensional structure, thereby increasing the paratope repertoire [134, 132, 135].

Nanobodies have been used in basic science in manifold ways, e.g. as crystallization chaperones, enzyme inhibitors or to block protein function (reviewed in [136, 137]). A rather newly emerging field is the use of functionalized protein binders/nanobodies in multicellular organisms. The major advantage of nanobodies over classical antibodies, is the monomeric nature of the VHH domain. Monomeric VHHs can be used as synthetic protein binders that are easily functionalized by fusion to protein domains carrying specific functions. These fusion protein can be expressed in cells to

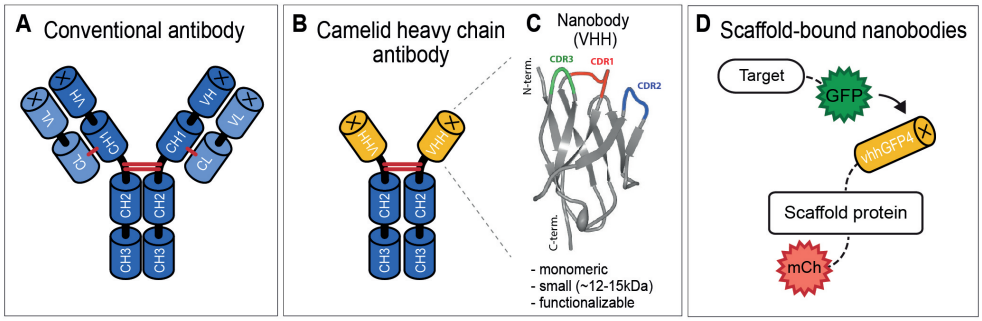

Figure 6: Functionalized-nanobodies as novel tools in developmental biology
A, Conventional antibodies consist of two heavy (dark blue) and two light chains (light blue), which are linked by disulphide bonds (red). Constant regions of heavy chain (CH1-3) and light chain (CL) build the framework of the antibody, while antigen binding specificity if give by the variable domains of the light (VL) and the heavy chain (VH). **B**, Heavy-chain antibodies (HCAbs) of the camelid family consist of two heavy chains only. Binding specificity is given by a single domain termed Variable-domain of the Heavy-chain of HCAbs (VHH, yellow) or nanobody. **C**, Structure of the anti-GFP nanobody (vhhGFP4, from Kubala *et.al.* [133]) used in this study. The three loops containing the complementarity determining regions (CDR1-3) are coloured. **D**, Schematic drawing of scaffold-bound nanobodies (SBNs). vhhGFP4 is fused to a scaffold protein of known localization, which has been tagged with mCherry (mCh) for visualization. SBNs can bind and immobilize GFP-tagged proteins of interest.

directly modify and study target protein function *in vivo*. The field of functionalized protein binders was strongly influenced by the isolation of a nanobody specifically recognizing GFP (termed vhhGFP4) [138, 139]. The 13kDa vhhGFP4 GFP-binding fragment was thoroughly characterized, and shown to retain its strong binding specificity (Equilibrium dissociation constant (K_D) = 0.32nM) *in vivo* when combined with fusion-proteins, also when expressed in the intracellular environment (as a so called intrabody) [138, 140]. Based on vhhGFP4 several tools to modify GFP-tagged proteins have been generated. So called chromobodies, fusion proteins of vhhGFP4 (or any other nanobody) and a fluorescent protein, allow to study protein localization and dynamics in living cells [139, 141, 142, 143]. Degradation of GFP-tagged proteins was achieved by a nanobody-based technique called deGradFP (degrade Green Fluorescent Protein). In deGradFP, vhhGFP4 was fused to a subunit of the ubiquitination machinery, resulting in ubiquitination and subsequent degradation of GFP-tagged proteins in *Drosophila* and human cell lines [144]. Recently an analogous approach was established to degrade nuclear GFP-tagged protein in mammalian cells and in zebrafish embryos [145]. Moreover, vhhGFP4 was used to directly control gene expression (T-DDOG - transcription device dependent on GFP) [146], or Cre recombinase activity (CRE-DOG - Cre-recombinase dependent on GFP) [147] by GFP in mouse embryos.

In order to modify the extracellular distribution of secreted, GFP-tagged proteins (e.g. morphogens), we developed and validated scaffold-bound nanobodies (SBNs) as novel tools to study morphogen gradient function. SBNs are fusion proteins consisting of vhhGFP4 fused to a "scaffold" protein of known localization and a fluorophor, to

visualize the localization of the SBN (Fig.6D). We have created SBNs that either localize to the cell surface, by fusing vhhGFP4 to transmembrane proteins, or to the extracellular matrix (ECM). In both cases, SBNs act as artificial morphogen traps, sequestering and immobilizing the EGFP::Dpp morphogen either along the cell surface or in the ECM. Expression of SBNs is controlled by binary expression systems (e.g. Gal4/UAS or LexA/LOP), and therefore can be tightly regulated in a spatial and temporal manner, allowing versatile experimental setups.

In the first part of this thesis I will make use of a specific SBN, we called morphotrap, which utilizes the mouse CD8 transmembrane protein as scaffold. Due to the membrane localization of morphotrap, the vhhGFP4 domain is presented outside of the cell along the cell surface, showing no bias in localization along the apical-basal axis when expressed in the polarized epithelial wing disc cells. Co-expression of EGFP::Dpp and morphotrap in source cells completely abolished gradient formation, and hence provides an elegant framework to study the requirement of Dpp spreading for wing disc patterning and growth control. In the second part, I will introduce SBNs that localize to specific sub-cellular compartments (e.g. to the apical or basolateral compartment only) or to the ECM. These differentially localized SBNs might allow us to investigate the route of Dpp dispersal and to modify the dispersal of specific sub-cellular fractions of Dpp. This will yield a basic understanding of their respective contributions to patterning and growth control of the wing disc. Finally, our studies illustrate the versatility and power of synthetic protein binders for biological research in multicellular organisms.

Part I

The requirement of Dpp and Wg spreading for patterning and growth control of the wing imaginal disc

2 Introduction

An outstanding question in developmental biology is how pattern and size of tissues and organs are controlled and coordinated during embryonic development. Transplantation experiments performed already in the 1920s suggested that organs 'know' how big to grow. In a striking experiment Victor C. Twitty and Joseph L.Schwind transplanted the leg primordium of a large salamander species, *Ambystoma tigrinum*, to a small salamander species, *Ambystoma punctatum* [148]. Despite developing in a different environment, the transplanted leg primordia developed to their original size, resulting in either a small salamander with a longer-than-normal leg or a big salamander with a shorter-than-normal leg (Fig.7). These results demonstrated that embryonic primordia indeed possess intrinsic control mechanisms determining final organ size, which are clearly distinct from systemic mechanisms controlling individual size. Also in the *Drosophila* wing disc such intrinsic size control mechanisms have been observed. Modulation of cell proliferation in the posterior compartment of the wing disc can create compartments with much higher or lower cell numbers than control compartments, strikingly, these drastic changes in cell number do not affect the overall compartment size [149]. These observations clearly suggest that growing organs do not count their cell number, but possess mechanisms that can "measure" tissue size.

By which mechanisms organs measure their size and what might be the intrinsic factors controlling organ growth remained mysterious for a long time. The discovery that morphogens can link pattern with size provided the basis for a variety of morphogen-based models of organ-intrinsic growth and size control. The *Drosophila* wing disc provided a versatile and simple model system to study the role of morphogenetic growth control. Wing disc patterning and growth is mediated by the Dpp and Wg morphogen gradients, which are established from the two primary organizer regions along the A/P and D/V boundary, respectively (explained in detail in 1.3.1). Both, the *dpp* and the *wg* genes, are required for wing disc cells to form the central region, called the wing pouch, the area forming the adult wing blade. Mutations in

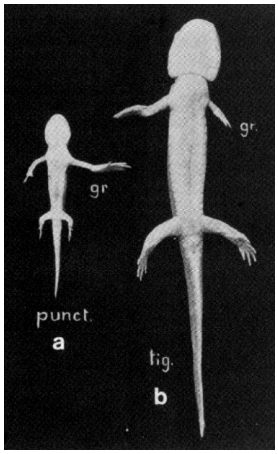

Figure 7: Organ intrinsic growth control
Two salamanders of the species *Ambystoma punctatum* (punc., left) and *Ambystoma tigrinum* (tig., right). The primordia forming the right facing leg have been transplanted during early embryonic development between the two species. Primordia intrinsic factors define leg size, such that the transplanted legs grow to the size they would have adapted in their original body. (Image from Twitty and Schwind, 1931 [148])

either the Dpp or the Wg pathway result in loss of cell proliferation and the adult wing blade [64, 61, 150, 151, 65, 66]. Both morphogen gradients have been studied extensively, and several models have been proposed to explain proliferation and size control by Dpp and Wg. However, the molecular mechanisms underlying these processes remain highly debated.

At this point, I want to clarify, that my work will focus on proliferation control (cell division) and on final size control of the wing disc tissue, which I will also referred to as growth control. Importantly, the term growth control is sometimes used in the literature to refer to the process of cellular mass increases ("cell growth"), a process I will not discuss in the scope of this work.

2.1 Models for Dpp-mediated growth and size control

Over the years, a variety of models were proposed to explain the mechanism of proliferation and size control by Dpp in the wing disc [152, 153, 127, 128, 154, 155, 156, 126]. These models can be mechanistically sub-divided into two distinct classes: (1) instructive (direct) or (2) permissive (indirect) (Fig.8). Instructive models imply that Dpp signalling activity directly controls the cellular proliferation rate and hence the growth rate of the tissue. In contrast, permissive models suggest that the proliferation rate is controlled by other factors than Dpp, but that Dpp signalling provides the competence to respond to these regulatory factors in a concentration/position-dependent manner. A major challenge for both types of models it to explain how the graded distribution of the growth factor Dpp can result in the uniform proliferation profile observed along the A/P axis of wing discs (Fig.9A) [157, 60, 158, 159].

The existence of two mechanistically distinct models has split the research community, one part favouring the instructive "Temporal Rule Model" (TRM) [126, 160, 125] (Fig.9B), the other part favouring the permissive "Growth Equalization Model"

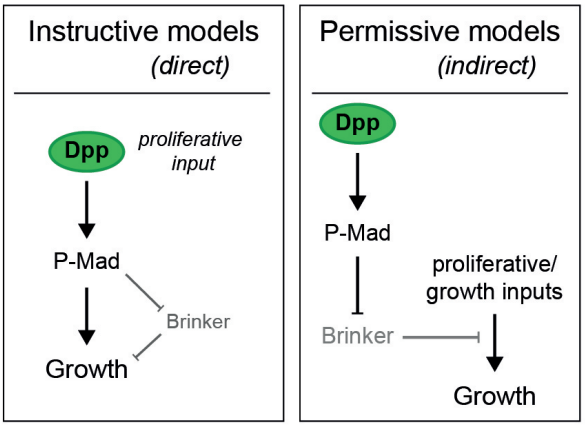

Figure 8: Instructive versus permissive models of growth control
Instructive models (left) suggest that Dpp signalling activity directly induces proliferation, ultimately resulting in tissue growth. Conversely, in permissive models (right) Dpp signalling gives competence to respond to other pro-proliferative/growth inputs. Competence is given to cells by removal of the growth repressor Brk by Dpp signalling.

(GEM) [128, 161, 129, 109] (Fig.9C). Both, the TRM and the GEM, suggest elegant ways to explain how graded Dpp distribution can result in uniform proliferation profiles along the A/P axis. In contrast, while the TRM can provide a mechanism for growth remination, the GEM model struggles to give conclusive suggestions on how Dpp controls the final size of the wing disc. In the following I will discuss the function of Dpp in the TRM and the GEM and how the two models explain control of the proliferation rate and tissue size control.

The "Temporal Rule Model" (TRM)

The TRM is based on quantitative observation of EGFP::Dpp distribution and levels during larval development. Wartlick *et.al.* observed that the amplitude of the EGFP::Dpp gradient increases over developmental time (Fig.9B). In addition, they found that the EGFP::Dpp gradient scales with tissue size, meaning that the gradient expands with the growing tissue in a way that the relative shape of the gradient remains unchanged (hence, the gradient "scales"). Combining these two observations, Wartlick *et.al.* concluded that all cells in the wing disc experience the same relative increases in EGFP::Dpp levels, independent of their position in the primordium. In a final step, they showed that the proliferation rate in the wing disc correlates well with the temporal increase in the amplitude of the Dpp activity gradient. It turns out, that cellular Dpp levels increase by 50% during the cell cycle, therefore the TRM suggests that cells divide once their cellular Dpp signalling levels have increased by 50%. Since the relative increase in Dpp signalling is position-independent along the A/P axis (because of gradient scaling), also the proliferation rate is uniform along this axis. An elegant feature of the TRM is that it can also explain growth termination at the end of larval development: relative Dpp signalling levels need to increase by 50% during each cell cycle. With each cell cycle, this increase becomes more difficult to obtain, resulting in a progressive reduction of the proliferation rate, until a threshold-point, where a 50% increase cannot be obtained any more and proliferation, and hence tissue growth, halts.

The TRM is supported by experiments in which the increase in Dpp signalling activity was modulated by inducible expression of Tkv^{QD}, a constitutively active version of the Dpp type-I receptor. In such clones, cell division also correlated with an increase in Dpp signalling activity by 50%. Furthermore, clones experiencing a faster increase in Dpp signalling also divided faster [126]. However, these results again only suggest a correlation between increasing Dpp signalling and the proliferation rate but do not provide evidence for such a mechanism under physiological conditions. Due to its simplicity and the mathematical framework provided by the authors the TRM gained support especially among computational biologists [162, 163]. A similar mechanism was suggested to control the growth of the *Drosophila* eye imaginal disc [125].

Recently, the TRM was challenged by two major findings: (1) Dpp signalling activity, visualized by p-Mad antibody staining, was not found to increase during larval developmental in wild type wing discs [164]. (2) Clones of cells that are mutant for both, the Dpp signal transducer *mad* as well as the growth repressor *brk*, showed

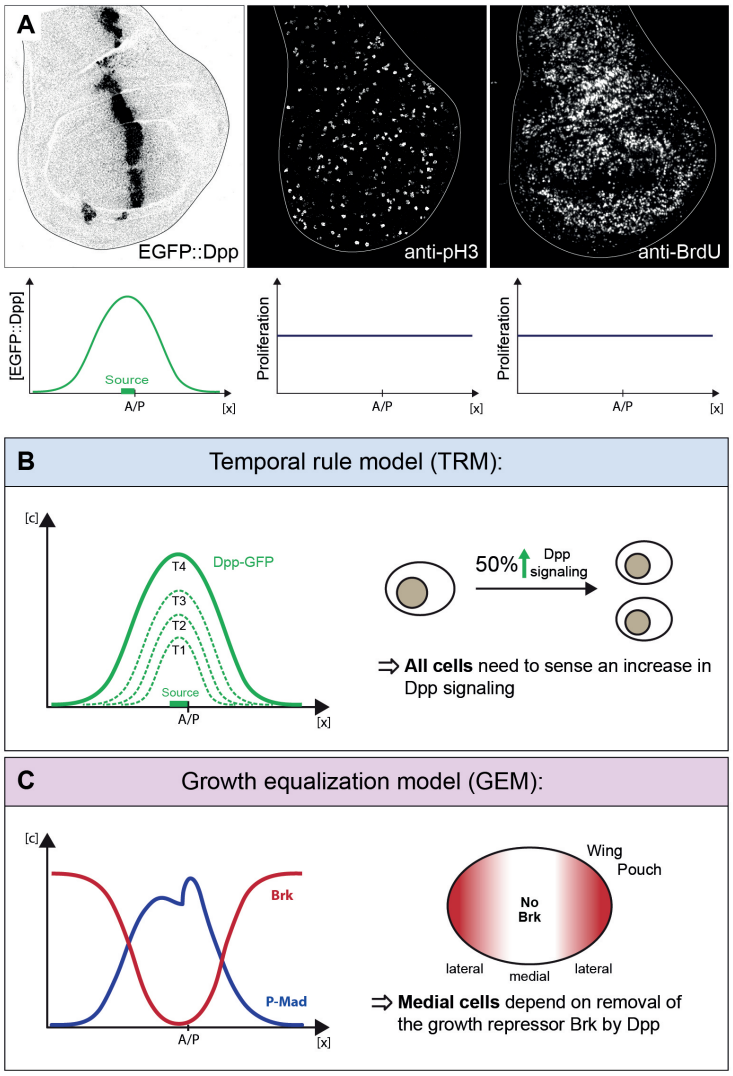

Figure 9: Proliferation control by the Dpp gradient

A, Dpp, visualized by the GFP::Dpp fusion protein, is expressed in a central stripe and forms a graded concentration profile in the wing disc tissue. Despite this graded distribution, cell proliferation, either visualized by staining for phospho-histone H3 (p-H3) or by BrdU labelling, is approximately uniform along the A/P axis. **B**, The "temporal rule model" (TRM) suggests an instructive function of Dpp. **C**, In contrast, the "growth equalization model" (GEM) suggests a permissive function of Dpp.

normal growth rates when located in the central region of the wing disc, and even overgrew when located in the periphery [129]. These clones cannot sense Dpp signalling input, and hence should not divide according to the TRM (or at a different rate), but do so at similar rates as wild type cells. These findings suggest that cell division does not depend on increasing Dpp levels, as long as the growth suppressor Brk is absent and not directly inhibiting growth; an idea that was picked up by the GEM.

The "Growth Equalization Model" (GEM)

The GEM is based on the finding that wing disc double mutant for *dpp* and *brk* grow normally, but non-uniform, showing increased proliferation in the periphery [128]. Analogous, clones mutant for both, *mad* and *brk* show similar growth rates as their twin-spots [129]. Based on these observations, the GEM suggests that the growth modulator function of Dpp is indirect and depends on the removal of medial Brk. This highlights that medial cell proliferation does not directly depend on Dpp signalling input, but requires the removal of the growth suppressor Brk. Such a mode of growth control emphasizes the role of other instructive growth promoters, such as the Insulin/dTOR and Hippo pathways [165], in controlling the basal proliferation rate.

The GEM proposes that the "basal" growth potential along the A/P axis is non-uniform, with lateral cells having a growth advantage over medial cells. This non-uniformity potentially arises from other signalling inputs [161], tissue geometry or mechanical feedback [166, 167, 168, 169]. Dpp balances this non-uniform growth potential by modulating Brk in a way that the lower growth potential of medial cells is elevated (by repression of Brk), while the higher growth potential of lateral cells is reduced (by the presence of Brk), such that the overall growth rates can be sustained by medial cells. Therefore, according to the GEM Dpp acts a growth modulator equalizing out a non-uniform growth potential along the A/P axis. Indeed, it was shown that Brk represses the growth promoter dMyc in lateral cells, reducing their growth potential [170]. Importantly, according to the GEM, Dpps' sole function is to remove medial Brk, hence Dpp input is not required to control proliferation in the lateral region.

This model was challenged by the observation that the levels of the Dpp signalling reporter *dad-nRFP* increase over time in wing disc mutant for *dpp* and *brk* [126], as well as in clones double mutant for *mad* and *brk* [160]. However, these findings only suggest that there are other potential inputs acting on the *dad* enhancer fragment used in these studies. Here, it is important to mention that the *dad-nRFP* reporter line used for these essays, expresses nuclear RFP (nRFP) under the control of the *dad* promoter. However, the half-life of nRFP in *Drosophila* cells has not been tested in Wartlick *et.al.* [126]. In a likely scenario, the nRFP protein stability exceeds the one of the unknown activating input; in this case nRFP levels do not reach a steady-state, and hence nRFP intensity is expected to increase over time. Furthermore, high Dpp pathway activation by clonal expression of Tkv^{QD} can also result in transiently increased proliferation in a non-autonomous manner [153]. This finding argues against

a solely permissive function of Dpp, and that strong signalling differences between neighbouring cells can have instructive effects on cell proliferation. However, whether such a response plays an active role during normal development remains to be shown.

2.1.1 Scaffold-bound nanobodies as novel tools to distinguish between an instructive or permissive function of Dpp

Here, we want to discriminate between the above introduced instructive and permissive models for growth control by Dpp. As pointed out before, both models predict the proliferation rate in dependence of the Dpp gradient profile. Importantly, the predicted proliferation rates for the two models would differ in a situation, where no Dpp gradient forms. Hence, a potential approach to distinguish between a instructive or a permissive mode of Dpp function would be to completely block Dpp spreading from its central stripe source and thereby abolishing gradient formation.

Situations in which Dpp spreading is impaired have been created before, e.g. by over-expression of the Dpp receptor Tkv [171, 172, 127]. However, such setups would not allow answering the above presented question because (1) the efficiency of Dpp immobilization is too low to completely abolish Dpp gradient formation (Dpp targets like Sal still form graded expression domains in the target field, see [172]) and (2) over-expression of a Dpp pathway component is not ideal, since it might results in artificial pathway activation due to high ectopic receptor levels or indirect effects. Another approach that specifically affects the protein of interests is genetic tethering to the cell surface, by fusion of the protein of interests to the extracellular domain of a transmembrane protein. This approach has been used to study the long-range function of Wg [173, 174, 82]. However, such a setup does not allow easy temporal and spatial control of protein tethering.

In order to overcome these limitation, we established a membrane-bound anti-GFP nanobody, we called morphotrap, as novel tool to directly modify spreading of GFP-tagged morphogens in a spatially and temporally controlled manner. Expression of morphotrap in the EGFP::Dpp source cells results in immobilization of EGFP::Dpp at the surface of source cells and a complete block of Dpp gradient formation. In such a situation, only the source cells and cells in direct contact with source cells experience Dpp signalling, while all other cells in the target tissue do not sense Dpp any more, but experience high levels of Brk. A result of this is that Brk is not repressed in the prospective medial region, and that all target cells, not in direct contact with source cells, do not experience temporally increasing Dpp signalling levels. Therefore this setup provides ideal conditions to distinguish between the GEM and the TRM.

Under normal developmental conditions, EGFP::Dpp spreads and forms a concentration gradient. Due to the repression by Dpp, Brk forms an inverse concentration gradient (Fig.10A, left). According to the GEM, central repression of Brk equalizes the growth of medial cells, such that they can sustain the overall proliferation rate, hence similar proliferation rates are observed in the medial and the lateral region. However, when Dpp spreading is blocked by morphotrap, Brk is only repressed in the first row of target cells; while high Brk levels should be present in the remaining target tissue (Fig.10A, right). According to the GEM, only medial proliferation

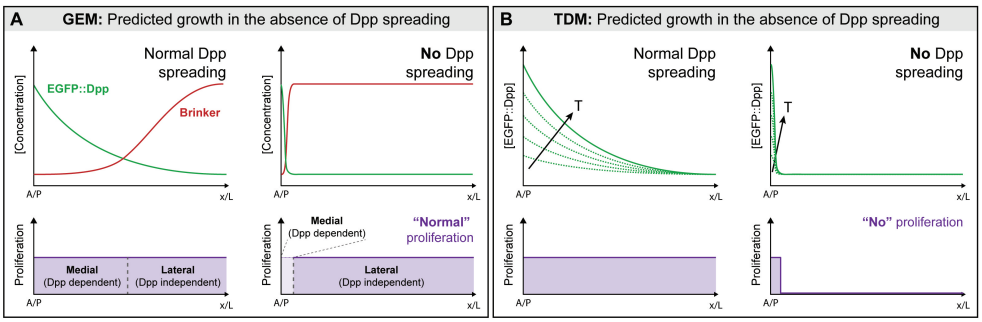

Figure 10: The proliferation profiles predicted by the GEM and the TRM differ in the absence of Dpp spreading
A, Predicted proliferation profiles for the GEM in the posterior compartment for the presence (left) and the absence (right) of Dpp spreading. Along the x-axis the relative position in the posterior compartment is shown, the left limit of the graph corresponds to the A/P boundary while the right limit corresponds to the posterior edge of the wing disc tissue. The y-axis shows the concentration of either EGFP:Dpp or Brk (top graphs) and the proliferative capacity (bottom graphs). **B**, Predicted proliferation profiles for the TRM in the presence (left) and the absence (right) of Dpp spreading. The temporal axis is marked by an arrow, labelled T.

depends on Dpp, while lateral cell proliferation is independent of Dpp. Hence, the GEM would predict that in the absence of Dpp spreading, the medial target region should not grow, while the lateral target cells should proliferate at rates similar to a control situation.

In striking contrast, according to the TRM, cell proliferation strictly depends on all individual cells sensing increasing Dpp signalling levels. In conditions with normal Dpp spreading and gradient scaling, all cells in the target tissue sense the same relative increase in Dpp, and hence proliferate at similar rates (Fig10B, left). However, in the absence of Dpp spreading (Fig.10B, right), all cells in the target tissue, apart from the ones in direct contact with source cells, will not sense any Dpp. Therefore the TRM predicts that in the absence of Dpp spreading no proliferation (or altered proliferation) should be observed in the target tissue, with exception of the target cells directly contacting Dpp source cells.

In conclusion, the GEM and the TRM predict two clearly different proliferation profiles in a situation where Dpp spreading is completely abolished. Using morphotrap-mediated blocking of EGFP::Dpp spreading, we want to create such a situation in an otherwise *dpp* mutant background. This experimental setup should allow us to distinguish between the two growth models presented.

2.2 Aim of the project

The *Drosophila* Dpp gradient in the wing imaginal disc has served as an excellent and intensely studied model system for morphogen mediated patterning and growth control. While the role of the Dpp gradient in pattern formation is well understood, its role in proliferation and growth control remains highly controversial and debated.

To better study the function of Dpp spreading in growth control, we aim to establish a novel nanobody-based method, that allows for the first time direct and specific modification of Dpp morphogen distribution *in vivo*. For this aim, we will create morphotrap, a membrane-bound anti-GFP nanobody, and characterize its function in the *Drosophila* wing disc. To complement this GFP-trap, we will establish a rescue system, in which the *dpp* mutant wing disc phenotype is rescued by the expression of an EGFP-tagged Dpp fusion protein, which can be specifically modified by morphotrap. Finally, we will combine these two novel tools and establish a genetic setup, using two binary expression systems, to independently control the spatial expression of the EGFP::Dpp transgene and the morphotrap transgene in a *dpp* mutant background. This setup will allow us to perform a multiplicity of versatile experiments, investigating the properties and function of Dpp spreading on patterning and growth control of the wing disc. In summary, nanobody-based morphogen trapping using morphotrap will allow us to:

(**1**) Understand the requirement of Dpp spreading for patterning the wing disc tissue.
(**2**) Distinguish between a direct versus a permissive function of Dpp in proliferation control.
(**3**) Test the requirement of Dpp spreading for wing disc growth and final tissue size control.

Moreover, we will show the versatile use of morphotrap by immobilizing Wg along source cells, testing the requirement of Wg spreading for *Drosophila* wing development. Finally, the morphotrap approach will allow us to study the role of the Dpp gradient from a novel perspective, complementary to existing genetic approaches, and provide an important novel tool to address highly debated questions in the morphogen field.

3 Material and Methods

3.1 Fly stocks

All fly strains used in Harmansa *et.al.* are listed in the methods section of the publication. Besides these the following lines were used:

UAS::dppRNA	Expresses dsRNA for RNAi of *dpp*. Bloomington stock number 33618, insertion on the 3rdchromosome.
Wg::GFP	Endogenous GFP-tagged Wg obtained from Simon Bullock [175]

3.2 Immunofluorescence

3.2.1 Standart immunostaining protocol for wing imaginal discs

Procedure Dissection was performed in ice cold PBS. Larvae were cut in the middle and the anterior part was inverted to expose the imaginal discs, which are attached the the larval cuticle. The whitish fat tissue was removed as much as possible. Dissected larvae were fixed in PBS fixative for 20 min. at RT, rinsed three times in PBT and washed four times in PBT for 15min. at RT on a rotor. After blocking in PBTN for 30 min. rotating at RT, the tissue was incubated with primary antibody in PBTN overnight at 4°C. The next day larvae were rinsed three times in PBT, followed by six washes in PBT for 15 min. Secondary antibody incubation was done in PBTN at RT for 1.5h. Afterwards, larvae were again rinsed three times with PBT and washed six times 15min in PBT at RT. Finally, all PBT was removed and discs were mounted in two drops of Vectashield fluorescent mounting medium (H-1000, Vecta Laboratories U.S.).

Solutions

10x PBS	2g KH_2PO_4, 1.25ml 10N NaOH, 80g NaCl, 2g KCl, 6.1g Na_2HPO_4, fill up to 1L with H_2O
PBS fixative	1x PBS + 4% Paraformaldehyde
PBT	1x PBS + 0.3% Triton-X100 (Sigma-Aldrich, Switzerland)
PBTN	PBT + 2% Normal Donkey Serum (Jackson Immuno Research)

3.2.2 Extracellular GFP immunostaining protocol for wing imaginal discs

Procedure Larvae were dissected in ice cold Schneider's Insect Medium (Sigma-Aldrich, Switzerland), followed by incubation in primary antibody (1:200 for α-GFP, Abcam ab6556) in Schneider's Insect Medium on ice for 1h (shaking occasionally). Incubation on ice is meant to reduce uptake of primary antibody in vesicular structures. Dissected discs were rinsed three times with ice cold PBS to wash off exessive antibody and fixed for 20 min at RT in PBS fixative. After four rinses with PBT and one wash in PBT for 20 min at RT tissue was blocked in PBTN for 2min at RT. After blocking tissue was either incubated in α-Wg/Ptc antibodies in PBTN for 1.5h at RT, subsequently rinsed three times in PBT and washed six times with PBT or directly incubated with secondary antibody in PBTN for 1.5h at RT. This was followed by

three rinses in PBT and three washes in PBT for 20 min each. Finally, PBT was removed and discs were mounted in Vectashield fluorescent mounting medium (H-1000, Vecta Laboratories U.S.).

Solutions

10x PBS	2g KH_2PO_4, 1.25ml 10N NaOH, 80g NaCl, 2g KCl, 6.1g Na_2HPO_4, fill up to 1L with H_2O
PBS fixative	1x PBS + 4% Paraformaldehyde
PBT	1x PBS + 0.3% Triton-X100 (Sigma-Aldrich, Switzerland)
PBTN	PBT + **5**% Normal Donkey Serum (Jackson Immuno Research)

3.2.3 Antibodies

All antibodies used in Harmansa *et.al.* are listed in the methods section of the publication. gp α-Dll was used preabsorbed at 1/2000 dilution (a gift from Carlos Estella).

3.3 Generation of transgenic flies

3.3.1 Cloning of EGFP::Dpp and vhhGFP4::CD8::mCherry contructs

pUASTLOTattB_EGFP::Dpp
In the Dpp-GFP plasmid obtained from S. Cohen, we replaced the GFP with EGFP. Then, we inserted the EGFP::Dpp in the multiple cloning site of the pUASTLOTattB vector [176] using standard cloning procedures.

pUASTLOTattB_VHH-GFP4::CD8::mCherry
In the pUAS::CD8::GFP plasmide [177] we inserted the vhh-GFP4 fragment between the signal peptide and the coding sequence of the mouse CD8 protein. Since we wanted to use this construct in combination with EGFP::Dpp, we replaced the GFP by a mCherry (Clonetech). Finally, the vhh-GFP4::CD8.mCherry fragment was cloned into the multiple cloning site of the pUASTLOTattB vector [176].

pUASTattB_VHH-KDRL
The signal peptide of CD8 was fused to the vhhGFP4 fragment and the KDRL sequence (AAGGACGAGCTG) [178] was inserted c-terminally to vhhGFP4. Finally, the construct was cloned into pUASTattB [179].

3.3.2 Transgenesis using the attB/attP system

For generation of transgenic flies we used the attB/attP system developed by Bischof et.al.[179]. For injection in wild type background flies homozygous for attP 35B landing site on the second and the ΦC31 integrase on the first chromosome were used. In order to create fly lines carrying these constructs in *dpp* mutant background, the attP 35B landing site was recombined with either the dpp^{d8} or dpp^{d12} mutant allel and balanced over CyO and carrying the ΦC31 integrase on the first chromosome. For injection endotoxin free plasmid DNA was prepared using the Nucleo Bond Xtra Midi

Plus EF kit (Macherey-Nagel). Endotoxin free DNA was used at 300ng/µl concentration and centrifuged at 4°C max. speed for 30 min. before injection and subsequently kept on ice. Embryos of above described genotypes were collected on grape juice plates with some yeast paste, dechorionized in 3.5% sodium hypochloride solution (2 min.), aligned and transferred onto a glass slide using embryo glue. Embryo glue is obtained by dissolving the glue of adhesive tape in heptane. Aligned embryos were dried with a standard cold-air hair dryer for 5 min., covered with VOLTALEF H10S oil (ATOFINA) and injected with the DNA solution (300ng/µl) into the posterior end. Freshly injected embryos were kept at 18°C for one day and then transferred to 25°C until hatching. Adult survivors were crossed with balancer flies (w ; IF / CyO ; TM3 / TM6) and the progeny was screened for w^+ eye colour, indicating successful germ line transformation.

3.3.3 Removal of either UAS or LOP sites

The resulting fly lines respond to LexA[86] and Gal4[85] transcriptional activators. In order to excise either the UAS or the LOP site in a mutually exclusive manner flies were crossed to flies carrying the Cre^y recombinase. Resulting fly lines either respond to Gal4 or LexA transcriptional activator. The response was either screened for by transgene expression, crossing the resulting lines to Gal4 and LexA driver lines, or by PCR as described in Kanca *et.al.*[176]. For PCR screening, we extracted DNA from single flies (see protocol below) which was used as a PCR template using the following primers:

Lex	5' GCT AGC GGA TCC TAA TCT TAC CTC G 3'
UAS	5' GTT ATG CCT GCA GGT CGG 3'
HS_linker_rev	5' GGA GAG AAC TCT GAA TAG GGA ATT GG 3'

Excision of the LOP site (UAS site present) results in a ~420bp band using primers UAS + HS_linker_rev, whereas excision of the UAS site (LOP site present) results in a ~500bp band using primers Lex + HS_linker_rev. Using this approach allowed us to generate Morphotrap lines that either respond to both Gal4 and LexA (LOP/UAS-morphotrap), only to LexA (LOP-morphotrap) or only to Gal4 (UAS-morphotrap).

3.3.4 Single fly DNA extraction

Squishing buffer:

- 970µl ddH_2O
- 10µl 1M Tris-HCl (pH 7.5)
- 5µl 500mM EDTA (pH 8.0)
- 5µl 5M NaCl
- 10µl proteinase K (20µg/µl)

Single anesthetized flies (kept over CO_2 for several minutes) are transferred into PCR tubes and crushed using a pipet tip loaded with 50µl of squishing buffer. Once crushed,

the squishing buffer is expelled and mixed with the crushed fly by pipetting up and down several times. For protein degradation this mixture is incubated for 30 min. at 37°C, followed by 2 min. at 95°C for heat-inactivation of proteinase K. 1µl of this mixture was used as PCR template. Extracted DNA can be stored at 4°C for up to one month.

3.4 Staging of *Drosophila* larvae and generation of quantitative data sets

3.4.1 Staging of embryos and collection of larvae

Fly stocks used for experiments were feed well over several generations to ensure that flies are in good shape, reducing variability in offspring size. For embryo collections flies were kept in standard fly vials (with polenta and yeast). Best results were obtained under non-crowded conditions with ~30-40 female and ~10 male flies per tube. Crosses were preferentially set a few days before the actual collection. Before collection flies were anesthetized over CO_2 for 3 min. and afterward allowed to recover for minimum 30 min. The CO_2 anesthetization is meant to relax abdominal muscles of females flies, allowing deposition of old eggs, as described in Hamaratoglu *et.al.*[164]. Embryo were collected and grown in an incubator at 26°C. When larvae had reached the stage of interest, they were dissected, stained and processed according to the protocols in 3.2.1 and 3.2.2. Since only larvae older than approximately 100h AEL crawl out of the food, we used 30% Glycerol, which makes larvae float and easy to collect. Whenever genotypes were clearly distinguishable from each other under the microscope, larvae of different genotypes were processed and stained in the same tubes to further reduce variation. Dissected larvae were stained for the targets of interest, Wg and Ptc. The later two markers were used as landmarks that marks the A/P (Ptc) and the D/V boundary (Wg).

3.4.2 Mounting and imaging of quantitative data sets

To minimize variation, all wing discs of one data set were mounted on the same slide, using larval brains as spacers. Imaging was done using a Leica SP5 confocal microscope (40x oil objective). Stacks were aquired with 1µm distance between single slices. For each data set aquired we tested if imaging conditions were within the linear imaging range. To do so, a dilution series of the secondary antibody in Vectashield was imaged with the identical setting used to image the data set. A slide only containing Vectashield was imaged as background measurement. In ImageJ mean intensities of the different dilutions were computed using the histogram function on the average projection of 10 consecutive slices. After subtraction of the background value, mean intensities were plotted against the relative concentration in Excel software (Microsoft). If imaging conditions are within the linear range, fluorescence intensities are proportional to secondary antibody concentration, i.e. they fall on a straight line when plotted against secondary antibody concentration.

Further computation was done in ImageJ using the WingJ plug-in [180] (http://

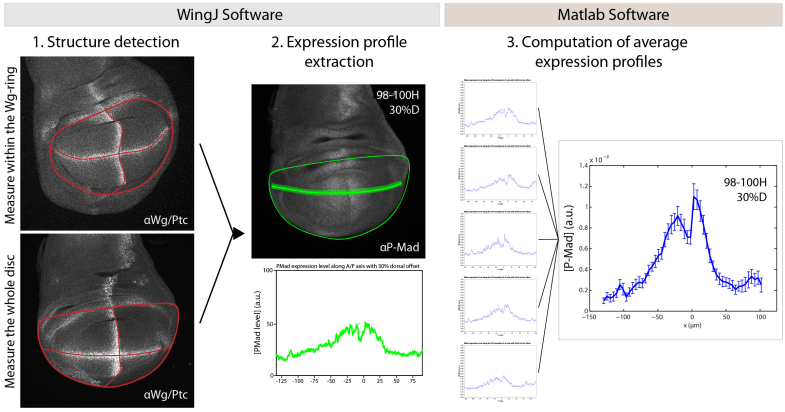

Figure 11: Computation of average concentration profiles
1, The ImageJ plug in WingJ semi-automatically detects the A/P and D/V boundary and the pouch outlines (1 top). To extract profiles, the area of interest can be expanded manually to the whole disc width (1 bottom). **2**, Using the before computed structure model, concentration profiles are extracted parallel to the D/V boundary. **3**, Single profiles are fused to an average concentration profile in Matlab.

---

lis.epfl.ch/wingj). WingJ allows a semi-automated detection of the wing pouch structure using the pattern of the Wg/Ptc staining (see Fig.11-1 top). However this allows only to extract and measure protein levels within the pouch region of the disc. Especially for visualization of Brk concentrations (which are highest at the lateral edges of the wing disc) concentration profiles covering the whole disc primordium are advantageous. We therefore manually expanded the are of measurement to the whole width of the wing disc (see Fig.11-1 bottom). Using this structure "model" WingJ can extract concentration profiles at different distances, parallel to the D/V boundary (Fig.11-2). For the EGFP::Dpp rescued genotypes we obtained the best profiles measuring with a 30% dorsal offset. In a final step, single profiles were computed in Matlab software (MathWorks) using the benchmark_expression_profile.m script to create average concentration profiles (Fig.11-3).

4 Results

The results of this study concerning the impact of Dpp spreading on wing disc growth control were released in the interdisciplinary journal Nature and the results of the publication are found in the following section. In addition, some unpublished results investigating the impact of Dpp originating from the posterior edge of the wing disc on growth control are included in section 4.2.1. We also tested the dependence of the expression of the inhibitory Smad Dad on the spreading of Dpp in section 4.2.2. In order to illustrate the diverse use of the morphotrap technique for developmental biology, I also tested the requirement for Wg spreading on pattering and size control using morphotrap. Finally, I will show preliminary results on the characterization of a morphotrap construct localized to the endoplasmic reticulum and its use in blocking morphogen secretion, and hence signalling. These results are found in section 4.3.

4.1 Publication - Dpp spreading is required for medial but not for lateral wing disc growth

---

Stefan Harmansa[1], Fisun Hamaratoglu[2], Markus Affolter[1*] & Emmanuel Caussinus[1,3*]
[1]Growth & Development, Biozentrum, Klingelbergstrasse 50/70, University of Basel, 4056 Basel, Switzerland.
[2]Center for Integrative Genomics, University of Lausanne, 1015 Lausanne, Switzerland.
[3]Institute of Molecular Life Sciences (IMLS), University of Zurich, 8057 Zurich, Switzerland.

Abstract

Drosophila Decapentaplegic (Dpp) has served as a paradigm to study morphogen-dependent growth control. However, the role of a Dpp gradient in tissue growth remains highly controversial. Two fundamentally different models have been proposed: the 'temporal rule' model suggests that all cells of the wing imaginal disc divide upon a 50% increase in Dpp signalling, whereas the 'growth equalization model' suggests that Dpp is only essential for proliferation control of the central cells. Here, to discriminate between these two models, we generated and used morphotrap, a membrane-tethered anti-green fluorescent protein (GFP) nanobody, which enables immobilization of enhanced (e)GFP::Dpp on the cell surface, thereby abolishing Dpp gradient formation. We find that in the absence of Dpp spreading, wing disc patterning is lost; however, lateral cells still divide at normal rates. These data are in line with the growth equalization model, but do not fit a global temporal rule model in the wing imaginal disc.

Introduction

Morphogens regulate patterning and growth of tissues and organs by forming long-range gradients from regions of high concentration (the source) to regions of low concentration (the adjacent target field)[1–5]. In *Drosophila*, the vertebrate bone morphogenetic protein (BMP)2/4 homologue Dpp is studied extensively in the wing imaginal disc. This larval precursor of the fly wing is subdivided into an anterior and a posterior compartment[6,7]. Dpp is expressed in a stripe of anterior cells adjacent to the compartment boundary[8], forming long-range anterior and posterior extracellular gradients in the target field[9–11]. The Dpp gradient is transduced by its receptors Thickveins (Tkv)[12] and Punt[13] and translated into an intracellular gradient of phosphorylated Mothers against dpp (p-Mad)[14]. Dpp signalling suppresses transcription of *brinker* (*brk*)[15–17], a repressor of Dpp target gene transcription[14] and a repressor of growth[18]. This results in high p-Mad levels (high Dpp signalling) in the medial region of the wing disc and high Brk levels (low Dpp signalling) in the lateral region of the wing disc. The interplay of p-Mad and Brk coordinates the expression profiles of other Dpp targets, such as *spalt* (*sal*), *optomoter blind* (*omb*; also known as *bifid*) and *daughters against dpp* (*dad*)[19–21]. In addition to its role in patterning, Dpp is a key regulator of growth; overexpression of Dpp promotes wing disc overgrowth[22,23], while dpp mutant wing discs remain very small[24].

To our knowledge, the requirement for Dpp spreading has never been explicitly tested by, for example, blocking Dpp dispersal by tethering it to the cell membrane, as has been done for the Wingless (Wg) morphogen[25–27]. The available experimental evidence strongly supports an instructive and essential role for Dpp spreading in the control of patterning (reviewed in refs 14, 28, 29). However, the role of Dpp spreading in growth control is highly controversial[5,28,30,31]. Two major models have been suggested to explain how the Dpp gradient controls uniform proliferation and growth of the wing disc. One model, the temporal rule, suggests that all cells of the wing imaginal disc compute the level of Dpp and divide upon a 50% increase in Dpp signalling. In contrast, the growth equalization model proposes that Dpp sustains the proliferation of medial cells by the removal of the growth repressor Brk, while the proliferation rate of lateral cells is limited by Brk to rates that can be sustained by medial cells, resulting in a uniform proliferation profile along the wing disc tissue[28,32–34]. In the growth equalization model, the Dpp/Brk system is not a growth promoter but is rather a growth-modulatory system, ironing out inherent regional differences in proliferation rates[32]. To study the role of Dpp spreading in wing disc patterning and growth better, we designed and experimentally established a novel approach to manipulate morphogen spreading *in vivo*.

Nanobody-mediated morphogen trapping

To manipulate the Dpp gradient *in vivo*, we designed and implemented a synthetic morphogen trapping system consisting of a GFP-tagged morphogen (in our case, eGFP::Dpp) and a generic extracellular GFP trap (VHH-GFP4::CD8::mCherry; referred to as morphotrap) (Fig. 1a). Our eGFP::Dpp construct is based on a previously published fusion protein[9] and was implemented as a LexA inducible transgene (see

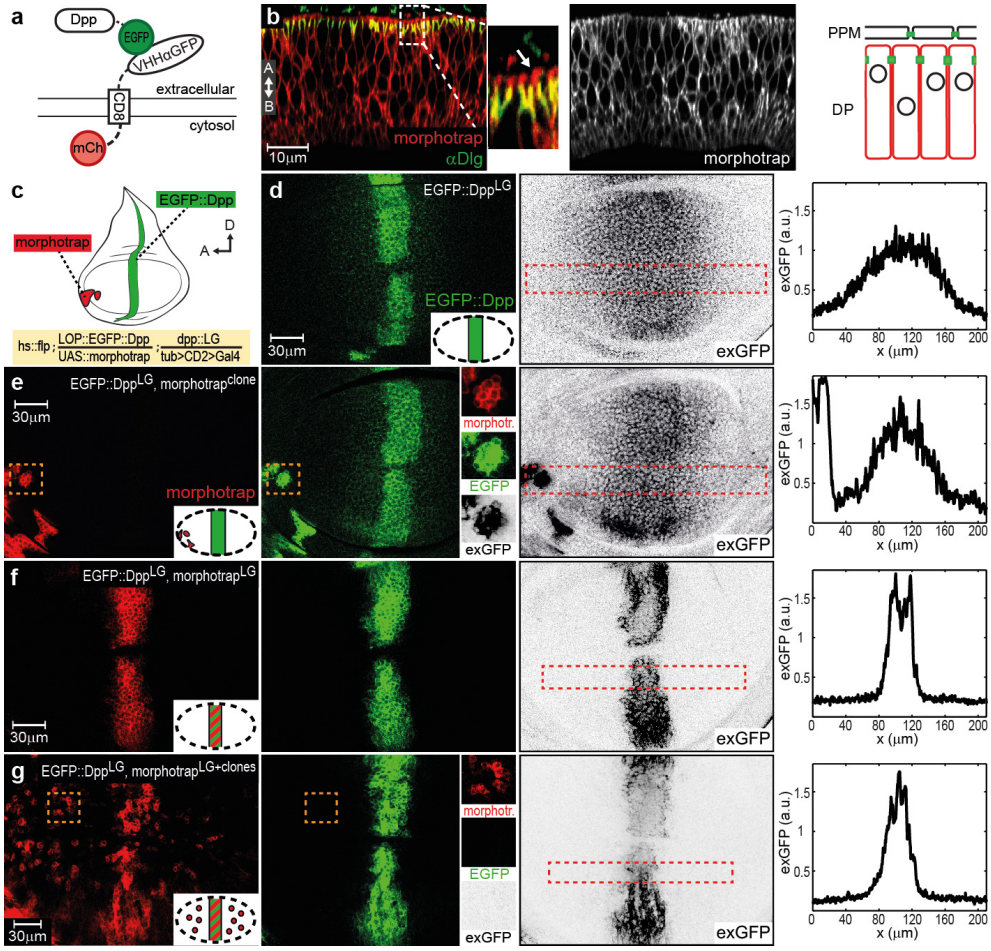

Figure 1 - Morphotrap can block eGFP::Dpp spreading.
a, The morphotrap system. **b**, Optical cross-section (left, middle) and schematics (right) along the apical-basal (A-B) axis of a wing disc expressing morphotrap in the wing pouchdisc proper (DP) cells only (*nubbin::Gal4*). Morphotrap is localized all along the cell membrane (in red), both apical (arrow) and basal to the junctional marker Discs-large (Dlg; in green). Peripodial membrane (PPM). **c**, Schematic representation of eGFP::Dpp (LexA/LOP) and morphotrap clones (Gal4/UAS). For all discs anterior (A) is oriented to the left and dorsal (D) is oriented to the top. **d**, A wild-type wing disc expressing eGFP::Dpp in the Dpp stripe (*dpp::LG*), visualized by eGFP fluorescence (left) or by extracellular GFP staining (exGFP) (middle). Fluorescence intensity profile of the region marked by a red rectangle (right). a.u., arbitrary units. **e**, Lateral morphotrap clones trap extracellular eGFP::Dpp. **f**, Gradient formation is blocked by co-expression of eGFP::Dpp and morphotrap in the Dpp stripe (both expressed by *dpp::LG*). **g**, Co-expression of eGFP::Dpp and morphotrap in the stripe fully blocks Dpp spreading since additional morphotrap clones do not show eGFP signal (see insets in second panel from the left).

Methods and Extended Data Fig. 1a). Morphotrap (VHH-GFP4::CD8::mCherry) represents a fusion protein consisting of an extracellular, single-domain nanobody against GFP[35] (and cognate fluorescent tags, including eGFP), followed by the mouse CD8 transmembrane domain and a cytoplasmic mCherry fluorescent tag. Morphotrap was implemented as a Gal4-inducible transgene as well as a LexA-inducible transgene (see Methods). The principle idea behind morphotrap is to immobilize the extracellular fraction of eGFP::Dpp in *Drosophila* tissues in a controlled spatial manner, either in the presence or the absence of wild-type Dpp (Fig. 1a).

Expression of eGFP::Dpp by the *dpp-LG* LexA driver line in a $dpp^{d8/d12}$ mutant background restored proper Dpp signalling in the wing tissue such that the size and pattern was rescued to a large extent and adult flies developed (Extended Data Fig. 1). These results show that our eGFP::Dpp fusion protein acts as a good surrogate for Dpp in the wing disc.

Morphotrap localizes along the basolateral and apical surface of wing disc cells (Fig. 1b), and does not interfere with Dpp signalling or cell survival when expressed at high levels (Extended Data Fig. 2a–e). Therefore, morphotrap can be expressed at high levels and accumulates around the expressing wing disc cells without interfering with cell division and patterning.

Morphotrap can modify the Dpp gradient

We then tested whether exposing morphotrap on the cell surface locally modified the extracellular concentration of eGFP::Dpp. We generated random small clones of morphotrap in wild-type wing discs expressing eGFP::Dpp in the domain of *dpp* transcription. To set apart the induced morphotrap clones from the cells expressing eGFP::Dpp, we used Gal4 and LexA drivers to induce morphotrap and eGFP::Dpp, respectively (Fig. 1c; see Methods). In control discs, in which no clones were generated, eGFP::Dpp formed a bilateral extracellular concentration gradient visualized by sensitive extracellular immunostainings against eGFP (Fig. 1d). The eGFP signal dropped below detection levels at a distance of approximately 60 µm from the medial eGFP::Dpp source. In discs in which small clones expressing morphotrap had been generated, we detected high levels of extracellular eGFP::Dpp coating the surface of the clone cells, even when the clones were located in regions in which eGFP::Dpp was not detected otherwise (Fig. 1e). These results show that morphotrap is able to sequester extracellular eGFP::Dpp, even in areas of low or non-detectable eGFP::Dpp.

Trapped eGFP::Dpp was active in signalling, since morphotrap clones located in the lateral region of the disc showed increased p-Mad levels, mainly along the edge facing the eGFP::Dpp source (Extended Data Fig. 2f, g). The results show that eGFP::Dpp disperses over the entire width of the disc, although its levels cannot normally be detected above background levels in the lateral regions using fluorescent microscopy (see also ref. 30). We conclude that eGFP::Dpp can interact with its receptors when bound to the cell surface by morphotrap and that lateral cells can respond to Dpp.

To investigate whether morphotrap was able to interfere with the formation of the extracellular concentration gradient of eGFP::Dpp when expressed in the source

cells, we expressed both eGFP::Dpp and morphotrap in wild-type wing discs in the domain of *dpp* transcription. Under these conditions, we did not detect any dispersal of eGFP::Dpp using antibody staining (Fig. 1f), suggesting that eGFP::Dpp cannot leave the source region owing to tethering to secreting cells. Furthermore, clones expressing morphotrap in lateral cells did not accumulate any eGFP::Dpp on the cell surface in these conditions, neither did clones in the vicinity of the eGFP::Dpp source (Fig. 1g, middle; see insets). These results demonstrate that morphotrap fully retains eGFP::Dpp on source cells and completely abolishes the formation of the extracellular concentration gradient of eGFP::Dpp.

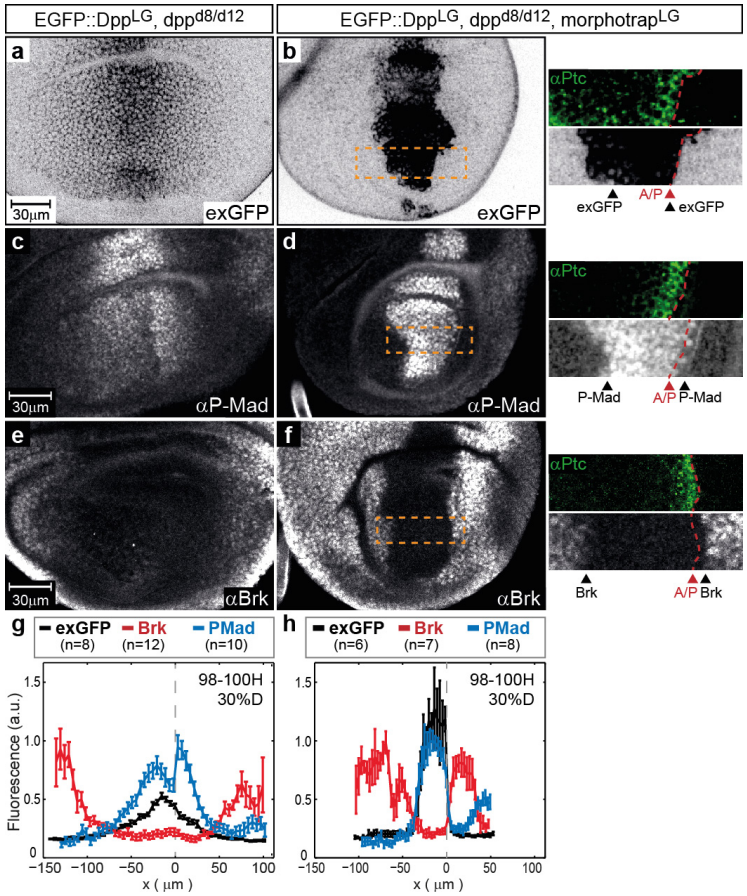

Figure 2 - Blocking Dpp spreading results in a sharp p-Mad/Brk transition. **a**, Representative $dpp^{d8/d12}$ mutant wing disc rescued with eGFP::Dpp (rescue) and stained for exGFP (grey). **b**, Left, exGFP signal in a disc co-expressing eGFP::Dpp and morphotrap (*dpp-LG*, co-expression) in a $dpp^{d8/d12}$ mutant. Right, magnification of the region marked by the rectangle on the left, showing that all signal is from anterior cells where Dpp is expressed. A/P boundary is determined by Ptc staining (green) and marked by a dotted line. Approximate domain size is marked by arrowheads. **c**, **d**, p-Mad staining in rescue (**c**) and co-expression (**d**) wing discs. **e**, **f**, Brk staining in rescue (**e**) and co-expression (**f**) wing discs. **g**–**f**, Average fluorescence intensity profiles of 98-100h after egg laying (AEL) old larvae measured to the edge of the wing disc of rescued (**g**) and co-expression (**h**) wing discs. Profiles were measured with 30% dorsal (D) offset parallel to the dorso/ventral (D/V) boundary (see Methods for details). Error bars show standard deviation (s.d.).

Dpp spreading is required for patterning

The function of *dpp* for patterning the wing disc has been studied extensively[11,36,37]. However, how a loss of Dpp spreading would affect target gene expression has not been tested directly. To compare Dpp signalling responses in control $dpp^{d8/d12}$ wing discs rescued by eGFP::Dpp (eGFP::Dpp gradient is present) to Dpp signalling responses in $dpp^{d8/d12}$ wing discs expressing both eGFP::Dpp and morphotrap in the expression domain of dpp (eGFP::Dpp gradient is absent; Methods and Fig. 2), we performed immunostainings against p-Mad, Brk, Sal and Omb. In control discs, p-Mad, Sal and Omb formed three bilateral gradients of different widths, Sal being the narrowest and Omb being the widest (Fig. 2c, g and Extended Data Fig. 3a); Brk was only detected in the most lateral regions of the discs (Fig. 2e, g). In contrast, when eGFP::Dpp and morphotrap were co-expressed, Dpp spreading and hence gradient formation was fully blocked throughout development (Extended Data Fig. 4a–c). In these discs, the p-Mad, Sal and Omb gradients collapsed in the posterior compartment to a single row of cells abutting the anterior source of eGFP::Dpp (Fig. 2d, h and Extended Data Fig. 3b); high levels of Brk were detected in the posterior compartment up to the source of Dpp, except for a single row of cells abutting the compartment boundary (Fig. 2f, h). Similar results were obtained regarding target gene expression in the anterior compartment upon trapping eGFP::Dpp in source cells (Fig. 2h and Extended Data Fig. 3). In addition, we inhibited eGFP::Dpp dispersal in posterior cells only (Extended Data Fig. 5); under these conditions p-Mad failed to form a posterior long-range gradient and both Sal and Omb expression collapsed onto the narrow p-Mad domain. Hence, wing disc patterning in the posterior compartment was abolished (Extended Data Fig. 5a–f). Wings of flies with blocked or reduced Dpp spreading lacked proper wing vein patterning (Extended Data Figs 3f and 9d, f). Altogether, these results show that dispersal of Dpp is strictly required for the patterning function of Dpp.

Dpp spreading and growth control

Despite numerous studies addressing the role of Dpp in the control of growth of the wing imaginal disc, the conclusions drawn from different sets of experiments have remained controversial. In the temporal rule model[30,38], all disc cells compute the increase in Dpp levels and divide upon a gain of 50%. In sharp contrast, the growth equalization model[28] proposes that lateral cells proliferate independently of Dpp (Fig. 3a). In line with this later model, Dpp signalling has been blocked in regions outside of the wing pouch in several studies, without much effect on cell proliferation[39,40]. However, it has not been possible to directly modulate the Dpp gradient at the protein level until now, making it difficult to interpret the requirement of Dpp long-range function in growth control.

To discriminate between these two growth control models, we aimed at using a different experimental approach, directly eliminating the Dpp gradient at the protein level using morphotrap. As described earlier, the elimination of the gradient leads to the absence of Dpp signalling, that is, the target genes *sal* and *omb* are not expressed in the wing epithelium beyond the source cells and the immediate neighbours, and the

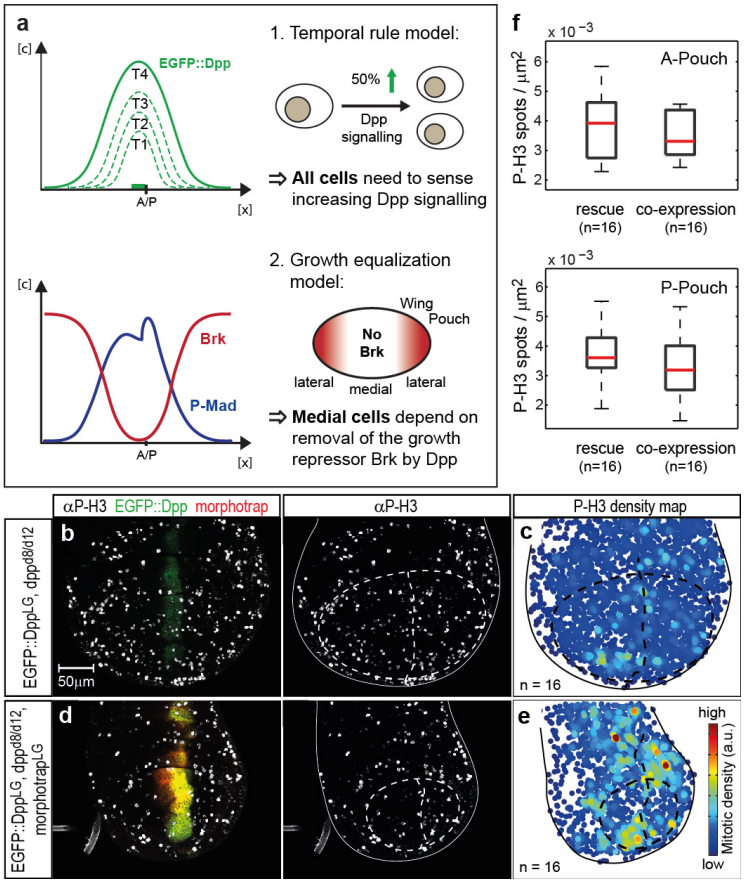

Figure 3 - The uniform proliferation pattern is independent of Dpp spreading. **a**, Top, the temporal rule model of growth control. Bottom, the growth equalization model. **b**, p-H3 staining in a representative $dpp^{d8/d12}$ mutant wing disc rescued with eGFP::Dpp. The A/P boundary and the pouch outline are marked by dotted lines (right). **c**, **e**, Computed p-H3 spots density (of $n = 16$ discs) in rescue (**c**) and co-expression (**e**) wing discs (see Methods). **d**, p-H3 signal in a $dpp^{d8/d12}$ mutant wing disc co-expressing eGFP::Dpp and morphotrap. **f**, Mitotic density in the anterior ($P > 0.05$) and posterior pouch ($P > 0.05$); whiskers correspond to minimum and maximum data points.

Brk repressor is present at high levels in all cells beyond the Dpp source. We thus compared the proliferation pattern of control $dpp^{d8/d12}$ wing discs rescued by eGFP::Dpp to the proliferation pattern of $dpp^{d8/d12}$ wing discs expressing both eGFP::Dpp and morphotrap in the expression domain of *dpp*, that is, we compared the growth rates of wing disc cells in the presence and in the absence of eGFP::Dpp spreading. We visualized the proliferation pattern of such wing discs by staining for phospho-histone H3 (p-H3), a marker for mitotic cells. In wild-type wing discs, cell proliferation was shown to be rather homogeneous in third instar wing discs[7,41,42]. Our quantitative analyses showed that in discs rescued with eGFP::Dpp, the proliferation profile was also uniform (Fig. 3b, c). Interestingly, blocking Dpp spreading neither affected the uniform proliferation pattern (Fig. 3d, e) nor did we detect significant changes in the mitotic density in wing imaginal discs during the observed developmental stages (Fig. 3f and Extended Data Fig. 4g–i).

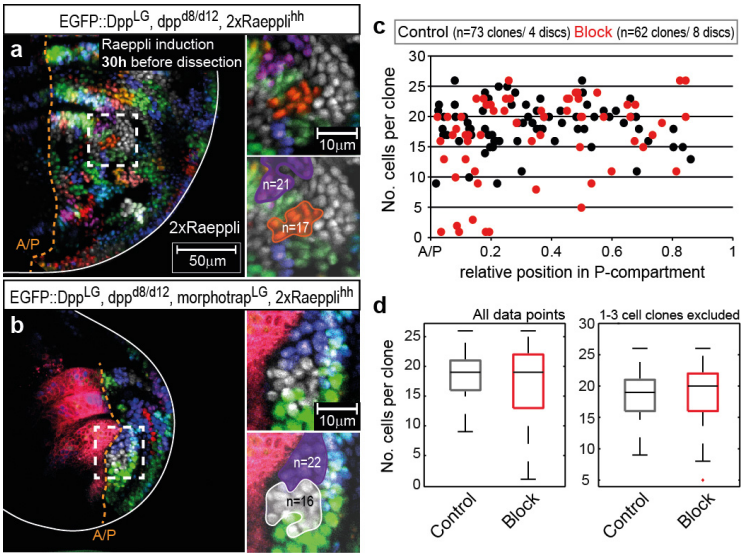

Figure 4 - Block of Dpp spreading does not affect clonal proliferation rates. **a–d**, To estimate clonal proliferation rates in the posterior compartment, Raeppli was induced 30 h before dissection (66–70 h AEL) and larvae were dissected at 96–100 h AEL. **a**, Control disc. **b**, Disc with blocked Dpp spreading. **c**, Cell numbers per clone were counted and plotted against the relative position in the posterior compartment (0 corresponding to the A/P boundary and 1 to the posterior edge of the disc). **d**, Boxplots showing the number of cells per clone for all data points (left plot, $P > 0.05$) or when the 1–3 cell clones are excluded (right plot, $P > 0.05$).

To obtain a more global and more quantitative view of the cell division patterns, we used the whole-tissue labelling tool Raeppli[43] to induce differently marked clones in control wing discs and in wing discs in which Dpp spreading was blocked by morphotrap (Fig. 4 and Extended Data Fig. 6). To compare the proliferation rates in the presence or absence of Dpp spreading, we induced colour selection in clones at different time points of development and quantitatively evaluated the resulting clone size after defined time points (number of cells per clone). In control wing discs, clonal growth rates were homogeneous along the anterior–posterior (A/P) axis (Fig. 4c, black dots). When Dpp spreading was blocked, we observed that the majority of clones showed similar growth rates to control clones, and we did not find a significant difference in clonal proliferation between controls and discs with blocked Dpp spreading (Fig. 4d). However, with blocked Dpp spreading, we also found low numbers of small clones (1–3 cells) next to the A/P boundary (Extended Data Fig. 7). These small clones were not found in control discs, in which Dpp spreading was normal. The presence of such small clones might hint towards the fact that a subpopulation of wing disc cells depend on Dpp signalling to divide and/or survive.

Both the p-H3 data and the Raeppli results demonstrate that the cells in the lateral Brk domain do not depend on Dpp spreading to proliferate (in contradiction with the temporal rule model), but rather that the proliferation rate is set by a Dpp-independent system (in line with the growth equalization model).

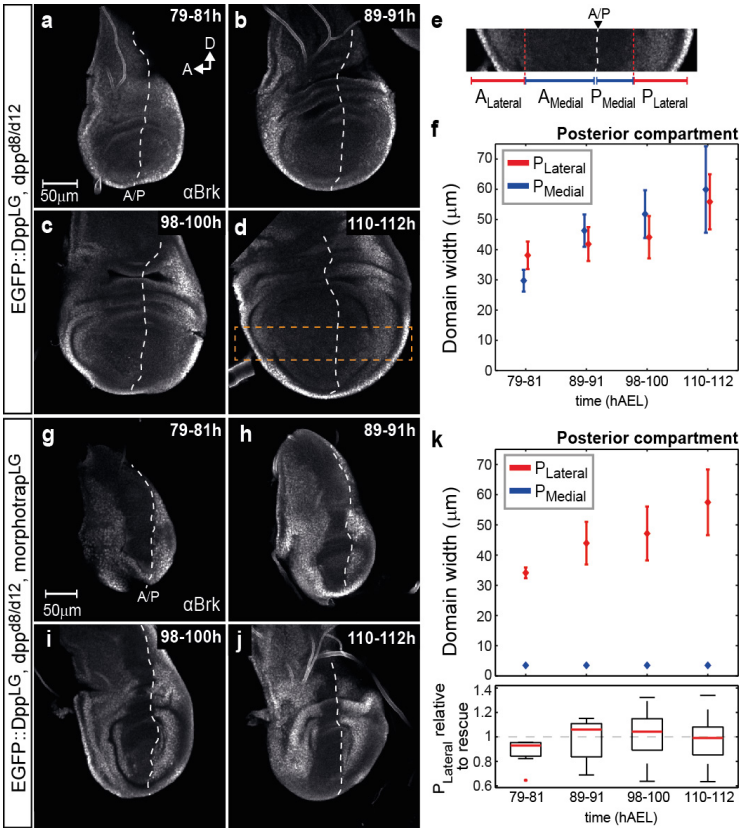

Figure 5 - The development of the medial but not the lateral wing disc requires Dpp spreading.
a–**k**, Data set from 79–112 h AEL stained for Brk. **a**–**d**, Representative rescued wing discs of four time points investigated. e, Magnification of area marked in **d**, visualizing the location of medial (high Dpp signalling) and lateral (low Dpp signalling) domain (see Methods). **f**, Temporal development of domain width in the posterior compartment in rescued discs. **g**–**j**, Representative co-expression wing discs. **k**, Temporal development of domain width in co-expression wing discs, and size change of the lateral domain relative to control discs (rescue $n = 34$, co-expression $n = 37$). **f**, **k**, Error bars show s.d.

Dpp spreading and size control

Using morphotrap in *dpp* mutant flies also allowed us to address how long-range spreading of Dpp affects wing disc size control. We quantified and compared the temporal growth profile of the posterior compartment of control $dpp^{d8/d12}$ wing discs rescued by eGFP::Dpp to the growth profile of $dpp^{d8/d12}$ wing discs co-expressing both eGFP::Dpp and morphotrap in the expression domain of *dpp*. We performed immunostainings against Brk at different time points between 80 and 112 h after egg laying (AEL). In control discs, the posterior compartment doubled in width during the observed time window (Fig. 5a–d and Extended Data Fig. 8d). We delimited a medial low Brk (indicating high Dpp signalling) zone and a lateral high Brk (indicating low Dpp signalling) zone (Fig. 5e; see Methods); both zones increased in width at the same speed, keeping a constant relative proportion of 1:1 (Fig. 5f), consistent with published data[44]. In discs in which spreading of Dpp was abolished, the low

Brk zone in the centre of the disc was reduced to a single medial row of cells in the posterior compartment (see earlier and Fig. 5g–j). During the observed time window, the lateral part of the posterior compartment showed similar widths and width increases as the lateral high Brk zone of the posterior compartment of control discs (Fig. 5k). Similar growth profiles were seen in discs expressing eGFP::Dpp in the source stripe and morphotrap in the posterior compartment (Extended Data Fig. 5g). These results demonstrate that growth in the lateral region of the wing disc is independent of the extracellular Dpp gradient and does not depend on the dynamics of Dpp signalling. In support of this finding, similar growth dynamics were observed for the anterior compartment (Extended Data Fig. 8a, b).

In contrast, the medial, Brk-negative region is lost when Dpp spreading is blocked, suggesting that Dpp dispersal is important for growth control of the medial region, in particular in the central wing pouch area. We therefore quantified wing pouch size using the inner Wg-expression ring as a pouch marker. We measured the size of the pouch in *dpp* mutant discs rescued with eGFP::Dpp, and compared it to the pouch of discs in which either eGFP::Dpp dispersal was hindered in the posterior compartment only, or in which the release of eGFP::Dpp from the anterior source was completely blocked (Extended Data Fig. 9). Upon hindering Dpp spreading in the posterior compartment, the size of the posterior pouch was reduced by approximately 40%. Strikingly, when we trapped eGFP::Dpp in the source, the size of the posterior wing pouch was even further reduced (by more than 60%). These results indicate that eGFP::Dpp spreading is essential for wing pouch growth. The analyses using the whole-tissue labelling technique Raeppli (Extended Data Fig. 7) further showed that small clones were found in the posterior compartment close to the compartment boundary when morphotrap is expressed in source cells. Such clones were not found in control discs. Together, these data show that Dpp signalling has an important role in proliferation control of medial wing pouch cells, as indicated by earlier studies[33,39,40], and further suggest that the range of Dpp spreading might be crucially linked to the size of the wing pouch region along the A/P axis.

Discussion

We used morphotrap, a novel approach to manipulate the extracellular Dpp gradient in the wing imaginal disc. Expressing morphotrap in small clones of lateral wing disc cells captures eGFP::Dpp in regions of the disc in which eGFP::Dpp cannot be detected above background levels. This finding demonstrates that Dpp does disperse over the entire wing imaginal disc, and that low Dpp levels could control cell behaviour even in lateral regions. However, we find that while Dpp spreading is strictly required for wing disc patterning, it is not essential for cell proliferation in the lateral region of the wing disc. These results are in line with the growth equalization model but are in disagreement with a disc-wide temporal rule model, and suggest that lateral cells do not compute Dpp signalling levels to trigger cell division. It has been argued that Dpp-independent Dpp signalling (in addition to Dpp-dependent Dpp signalling) might control cell proliferation according to the temporal rule model[45]. This interpretation was based on the observation that in genetic experiments in which Dpp signalling

was eliminated by the concomitant genetic removal of *brk* and *tkv* (or *brk* and *dpp*), certain Dpp targets were active owing to the absence of the potent Brk repressor[31,38]. However, in our experiments using morphotrap, Dpp signalling was eliminated via the removal of the Dpp gradient and led to the absence of Dpp target gene expression and to the presence of high levels of Brk in the entire lateral wing disc. Therefore, in our experimental setting, Dpp signalling was turned off in the lateral cells, yet these cells divided at a normal rate, as quantitatively shown by our experiments using Raeppli. Since cell division should be abolished (or altered) in the absence of Dpp signalling, according to the temporal rule, our experiments reject a general, disc-wide temporal rule model for wing disc growth control.

However, our data are entirely consistent with the proposal of the growth equalization model, suggesting that Dpp spreading results in medial removal of Brk and that this repression of *brk* represents an essential step in the formation of the wing pouch tissue[33]. Our results support the suggestion made by the growth equalization model that the wing disc tissue consists of two regions with different requirements for Dpp signalling, namely a medial region that depends on Dpp signalling to grow and a lateral region that grows independent of Dpp.

While the growth equalization model does not explain final organ size, our results suggest that the range of Dpp spreading is linked to the size of the wing pouch (albeit not to the entire disc). In a number of elegant studies, the range of Wg signalling was suggested to control pouch growth via a feed-forward recruitment mechanism[27,46], presumably together with Dpp. Interestingly, the replacement of the major endogenous *Drosophila* Wnt, Wg, with one that expresses a membrane-tethered form of the protein, showed that Wg spreading and gradient formation is dispensable for patterning and to some extent for growth of the pouch[26]. In contrast, our results on Dpp strongly support the notion that Dpp spreading is essential for its role in pouch patterning and size control. Getting a better understanding of the control of wing pouch growth will require the combinatorial manipulation of the Dpp and the Wg signalling pathways to study individual pathway outputs as well as their mutual interactions at different time points throughout larval development. Furthermore, it will be of major importance to study the interactions of the morphogen systems with other growth control systems (for example, the insulin–phosphatidylinositol-3-OH kinase and the Hippo pathways) to better understand the control of final organ size[47]. The addition of the morphotrap and the Raeppli techniques to such analyses will help gain better insight into how morphogens control organ growth.

References

1 Ashe, H. L. & Briscoe, J. The interpretation of morphogen gradients. *Development* 133, 385–394 (2006).

2 Baena-Lopez, L. A., Nojima, H. & Vincent, J. P. Integration of morphogen signalling within the growth regulatory network. *Curr. Opin. Cell Biol.* 24, 166–172 (2012).

3 Rogers, K. W. & Schier, A. F. Morphogen gradients: from generation to interpretation. *Annu. Rev. Cell Dev. Biol.* 27, 377–407 (2011).

4 Schwank, G. & Basler, K. Regulation of organ growth by morphogen gradients. *Cold Spring Harb. Perspect. Biol.* 2, a001669 (2010).

5 Wartlick, O., Mumcu, P., Jülicher, F. & Gonzalez-Gaitan, M. Understanding morphogenetic growth control—lessons from flies. *Nature Rev. Mol. Cell Biol.* 12, 594–604 (2011).

6 Martín, F. A., Herrera, S. C. & Morata, G. Cell competition, growth and size control in the *Drosophila* wing imaginal disc. *Development* 136, 3747–3756 (2009).

7 Garcia-Bellido, A. & Merriam, J. R. Parameters of the wing imaginal disc development of *Drosophila melanogaster*. *Dev. Biol.* 24, 61–87 (1971).

8 Masucci, J. D., Miltenberger, R. J. & Hoffmann, F. M. Pattern-specific expression of the *Drosophila decapentaplegic* gene in imaginal disks is regulated by 3´ cis-regulatory elements. *Genes Dev.* 4, 2011–2023 (1990).

9 Teleman, A. A. & Cohen, S. M. Dpp gradient formation in the *Drosophila* wing imaginal disc. *Cell* 103, 971–980 (2000).

10 Entchev, E. V., Schwabedissen, A. & González-Gaitán, M. Gradient formation of the TGF-β homolog Dpp. *Cell* 103, 981–992 (2000).

11 Nellen, D., Burke, R., Struhl, G. & Basler, K. Direct and long-range action of a DPP morphogen gradient. *Cell* 85, 357–368 (1996).

12 Nellen, D., Affolter, M. & Basler, K. Receptor serine/threonine kinases implicated in the control of *Drosophila* body pattern by decapentaplegic. *Cell* 78, 225–237 (1994).

13 Ruberte, E., Marty, T., Nellen, D., Affolter, M. & Basler, K. An absolute requirement for both the type II and type I receptors, *punt* and *thick veins*, for Dpp signaling *in vivo*. *Cell* 80, 889–897 (1995).

14 Affolter, M. & Basler, K. The Decapentaplegic morphogen gradient: from pattern formation to growth regulation. *Nature Rev. Genet.* 8, 663–674 (2007).

15 Jaźwińska, A., Kirov, N., Wieschaus, E., Roth, S. & Rushlow, C. The *Drosophila* gene *brinker* reveals a novel mechanism of Dpp target gene regulation. *Cell* 96, 563–573 (1999).

16 Minami, M., Kinoshita, N., Kamoshida, Y., Tanimoto, H. & Tabata, T. *brinker* is a target of Dpp in *Drosophila* that negatively regulates Dpp-dependent genes. *Nature* 398, 242–246 (1999).

17 Campbell, G. & Tomlinson, A. Transducing the Dpp morphogen gradient in the wing of *Drosophila*: regulation of Dpp targets by *brinker*. *Cell* 96, 553–562 (1999).

18 Doumpas, N. et al. Brk regulates wing disc growth in part via repression of Myc expression. *EMBO Rep.* 14, 261–268 (2013).

19 Barrio, R. & de Celis, J. F. Regulation of *spalt* expression in the *Drosophila* wing blade in response to the Decapentaplegic signaling pathway. *Proc. Natl Acad. Sci.* USA 101, 6021–6026 (2004).

20 Weiss, A. et al. A conserved activation element in BMP signaling during *Drosophila* development. *Nature Struct. Mol. Biol.* 17, 69–76 (2010).

21 Sivasankaran, R., Vigano, M. A., Müller, B., Affolter, M. & Basler, K. Direct transcriptional control of the Dpp target *omb* by the DNA binding protein Brinker. *EMBO J.* 19, 6162–6172 (2000).

22 Capdevila, J. & Guerrero, I. Targeted expression of the signaling molecule decapentaplegic induces pattern duplications and growth alterations in *Drosophila* wings. EMBO J. 13, 4459–4468 (1994).

23 Zecca, M., Basler, K. & Struhl, G. Sequential organizing activities of engrailed, hedgehog and decapentaplegic in the *Drosophila* wing. *Development* 121, 2265–2278 (1995).

24 Spencer, F. A., Hoffmann, F. M. & Gelbart, W. M. Decapentaplegic: a gene complex affecting morphogenesis in *Drosophila melanogaster*. *Cell* 28, 451–461 (1982).

25 Zecca, M. & Struhl, G. Recruitment of cells into the *Drosophila* wing primordium by a feed-forward circuit of vestigial autoregulation. *Development* 134, 3001–3010 (2007).

26 Alexandre, C., Baena-Lopez, A. & Vincent, J. P. Patterning and growth control by membrane-tethered Wingless. *Nature* 505, 180–185 (2014).

27 Zecca, M. & Struhl, G. A feed-forward circuit linking Wingless, Fat-Dachsous signaling, and the Warts-Hippo pathway to *Drosophila* wing growth. *PLoS Biol.* 8, e1000386 (2010).

28 Restrepo, S., Zartman, J. J. & Basler, K. Coordination of patterning and growth by the morphogen DPP. *Curr. Biol.* 24, R245–R255 (2014).

29 Hamaratoglu, F., Affolter, M. & Pyrowolakis, G. Dpp/BMP signaling in flies: from molecules to biology. *Semin. Cell Dev. Biol.* 32, 128–136 (2014).

30 Wartlick, O. et al. Dynamics of Dpp signaling and proliferation control. *Science* 331, 1154–1159 (2011).

31 Schwank, G., Yang, S. F., Restrepo, S. & Basler, K. Comment on "Dynamics of Dpp signaling and proliferation control". *Science* 335, 401 (2012).

32 Schwank, G., Restrepo, S. & Basler, K. Growth regulation by Dpp: an essential role for Brinker and a non-essential role for graded signaling levels. *Development* 135, 4003–4013 (2008).

33 Martín, F. A., Pérez-Garijo, A., Moreno, E. & Morata, G. The brinker gradient controls wing growth in *Drosophila*. *Development* 131, 4921–4930 (2004).

34 Schwank, G. et al. Antagonistic growth regulation by Dpp and Fat drives uniform cell proliferation. *Dev. Cell* 20, 123–130 (2011).

35 Saerens, D. et al. Identification of a universal VHH framework to graft non-canonical antigen-binding loops of camel single-domain antibodies. *J. Mol. Biol.* 352, 597–607 (2005).

36 Lecuit, T. et al. Two distinct mechanisms for long-range patterning by Decapentaplegic in the *Drosophila* wing. *Nature* 381, 387–393 (1996).

37 Müller, B., Hartmann, B., Pyrowolakis, G., Affolter, M. & Basler, K. Conversion of an extracellular Dpp/BMP morphogen gradient into an inverse transcriptional gradient. *Cell* 113, 221–233 (2003).

38 Wartlick, O., Mumcu, P., Jülicher, F. & Gonzalez-Gaitan, M. Response to Comment on "Dynamics of Dpp Signaling and Proliferation Control". *Science* 335, 401 (2012).

39 Martín-Castellanos, C. & Edgar, B. A. A characterization of the effects of Dpp signaling on cell growth and proliferation in the *Drosophila* wing. *Development* 129, 1003–1013 (2002).

40 Burke, R. & Basler, K. Dpp receptors are autonomously required for cell proliferation in the entire developing *Drosophila* wing. *Development* 122, 2261–2269 (1996).

41 Milán, M., Campuzano, S. & García-Bellido, A. Cell cycling and patterned cell proliferation in the wing primordium of *Drosophila*. *Proc. Natl Acad. Sci.* USA 93, 640–645 (1996).

42 Mao, Y. et al. Differential proliferation rates generate patterns of mechanical tension that orient tissue growth. *EMBO J.* 32, 2790–2803 (2013).

43 Kanca, O., Caussinus, E., Denes, A. S., Percival-Smith, A. & Affolter, M. Raeppli: a whole-tissue labeling tool for live imaging of *Drosophila* development. *Development* 141, 472–480 (2014).

44 Hamaratoglu, F., de Lachapelle, A. M., Pyrowolakis, G., Bergmann, S. & Affolter, M. Dpp signaling activity requires Pentagone to scale with tissue size in the growing *Drosophila* wing imaginal disc. *PLoS Biol.* 9, e1001182 (2011).

45 Wartlick, O., Jülicher, F. & Gonzalez-Gaitan, M. Growth control by a moving morphogen gradient during *Drosophila* eye development. *Development* 141, 1884–1893 (2014).

46 Zecca, M. & Struhl, G. Control of *Drosophila* wing growth by the vestigial quadrant enhancer. *Development* 134, 3011–3020 (2007).

47 Hariharan, I. K. Organ size control: lessons from *Drosophila*. *Dev. Cell* 34, 255–265 (2015).

Methods

Fly strains

The following fly lines were used: $y^1 w^{1118}$ (wild type), *dpp-LG86Fb* and *LOP::mCherry-CAAX* (K. Basler[48]), *tub > CD2,Stop > Gal4* (F. Pignioni). *P{Cre}1b* was obtained from Bloomington. *hh-Gal4*, *dpp-Gal4*, *nub-Gal4*, dpp^{d8} and dpp^{d12} are described in FlyBase (http://www.flybase.org).

Genotypes by figure

Figure 1b: *w*; *nub-Gal4 / UAS-morphotrap*; Fig. 1d: *w*; *LOP-eGFP::Dpp / +*; *dpp-LG / +*; Fig. 1e: *yw, hsFlp*; *tub > CD2,Stop > Gal4, LOP-eGFP::Dpp / UAS-morphotrap* ; *dpp-LG / +*; Fig. 1f: *w*; *LOP-eGFP::Dpp / LOP-morphotrap* ; *dpp-LG / +*; Fig. 1g: *w, hsFlp* ; *LOP-eGFP::Dpp, tub > CD2,Stop > Gal4 / LOP/UAS-morphotrap* ; *dpp-LG / +*.

Fig. 2a, c, e: *w*; *LOP-eGFP::Dpp,* dpp^{d12} */* dpp^{d8} *; dpp-LG / +*; Fig. 2b, d, f: *w*; *LOP-eGFP::Dpp,* dpp^{d12} */ LOP-morphotrap,* dpp^{d8} ; *dpp-LG / +*;

Fig. 3b, c: *w*; *LOP-eGFP::Dpp,* dpp^{d12} */* dpp^{d8} ; *dpp-LG / +*; Fig. 3d, e: *w*; *LOP-eGFP::Dpp,* dpp^{d12} */ LOP-morphotrap,* dpp^{d8} ; *dpp-LG / +*;

Fig. 4a: *yw, hsFlp*; *LOP-eGFP::Dpp,* dpp^{d12} */* dpp^{d8} ; *dpp-LG, hh-Gal4 / 2×LOP / UAS::Raeppli*; Fig. 4b: *yw, hsFlp*; *LOP-eGFP::Dpp,* dpp^{d12} */ LOP-morphotrap,* dpp^{d8} ; *dpp-LG, hh-Gal4 / 2×LOP / UAS::Raeppli*; Fig. 5a–d: *w*; *LOP-eGFP::Dpp,* dpp^{d12} */* dpp^{d8} ; *dpp-LG / +*;

Fig. 5g–j: *w*; *LOP-eGFP::Dpp,* dpp^{d12} */ LOP-morphotrap,* dpp^{d8} ; *dpp-LG / +*.

Molecular cloning

For pUASTLOTattB_eGFP::Dpp, GFP was replaced by eGFP in the Dpp-GFP plasmid[9] (obtained from S. Cohen). Then, eGFP::Dpp was inserted in the multiple cloning site of pUASTLOTattB vector[43] by standard cloning procedures.

To create pUASTLOTattB_VHH-GFP4::CD8::mCherry, we inserted the VHH-GFP4 fragment after the signal peptide sequence of the mouse CD8 domain in the pUAS::CD8::GFP plasmid[49]. We replaced the GFP by a mCherry (Clonetech) and finally cloned the VHH-GFP4::CD8::mCherry fragment into the pUASTLOTattB vector[43].

Transgenes were inserted by phiC31-integrase-mediated recombination into the 35B region on the 2nd chromosome. Resulting fly lines are responsive to LexA (ref. 48) and Gal4 (ref. 50) transcriptional activators. By crossing these flies to Cre^y-expressing flies, either the UAS or the LOP site is being excised in a mutually exclusive manner. Excision was screened for by PCR as described previously[43].

Creation of wing disc data sets

Flies were kept in standard fly vials (containing polenta and yeast) in a 26 °C incubator. Larvae were staged as described previously[44]. In our data sets, we only included male larvae, which were positively selected for the presence of the genital disc. All male larvae of a collection were dissected and further processed to obtain maximum sample numbers.

Statistics and data representation

The phenotypes observed and quantified (pattern and size) differ strikingly from controls; therefore no sample size estimation was performed. However, sample number was chosen to ensure statistical significance, which was assessed using a two-sided Student's *t*-test with unequal variance. No randomization was done, however all larvae of an experiment were kept in the same incubator, as well as dissected and processed together using identical solutions in order to minimize variation between the different experimental groups. Blinding was not possible due to the obvious phenotypes observed. For quantitative measurements, the centre values represent the arithmetic mean and the error bars show standard deviation, expect for boxplots (Fig. 3f, Fig. 4d and Fig. 5k, bottom), where centre value correspond to the median and the whiskers mark the maximum and minimum data points.

Immunostainings and image acquisition

Staged larvae were dissected and transferred directly to cold fixative (4% PFA in PBS) and fixed for 20 min at room temperature or 40 min at 4 °C (for p-Mad and Brk stainings) rotating. After fixation, discs were extensively washed with PBT (PBS plus 0.3% Triton-X) and blocked in PBTN (PBT plus 2% normal donkey serum; Jackson Immuno Research Laboratories) for 30 min at room temperature, followed by incubation with primary antibody overnight at 4 °C. The next day discs were washed in PBT six times for 20 min and incubated in secondary antibody for 1.5 h at room temperature on a rotor. After another round of washes with PBT, samples were mounted in Vectashield (H-1000, Vector Laboratories). All discs of one data set were mounted on the same slide using larval brains as spacers. For all quantitative data sets we made sure that imaging conditions allowed acquisition of data in the linear range (Extended Data Fig. 10). For high-resolution imaging along the z-axis (Fig. 1b), discs were mounted with double-sided tape as spacers to avoid squeezing of the discs. The extracellular GFP staining was done as described previously[51]. Images were acquired on a Leica SP5 confocal microscope (section thickness 1 µm for data sets, 0.13 µm for optical cross-section in Fig. 1b).

BrdU labelling

Discs were dissected in Schneider's insect medium, followed by a 1 h incubation in Schneider's plus 75 µg ml−1 BrdU (Sigma, B5002) at room temperature. This was followed by two 5 min washes in Schneider's and one 5 min wash in PBS. Then discs were fixed for 15 min in PBS plus 4% PFA, followed by another 15 min fixation in PBS plus 4% PFA plus 0.6% Triton-X-100. Discs were permeabilized for 60 min in PBS plus 0.3% Triton-X-100 and transferred to a 1:1 mixture of PBS plus 0.6% Triton-X-100: 4 N HCl for 30 min. This was followed by extensive washes in PBS plus 0.3% Triton-X-100. Discs were incubated overnight in anti-BrdU (1:100, Becton Dickson, 347580) in PBS plus 0.3% Triton-X-100. Washing, incubation in secondary antibody and mounting were done as described earlier.

Antibodies

rb-anti-p-Mad (1:1,500; E. Laufer[52,53]); rb-anti-phospho-Smad1/5 (1:200; Cell Signaling, 9516S; used in Extended Data Fig. 4d–f); gp-anti-Brk (1:1,000; Gines Morata);

rb-anti-Sal (1:40; R. Schuh[54]); rat-anti-Sal (1:700; R. Barrio[55]); rb-anti-Omb (1:1,200; G. O. Plugfelder[56]); m-anti-Wg (also known as 4D4-s; 1:120; DSHB, University of Iowa); m-anti-Ptc (also known as Apa1-s; 1:40; DSHB, University of Iowa); rb-anti-GFP (1:200 for extracellular staining; Abcam ab6556); anti-BrdU (1:100; Becton Dickson, 347580). All secondary antibodies from the AlexaFluor series were used at 1:750 dilutions except for Alexa405-anti-rb and Alexa680-anti-m, which were used at 1:500 dilutions; CF405S-anti-gp was used 1:1,000 (Sigma-Aldrich).

Image processing

Images were processed using ImageJ (National Institutes of Health) software. Concentration profiles in Fig. 1, Extended Data Fig. 3 and Extended Data Fig. 45f, right, were created using the Plot Profile function in ImageJ. Optical cross-section in Fig. 1b was created using the section function in Imaris (Bitplain) software. We made use of the Wg/Ptc co-staining[44], which outlines the wing pouch (Wg), the D/V boundary (Wg) and the A/P boundary (Ptc, see also Extended Data Fig. 2). Quantification of wing pouch size and extraction of average gradient profiles (Figs 2g, h, 3f and Extended Data Figs 1f, 2d, e, 4c,f, i, 5e, 8fg, 9g) were done using the WingJ software[57] (http://tschaffter.ch/projects/wingj/, last visited on October 20th 2015). For measuring gradient profiles in WingJ, we used average projections of ten consecutive slices spanning the disc proper epithelium only. Gradient profiles were extracted using WingJ software either only in the pouch (Extended Data Fig. 2) or up to the edge of the wing disc (Fig. 2 and Extended Data Fig. 4), which allowed a better representation of lateral Brk profiles. Profiles were measured with a Sigma of 4px and either 15% ventral offset (for Extended Data Fig. 2e) or 30% dorsal offset (for all other profiles) parallel to the D/V border (marked by the Wg staining). Plotting of average concentration profiles was done applying the Matlab toolbox included in WingJ using the Matlab (Matworks) software.

Generation of mitotic density maps

Wing discs were staged and stained for Wg/Ptc and p-H3, a marker labelling mitotic cells. p-H3-positive nuclei were detected using the Imaris software (Bitplane) spot detection tool; peripodial nuclei were excluded from the following computation. Each disc was marked at 15 landmarks (see Extended Data Fig. 8e). Sixteen discs of one time point were fitted to a reference disc using these landmarks by an affine transformation (least square, Fiji–Landmark correspondence plug-in). All data points of these 16 discs were included in a scatter plot using the Scatplot script (A. Sanchez-Barba; http://www.mathworks.com/matlabcentral/fileexchange/8577-scatplot) in Matlab. The Scatplot visualizes data point density by a colour map, with high-density regions appearing in red and low-density regions in blue.

The mitotic density in Fig. 3f was calculated by normalizing the number of p-H3-positive cells in the anterior or posterior pouch to the corresponding pouch area. Statistical significance was assessed using a two-sided Student's t-test with unequal variance.

Induction and computation of Raeppli clones

In our experiments we used two copies of nuclear Raeppli, resulting in ten different

colour combinations after induction (see Kanca et al.[43]). The larvae were staged as described earlier and dissected at 96–100 h AEL. Raeppli was induced by heat shock (38 °C for 15 min) at three different developmental time points: 55–59 h AEL (~41 h before dissection), 66–70 h AEL (~30 h before dissection) or 76–80 h AEL (~20 h before dissection). Discs were fixed in 4% PFA in PBS for 20 min at room temperature, washed in PBT extensively and mounted in Vectashield (H-1000, Vector Laboratories). Images were acquired on a Leica SP5 confocal microscope using the settings suggested previously[43]. Number of cells per clone was counted using the 'multi-point tool' in ImageJ software (National Institutes of Health). A two-sided Student's *t*-test with unequal variance was used to test for statistical significance.

Measuring growth of the medial and lateral domain of the wing disc

To compare the growth dynamics of the medial (high Dpp signalling) and the lateral domain (low Dpp signalling), we define the position of half-maximum Brk levels as the boundary between these two domains. The position of half-maximum Brk levels was accessed by extracting Brk intensity profiles along a straight line with 30% dorsal offset parallel to the D/V boundary (Extended Data Fig. 8f–l) in each disc individually. Subsequently single Brk profiles—separately for the anterior and the posterior compartment—were fit to a Hill function (see Extended Data Fig. 8f, graph 3) using the fitting-toolbox in Matlab. For fitting we excluded the lateral-most signal, which is noisy due to folds and signal form the peripodial membrane. The Hill function to which we fit the Brk profiles returns four parameters: the amplitude A, a measure for how sharp the profile drops n, a constant offset C, and the position of half-maximum Brk levels k (kA and kP for the anterior and the posterior compartment, respectively). To access the width of the lateral domain, we measured the width of the full compartment LA and LP for the anterior and the posterior compartment, respectively. Since kA equals the width of the anterior medial domain, $LA - kA$ equals the width of the anterior lateral region, and accordingly $LP - kP$ equals the width of the posterior lateral domain. Medial domain width in case of the posterior compartment in eGFP::Dpp morphotrap co-expressing wing discs was not fit to a Hill function, since in this condition only one cell row experiences Dpp signalling during the observed time window (equalling a width of 3.5 µm on average).

48 Yagi, R., Mayer, F. & Basler, K. Refined LexA transactivators and their use in combination with the *Drosophila* Gal4 system. *Proc. Natl Acad. Sci. USA* 107, 16166–16171 (2010).

49 Lee, T. & Luo, L. Mosaic analysis with a repressible cell marker for studies of gene function in neuronal morphogenesis. *Neuron* 22, 451–461 (1999).

50 Brand, A. H. & Perrimon, N. Targeted gene expression as a means of altering cell fates and generating dominant phenotypes. *Development* 118, 401–415 (1993).

51 Strigini, M. & Cohen, S. M. Wingless gradient formation in the *Drosophila* wing. *Curr. Biol.* 10, 293–300 (2000).

52 Tanimoto, H., Itoh, S., ten Dijke, P. & Tabata, T. Hedgehog creates a gradient of DPP activity in *Drosophila* wing imaginal discs. *Mol. Cell* 5, 59–71 (2000).

53 Persson, U. et al. The L45 loop in type I receptors for TGF-β family members is a critical determinant in specifying Smad isoform activation. *FEBS Lett.* 434, 83–87 (1998).

54 Kühnlein, R. P. et al. *spalt* encodes an evolutionarily conserved zinc finger protein of novel structure which provides homeotic gene function in the head and tail region of the *Drosophila* embryo. *EMBO J.* 13, 168–179 (1994).

55 de Celis, J. F., Barrio, R. & Kafatos, F. C. Regulation of the spalt/spalt-related gene complex and its function during sensory organ development in the *Drosophila* thorax. *Development* 126, 2653–2662 (1999).

56 Shen, J., Dahmann, C. & Pflugfelder, G. O. Spatial discontinuity of optomotor-blind expression in the *Drosophila* wing imaginal disc disrupts epithelial architecture and promotes cell sorting. *BMC Dev. Biol.* 10, 23 (2010).

57 Schaffter, T. From Genes to Organisms: Bioinformatics System Models and Software (École Polytechnique Fédérale de Lausanne, 2014).

58 Künnapuu, J., Björkgren, I. & Shimmi, O. The *Drosophila* DPP signal is produced by cleavage of its proprotein at evolutionary diversified furin-recognition sites. *Proc. Natl Acad. Sci. USA* 106, 8501–8506 (2009).

59 Foronda, D., Pérez-Garijo, A. & Martín, F. A. Dpp of posterior origin patterns the proximal region of the wing. *Mech. Dev.* 126, 99–106 (2009).

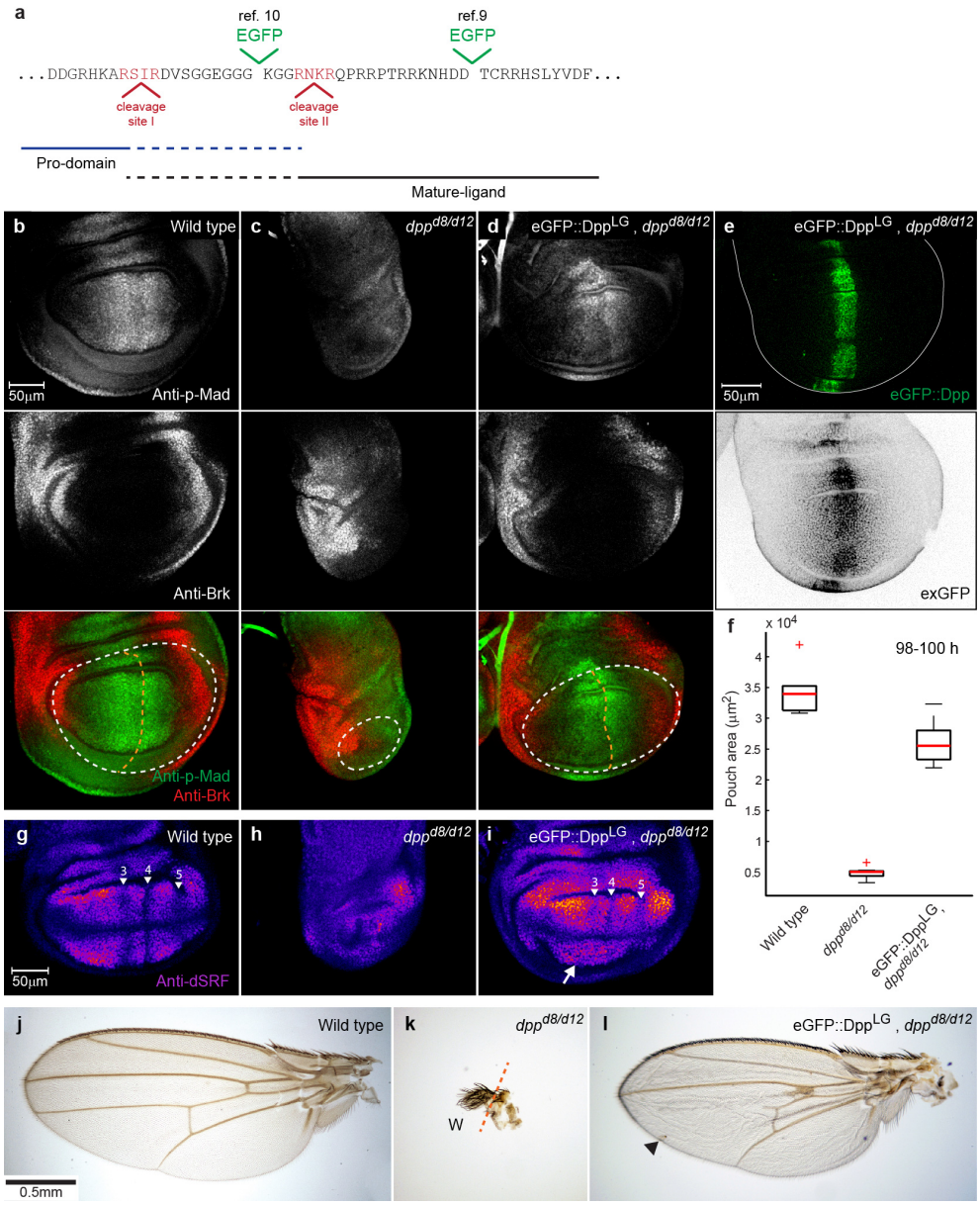

Extended Data Figure 1 - eGFP::Dpp can compensate for endogenous Dpp during wing disc development.

a, Part of the protein sequence of the Dpp protein. The two different eGFP insertion sites[9,10], and the two furin cleavage sites[58] located in this region are marked. Furin cleavage of the inactive pro-form yields the active carboxy-terminal mature ligand. However, potential processing at cleavage site II may result in uncoupling of the eGFP from the mature ligand in the construct described previously[10]. We therefore inserted the EGFP C-terminal to the second furin cleavage site as was done previously[9]. **b**–**d**, Immunostainings for p-Mad and Brk in wild-type (**b**), $dpp^{d8/d12}$ mutant (**c**) and $dpp^{d8/d12}$ mutant wing discs rescued with eGFP::Dpp expressed under control of the dpp::LG[48] line (**d**). In the $dpp^{d8/d12}$ mutant wing discs expressing eGFP::Dpp, the p-Mad and Brk profiles are rescued to a control-like pattern

(**d**, bottom). The pouch outline and the A/P boundary (assessed by Wg/Ptc pattern, data not shown) are marked by dotted lines. **e**, The eGFP::Dpp gradient visualized by eGFP fluorescence or by an immunostaining for the extracellular fraction of eGFP (bottom). **f**, Quantification of wing pouch area assessed by the inner Wg ring of 98–100 h old wing discs (wild type $n = 6$, $dpp^{d8/d12}$ mutant $n = 10$, rescue $n = 10$; red crosses are outliers). eGFP::Dpp expression in $dpp^{d8/d12}$ mutants rescues pouch area close to wild-type size. **g–i**, Wing discs of 98–100 h old larvae stained for the inter-vein marker *Drosophila* Serum response factor (DSRF, also known as blistered). DSRF is expressed in the future intervein tissue of the wing disc. Positions of prospective wing veins 3,4 and 5 are marked by arrowheads. The vein pattern is largely restored in mutant discs rescued by eGFP::Dpp expression (vein numbers are marked by arrows in (**g, i**)). **j–l**, Adult wings of a wild-type fly (**j**), a $dpp^{d8/d12}$ mutant (**k**) and a $dpp^{d8/d12}$ mutant expressing eGFP::Dpp (**l**) (W, wing). Rescued wings have a slightly elongated shape but their sizes are comparable to that of control wings. However, they show some additional vein tissue at the anterior cross-vein and wing vein 4 is absent in the distal part of the wing (marked by arrowhead). We speculate that this is due to lower eGFP::Dpp expression in the ventral compartment, which also manifests itself in lower ventral p-Mad levels (see **d**) and less well defined ventral vein patterns in the dSRF staining (**i**, arrow). Apart from these drawbacks, LexA-driven eGFP::Dpp can compensate for endogenous Dpp during wing disc development.

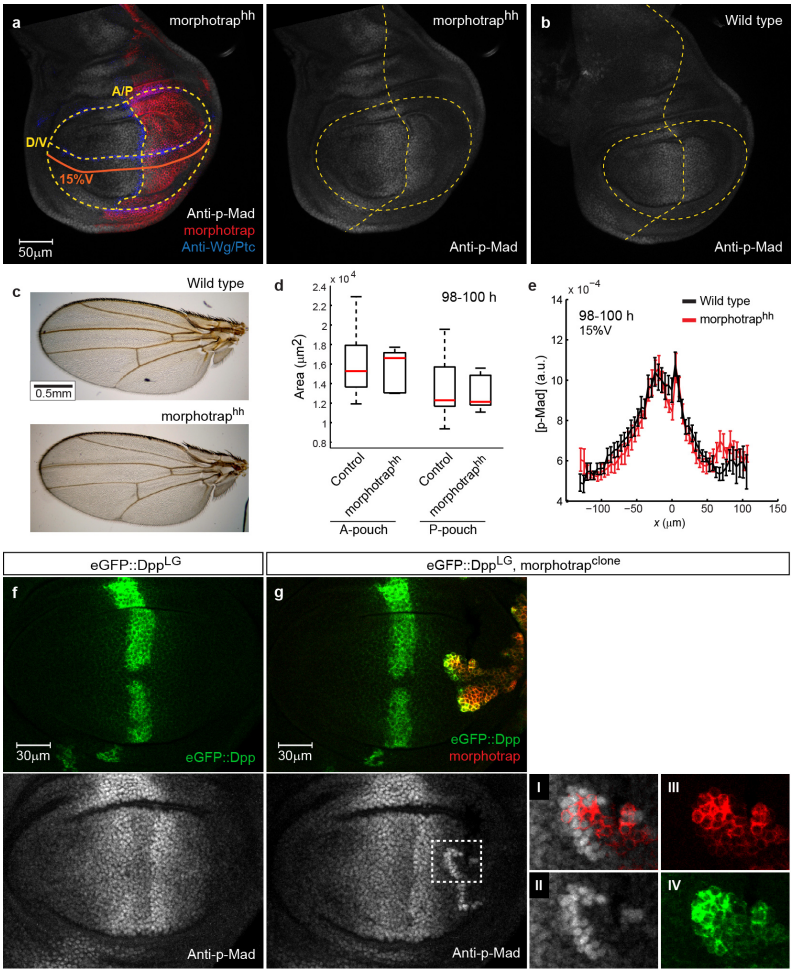

Reprinted by permission from Macmillan Publishers Ltd: *Nature* (Harmansa *et.al.* 2015, DOI: 10.1038/nature15712), copyright (2015)

Extended Data Figure 2 - Morphotrap expression does not affect growth or patterning of the wing disc.

a, Wing disc expressing morphotrap in the posterior compartment controlled by *hh-Gal4* (morphotrap^{hh}). The Wg/Ptc pattern is used as a coordinate system to assess pouch size (anterior (A) pouch, left two quadrants; posterior (P) pouch, right two quadrants). Gradient profiles are measured parallel to the dorso-ventral (D/V) boundary (for example, 15% ventral offset). **b**, Wild-type wing disc stained for p-Mad. **c**, Wings of a male wild-type fly and a fly expressing morphotrap in the posterior compartment under the control of *hedgehog::Gal4* (morphotraphh). **d**, Morphotrap^{hh} wing discs show no significant change in anterior or posterior pouch size (*t*-test two-sided, unequal variance: anterior compartment $P > 0.05$, posterior compartment $P > 0.05$). e, Posterior expression of morphotrap does not cause obvious changes to the p-Mad profile. **f**, p-Mad pattern of a wild-type wing disc expressing eGFP::Dpp in the endogenous Dpp source area. **g**, Lateral morphotrap clones show elevated p-Mad signal at the clone boundary facing the Dpp source due to eGFP::Dpp accumulation. The region marked by a white rectangle is enlarged to the right. **d**, **e**, Control $n = 11$, morphotrap^{hh} $n = 9$, error bars in **e** show s.d.

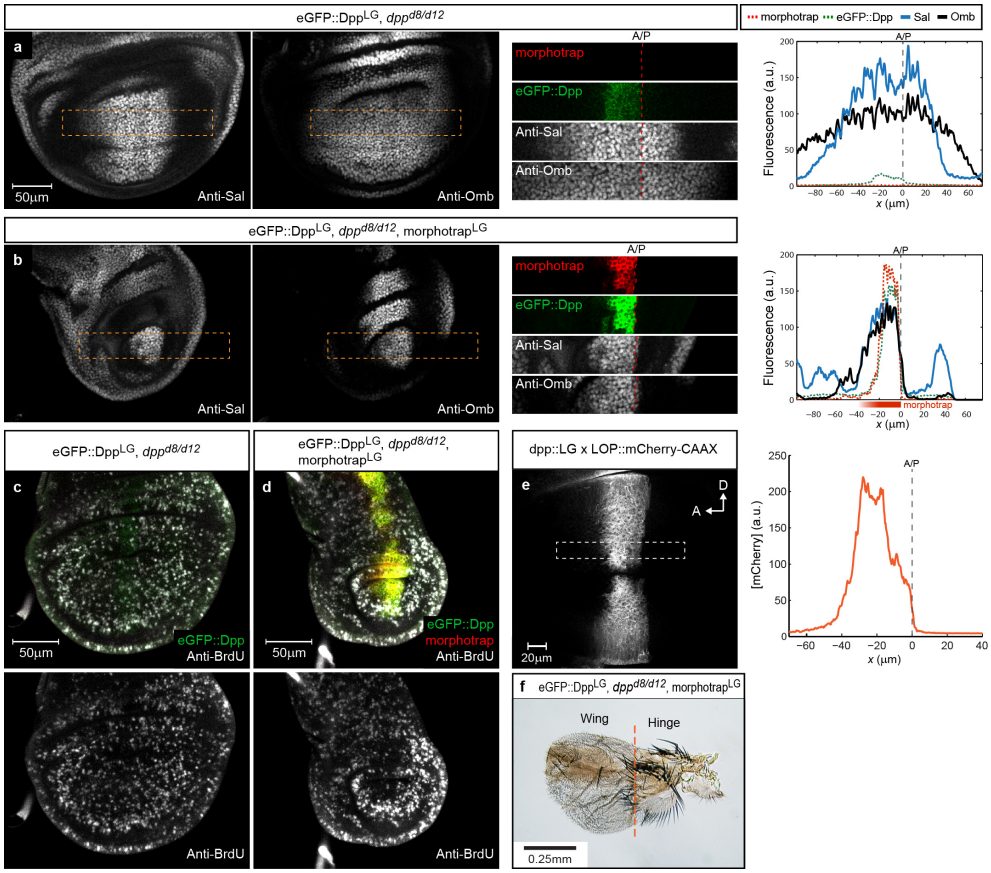

Reprinted by permission from Macmillan Publishers Ltd: *Nature* (Harmansa *et.al.* 2015, DOI: 10.1038/nature15712), copyright (2015)

Extended Data Figure 3 - Domain width of Dpp targets depends on Dpp spreading.

a, Discs of a $dpp^{d8/d12}$ mutant rescued with eGFP::Dpp stained for Dpp targets Sal and Omb. Omb shows a wider distribution than Sal. **b**, $dpp^{d8/d12}$ mutant wing discs co-expressing eGFP::Dpp and morphotrap. The regions marked by a dotted rectangle are enlarged to the right of the respective image. The dotted red line marks the A/P compartment boundary. In the absence of Dpp spreading, target domains collapse onto a single cell row in the posterior compartment. In the anterior compartment domain borders are less sharp. We hypothesize that this is due to morphotrap-bound eGFP::Dpp that is dragged into the anterior compartment by dividing cells (see also **e**). Intensity profiles of the enlarged regions are plotted to the right. **c**, Wing disc of a $dpp^{d8/d12}$ mutant rescued with eGFP::Dpp stained for the proliferation marked BrdU. Uniform BrdU signal is obtained along the entire disc tissue. **d**, Rescued wing disc with blocked Dpp spreading stained for BrdU. Also in the absence of Dpp spreading the uniform BrdU signal is not lost. **e**, Expression of mCherry–CAAX under the control of the *dpp::LexA* driver line used for the rescue. mCherry–CAAX is a protein with a long half-life that localizes to the membrane. Graph shows intensity plot of the region marked on the left. No posterior expression is observed; however, the protein profile is graded into the anterior compartment. Analogous to morphotrap-bound eGFP::Dpp, the stable mCherry–CAAX protein forms a concentration gradient into the anterior compartment due to dividing cells that are pushed further laterally into the anterior compartment.

f, Wing of a rescued fly with blocked Dpp spreading. The hinge region, arising from the lateral wing disc region, is present and well patterned. In contrast, the wing field, arising from the medial wing disc region, is strongly reduced in size and patterning is lost.

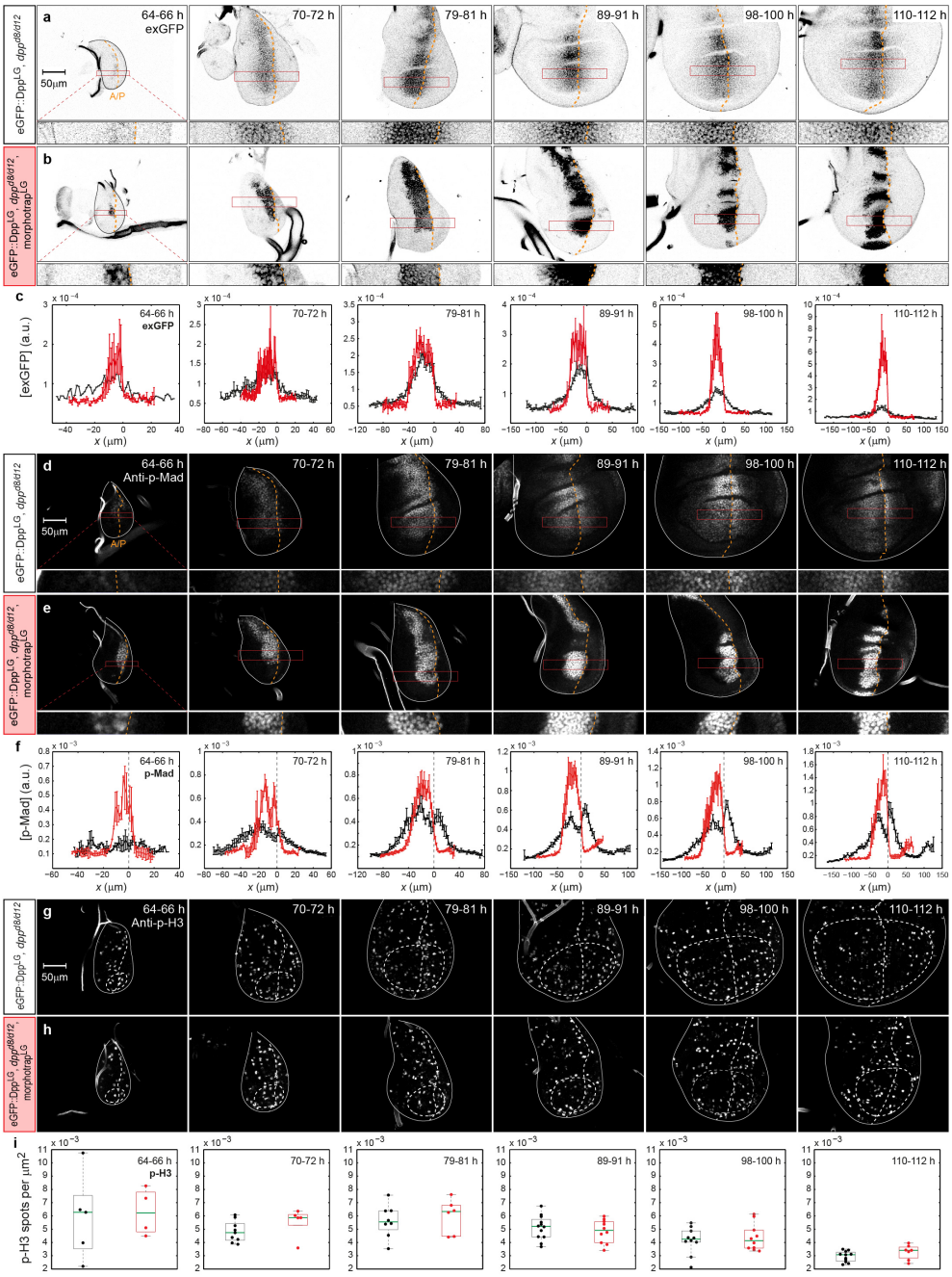

Reprinted by permission from Macmillan Publishers Ltd: *Nature* (Harmansa *et.al.* 2015, DOI: 10.1038/nature15712), copyright (2015)

Extended Data Figure 4 - Time course of eGFP::Dpp spreading, signalling and the mitotic index.

a–**i**, Time course of extracellular eGFP::Dpp (exGFP), Dpp signalling (p-Mad) and p-H3 from 64–112 h AEL of larval development. **a**, **b**, Representative discs of the six time points examined of control animals (**a**) and animals with blocked Dpp spreading (**b**) stained for exGFP. The region marked by a red rectangle is enlarged below each image. eGFP::Dpp spreading is tightly blocked by morphotrap at all time points. **c**, Average exGFP profiles for all time points (control in black/block in red: $n = 43/29$). **d**, **e**, Discs of control animals

(**d**) and animals with blocked Dpp spreading (**e**) stained for p-Mad. When Dpp spreading is blocked, the p-Mad gradient also collapses onto the source region at all time points. **f**, Average p-Mad profiles (control/block: $n = 50/35$). **g**, **h**, Control discs (**g**) and discs with blocked Dpp spreading (**h**) stained for p-H3. **i**, Quantification of the mitotic index (p-H3 spot density). No significant differences were observed between control discs (black, $n = 55$) and discs with blocked Dpp spreading (red, $n = 43$) at any time point ($n > 0.05$ for all time points, two-sided t-test, unequal variance).

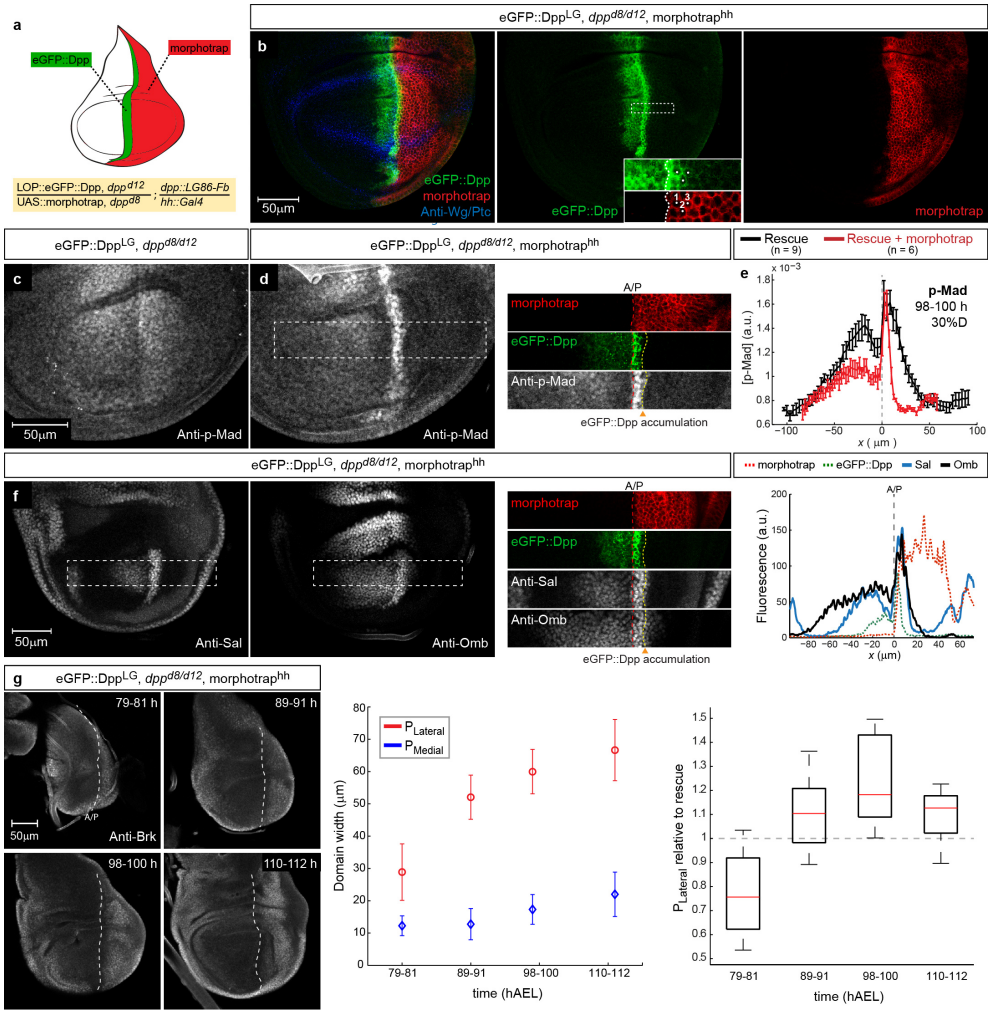

Extended Data Figure 5 - Shortening of the Dpp gradient by posterior morphotrap expression.

a, Scheme of morphotrap expression in the posterior compartment (using *hh::Gal4*) in $dpp^{d8/d12}$ mutant wing discs rescued with eGFP::Dpp. **b**, Posterior morphotrap expression in the rescue background results in strong eGFP signal in the first three cell rows of the posterior compartment due to eGFP::Dpp accumulation; after three cell rows the eGFP fluorescence signal drops. **c**, p-Mad staining in a $dpp^{d8/d12}$ mutant wing disc rescued with eGFP::Dpp. **d**, p-Mad staining in a $dpp^{d8/d12}$ mutant wing disc rescued by eGFP::Dpp and expressing morphotrap in the posterior compartment. Note that the eGFP::Dpp accumulation (marked by a yellow line) directly overlaps with the observed p-Mad signal. **e**, The average p-Mad profiles show that the p-Mad gradient range directly depends on the range of Dpp spreading (error bars are s.d.). **f**, $dpp^{d8/d12}$ mutant wing discs rescued with eGFP::Dpp expressing morphotrap in the posterior compartment stained for Sal and Omb (for control discs see Extended Data Fig. 3a). The A/P boundary is marked by a dotted red line and the range of the eGFP::Dpp accumulation is marked by a dotted yellow line. In this condition the domain width of both targets is strongly reduced. The Sal domain directly collapses

onto the eGFP::Dpp accumulation domain. However, Omb, which can be activated at lower Dpp signalling levels, shows a slightly wider distribution. We hypothesize that this is again due to morphotrap-stabilized eGFP::Dpp being dragged into the posterior compartment (as discussed in Extended Data Fig.3). Intensity profiles of the enlarged regions are plotted to the right. **g**, Representative $dpp^{d8/d12}$ mutant wing discs rescued with eGFP::Dpp expressing morphotrap in the posterior compartment stained for Brk at the indicated time points (79–112 h AEL). In this condition the medial region shows strongly reduced growth (compare to Fig. 5a–f). However, the growth dynamics of the lateral domain are similar to the lateral growth observed in control wing discs (right).

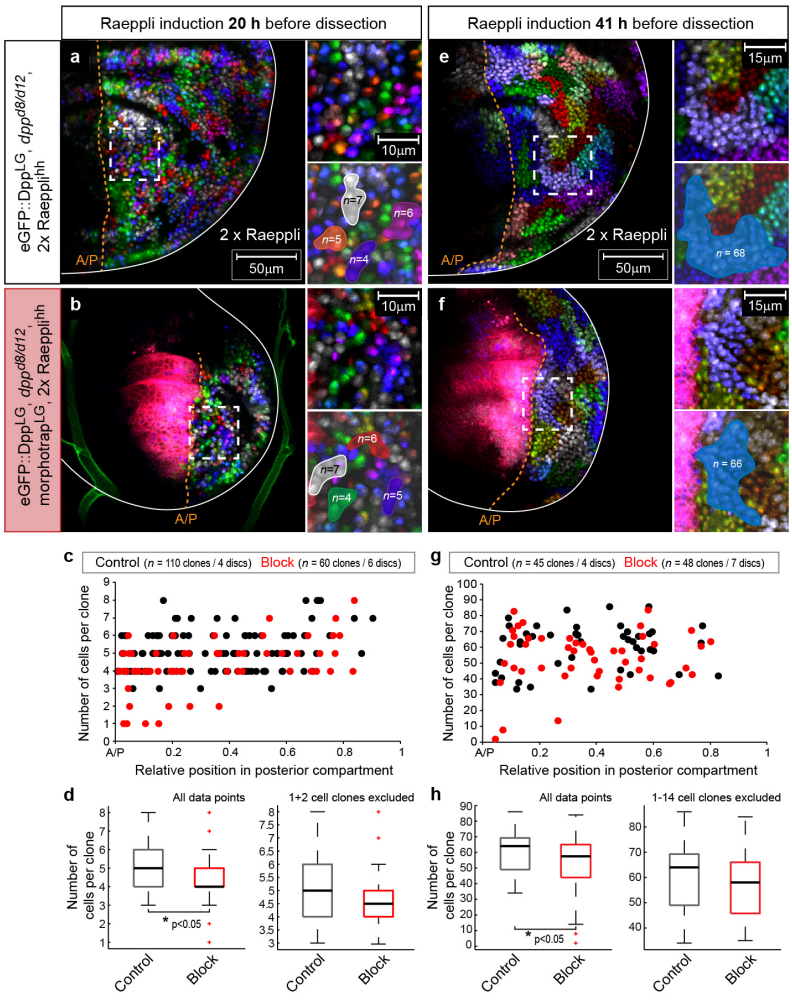

Reprinted by permission from Macmillan Publishers Ltd: *Nature* (Harmansa *et.al.* 2015, DOI: 10.1038/nature15712), copyright (2015)

Extended Data Figure 6 - Clonal growth rates do not change in the absence of Dpp spreading.

a–**h**, Estimation of clonal proliferation rates as shown in Fig. 4, inducing Raeppli at different time points: either 20 h before dissection (**a**–**d**) or 41 h before dissection (**e**–**h**). Discs were dissected at 96–100 h AEL. **a, e**, Representative control discs. **b**, **f**, Representative discs with blocked Dpp spreading. **c**, **g**, Clone size (number of cells per clone) plotted against the relative position in the posterior compartment (0 corresponding to the A/P boundary and 1 to the posterior edge of the disc). Low numbers of small clones in proximity to the A/P boundary are found in discs with blocked Dpp spreading (red dots), while these small clones are not present in control discs (black dots; see also Extended Data Fig. 7). **d**, **h**, Boxplots showing the number of cells per clone. When the small clones are excluded (right boxplots) no significant differences are detected in clonal proliferation between control discs and discs with blocked Dpp spreading ($P > 0.05$).

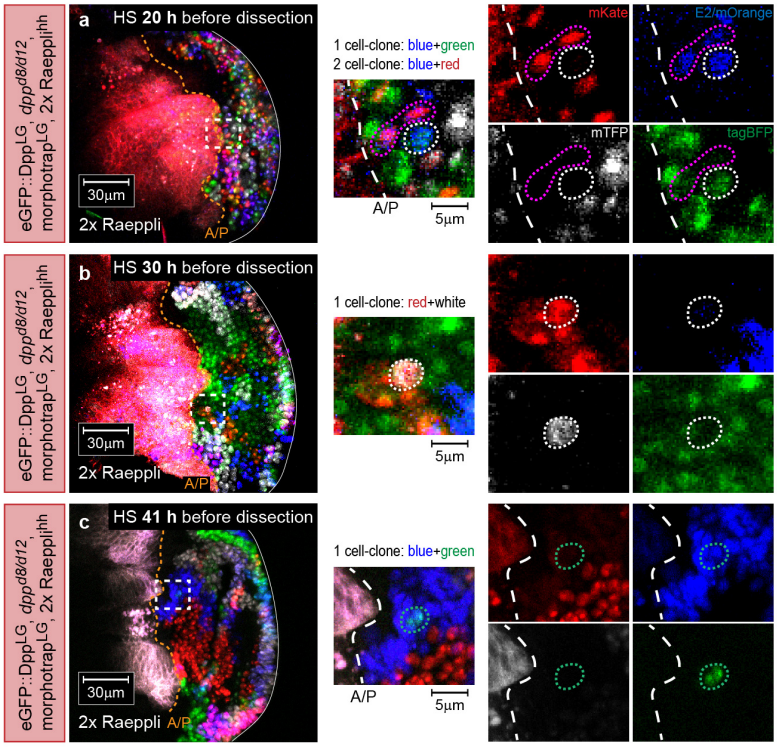

Extended Data Figure 7 - Small clones in discs with blocked Dpp spreading. **a–c,** Wing discs with blocked Dpp spreading carrying small Raeppli clones in proximity of the A/P boundary. Raeppli was induced at different time points during larval development: 20 h (**a**), 30 h (**b**) and 41 h (**c**) before dissection. The regions marked by a white rectangle in the left column are magnified to the right.

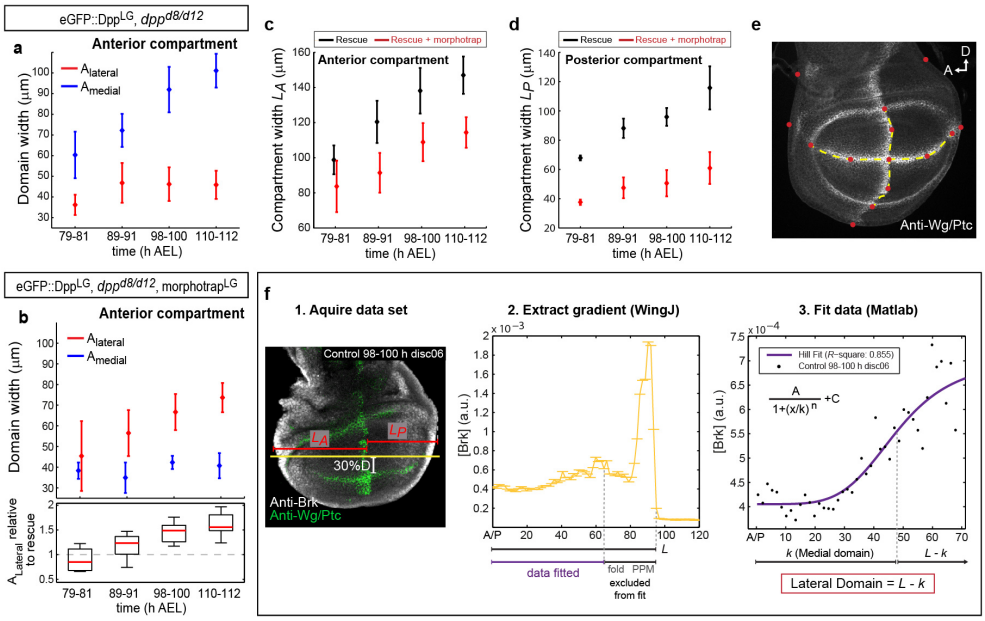

Extended Data Figure 8 - Temporal development and fitting procedure of Brk data set.

a, **b**, As can be seen in Fig. 2f, there is a gap in Brk expression in the lateral-most region of the posterior compartment, indicative of Dpp expression from another, laterally located source. Indeed, it has been shown that Dpp is expressed during the third instar larval stage in a posterior, lateral position and exerts a patterning role on the wing imaginal disc. However, this late Dpp expression does not affect the growth properties of wing disc cells[59]. Despite this, the additional Dpp source might complicate the interpretation of our growth analyses. To circumvent this problem, we also measured the growth properties in the anterior compartment in the presence (**a**) and in the absence of the eGFP::Dpp gradient (**b**; high uniform levels of Brk are indeed present in all cells outside the source). Indeed, we found that the lateral anterior region still grows despite the absence of the Dpp gradient and the lack of Dpp signalling. **c**, **d**, Width of the anterior and posterior compartment respectively in $dpp^{d8/d12}$ mutant wing discs rescued with eGFP::Dpp (black, $n = 34$) and $dpp^{d8/d12}$ mutant wing discs co-expressing eGFP::Dpp and morphotrap (red, $n = 37$, error bars show s.d.). **e**, The red dots mark the 15 points used as landmarks for the affine transformation. Using affine transformation allowed to overlay discs of slightly different shapes and sizes when generating the mitotic densitiy maps shown in Fig.3c, e (also see Methods for details). **f**, Computation of Brk data set shown for the posterior compartment: (1) The compartment width LA or LP was defined as the distance from the A/P boundary to the anterior or posterior edge of the wing tissue, respectively. Brk profiles were measured along a straight line with 30%D offset. (2) Profiles were extracted using WingJ software. (3) The single gradients were fitted to the shown Hill function. The fitting procedure returns the parameter k, which corresponds to the position of half-maximum Brk levels and hence to the width of the medial domain. Therefore, the lateral domain equals $L - k$.

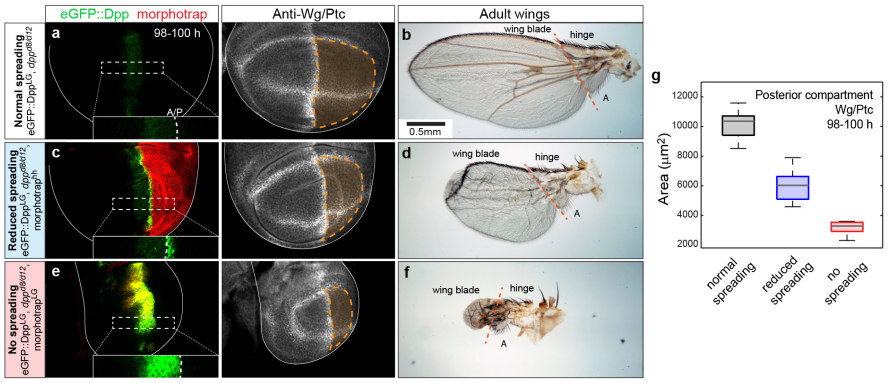

Extended Data Figure 9 - Impact of Dpp spreading on wing pouch and adult wing size.

a, Dpp mutant wing disc rescued with eGFP::Dpp stained for Wg (outlining the wing pouch) and Ptc (marking the A/P boundary). In this background eGFP::Dpp spreading is not hindered and a normal gradient forms. The size of the posterior wing pouch is estimated by the area enclosed by the Wg ring and the A/P boundary (coloured orange) and plotted in **g**. **b**, Adult wing of a rescued fly. The border between the hinge region and the wing blade is marked by a dotted orange line; the alula is labelled with an A. (Wing is the same as shown in Extended Data Fig. 1l). **c**, Rescued wing disc expressing morphotrap in the posterior compartment, reducing Dpp dispersal range in the posterior compartment. In this condition pouch size is significantly decreased (see **g**). **d**, Wing of a rescued fly expressing morphotrap in the posterior compartment. The wing blade area is strongly decreased and patterning in the posterior part of the wing is lost. **e**, Rescued wing disc expressing morphotrap in the Dpp stripe, completely blocking Dpp spreading, and hence gradient formation. Full block of Dpp spreading results in a further decrease of the Wg/Ptc-encircled posterior pouch area. **f**, Wing of a rescued fly co-expressing eGFP::Dpp and morphotrap. Full block of Dpp spreading results in a strong reduction of wing blade area. Only a small amount of unpatterned wing tissue is left, while the hinge region seems to be patterned normally (alula is present). **g**, Plot of the posterior pouch area, as accessed by the Wg/Ptc staining shown in (**a**, **c**, **e**, right) when Dpp spreads normally (black), Dpp spreading is reduced (blue) or when Dpp spreading is fully blocked (red). With decreasing Dpp dispersal range also the posterior pouch area decreases ($n = 22$).

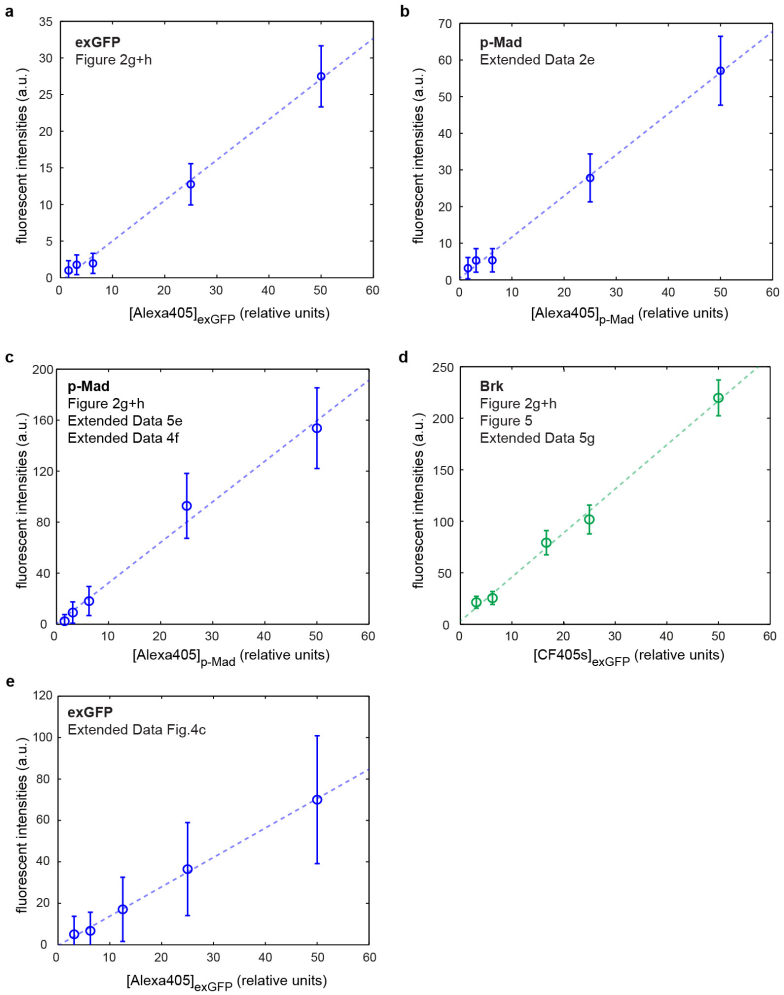

Extended Data Figure 10 - Linear range imaging conditions.

Linear range imaging for the quantitative data sets acquired (corresponding figure is labelled at top left in each plot). Dilutions of the secondary antibodies used (anti-rb-Alexa 405 (blue) and anti-gp-CF405S (green)) in Vectashield mounting medium yield fluorescent intensities proportional to their concentrations under the established imaging conditions. Mean intensities were extracted using the Histogram function in ImageJ on the whole imaging field of a mean projection. The background fluorescence was measured by imaging a slide only containing Vectashield and subtracted from the mean values. Dotted lines indicate linear fits.

4.2 Unpublished Results

4.2.1 Dpp of posterior origin is not required for growth of the wing disc

In the previous publication we characterized in detail the role of Dpp spreading for pattering and growth control of the wing imaginal disc. More precisely, we tested for the requirement of Dpp produced in the medial stripe source to spread, however neglected other sources of Dpp. Foronda *et.al.* showed that around the mid third instar stage another Dpp source, located at the posterior edge of the disc tissue comes up [181]. In this publication it was argued that posterior Dpp has a patterning function but no impact on growth. Still, the existence of another source of Dpp in the wing disc complicates the interpretation of our data. In the previous shown publication, we therefore also computed the proliferation and growth profiles for the anterior compartment, where no other source of Dpp exists, and where no p-Mad but high Brk levels are detected throughout the target field. Despite the lack of Dpp signalling in anterior target cells (shown by the lack of p-Mad and the lack of

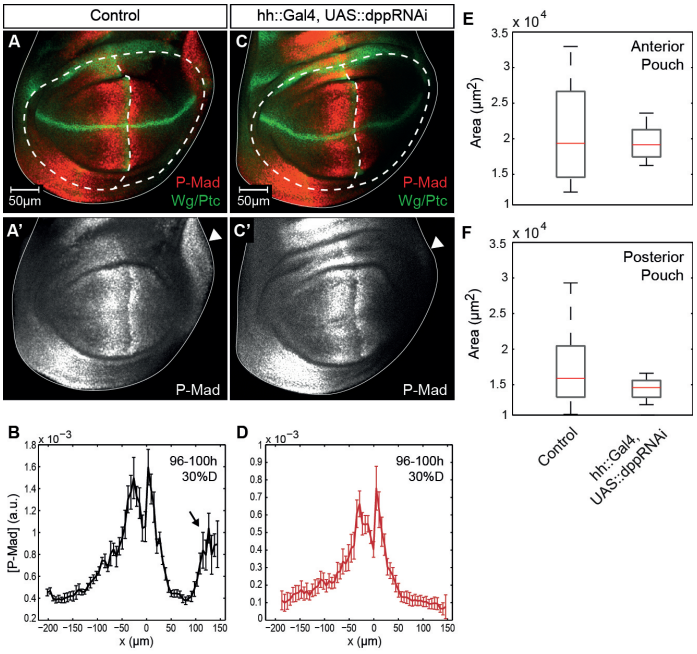

Figure 12: Dpp of posterior origin does not contribute to wing growth
A, Wild type control wing disc stained for p-Mad (Dpp signalling) and Wg/Ptc (Pouch outline and A/P boundary, respectively). Besides the stripe source of Dpp, there is a second source of Dpp in the posterior hinge region inducing p-Mad signalling (see arrow head in (**A'**)). **B**, Average plot of the control p-Mad profile (n=7). p-Mad induced by posterior Dpp is marked by an arrow. **c**, When the posterior Dpp source is eliminated, by posterior expression (hh::Gal4) of dppRNAi, also posterior p-Mad is lost (arrow head in (**C'**)). **D**, Loss of posterior p-Mad is also visible in the average p-Mad profile (n=5). **E**, No change in anterior pouch area, accessed by the Wg/Ptc staining (green in (**A**, **C**)), is observed. **F**, Also the posterior pouch area does not change significantly when the posterior source of Dpp is eliminated by dppRNAi. (n=7 for control and n=5 for RNAi, error bars in (**B**, **D**) show standard deviation)

target gene induction), the anterior compartment showed normal proliferation rates and increases in tissue size at similar speed as the control.

To further strengthen this conclusion and support the results obtained by Foronda *et.al.*, we expressed dppRNAi in the posterior compartment to eliminate p-Mad signalling induced by Dpp of posterior origin (Fig.12). Careful quantification of the results obtained show that expression of dppRNAi in the posterior compartment using *hh::Gal4* results in the loss of p-Mad signal in the posterior hinge region (Fig.12C-D). However, the loss of posterior Dpp signalling does not result in a reduction in wing pouch area (Fig.12F), and only leads to a loss of the region that gives rise to the alula, consistent with published results[181]. These experiments support the view that Dpp of posterior origin is not involved in growth control of the wing disc.

4.2.2 The Dad::EGFP domain width depends on Dpp spreading

Furthermore, we tested the impact of Dpp spreading on the expression pattern of Dad, the only inhibitory Smad in *Drosophila*. Dad is part of a negative-feedback circuit; its transcription is induced by Dpp, and Dad acts as a repressor of Dpp signalling activity [103, 104]. Since we have shown, that the Dpp targets Sal and Omb directly depend on Dpp spreading to define their proper expression patterns, we wanted to test if this is also the case for Dad. For this purpose, we made use of a reporter construct, expressing nuclear GFP (GFP^{NLS}) under the control of the *dad4* regulatory element (*dad-*GFP^{NLS}) [182].

Using a GFP reporter line might not be ideal in combination with EGFP::Dpp, however the nuclear GFP signal is clearly discernible from the extracellular/cytosolic EGFP::Dpp signal. Furthermore, when EGFP::Dpp spreading is blocked by morphotrap, no EGFP::Dpp signal is observed in the posterior compartment (Fig.2A of the

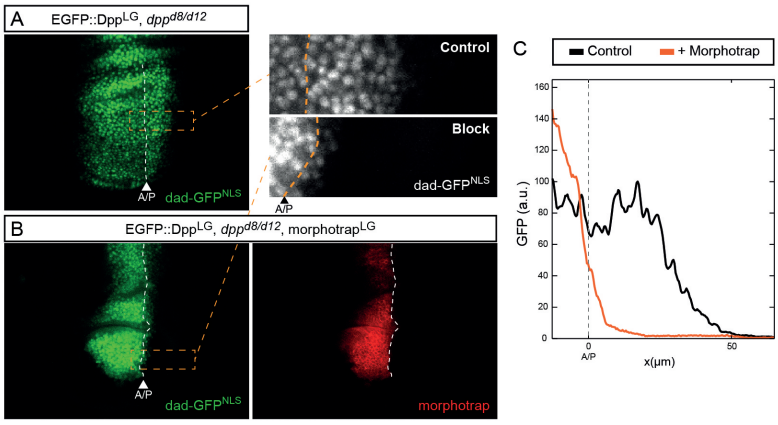

Figure 13: Dad::EGFP domain width depends on Dpp spreading
A, Expression of *dad-*GFP^{NLS} (green) in a $dpp^{d8/d12}$ mutant 3rd instar wing disc rescued by EGFP::Dpp expression. **B**, Expression of the dad reporter line, when EGFP::Dpp spreading is blocked by co-expression with morphotrap (red). **C**, *dad-*GFP^{NLS} (green) concentration profiles of the regions marked by rectangles in (**A**) and (**B**).

before shown publication). Hence, in a situation where Dpp spreading is blocked by morphotrap, all GFP signal observed in the posterior compartment must be signal from *dad-GFP^{NLS}*. We therefore restrict the following analysis to the posterior compartment only.

In wing discs of *dpp$^{d8/d12}$* mutant animals rescued by EGFP::Dpp expression (Dpp gradient present), GFP$^{\mathrm{NLS}}$expression is observed in a wide, graded domain in the posterior compartment (Fig.13A). However, when Dpp spreading is blocked by co-expression of EGFP::Dpp and morphotrap (Dpp gradient absent), GFP$^{\mathrm{NLS}}$is only observed in 1-2 cell rows in the posterior compartment adjacent to the compartment boundary (Fig.13B,C). This observation shows, that the expression domain of Dad, like the ones of Sal and Omb, is controlled by and depends on the spreading of Dpp.

4.3 Wg spreading is not required for patterning but for proper size control of the wing disc

Recently, the role of Wg spreading in *Drosophila* development was questioned by experiments, in which the endogenous *wg* gene was replaced by a membrane tethered-form of the protein [82]. Surprisingly, flies carrying endogenously-tethered, and hence completely immobilized Wg were viable and developed well patterned appendages of virtually normal size. This data suggested, that Wg spreading is dispensable for *Drosophila* development.

To verify this observation and to further validate morphotrap as a valuable tool for the scientific community and show its ease when combined with endogenously tagged proteins, we have used morphotrap to block spreading of endogenous, GFP-tagged Wingless (Wg-GFP). For this purpose, we used a fly strain generated by Port *et.al.*[175], in which the *wg* gene was tagged with GFP at the endogenous locus.

The results we obtain when blocking spreading of Wg-GFP using morphotrap are comparable to the ones obtained when tethering endogenous Wg to the cell membrane as reported by Alexandre *et.al.*[82]. Expression of morphotrap in the posterior compartment using *hh::Gal4* results in a clear shortening of the posterior extracellular Wg-GFP gradient (Fig.14A-B). In addition, the Wg target Distal-less (Dll) shows a reduction in its expression domain upon blocking Wg-GFP dispersal (Fig.14C), again similar to what has been observed by Alexandre *et.al.* Morphotrap-blocked posterior Wg-GFP spreading results in a ~25% decrease in posterior wing area (Fig.14D-G, compared to ~23% in Alexandre *et.al.* when modifying spreading in the entire wing). Interestingly, abolishing Wg spreading most strongly affects the growth of the posterior most region of the wing, between longitudinal vein L5 to the posterior edge (Fig. 14F and G, bottom). In summary, all the results we obtained are in agreement with the findings of Alexandre *et.al.*, validating morphotrap as a novel tool to modify the dispersal of secreted proteins.

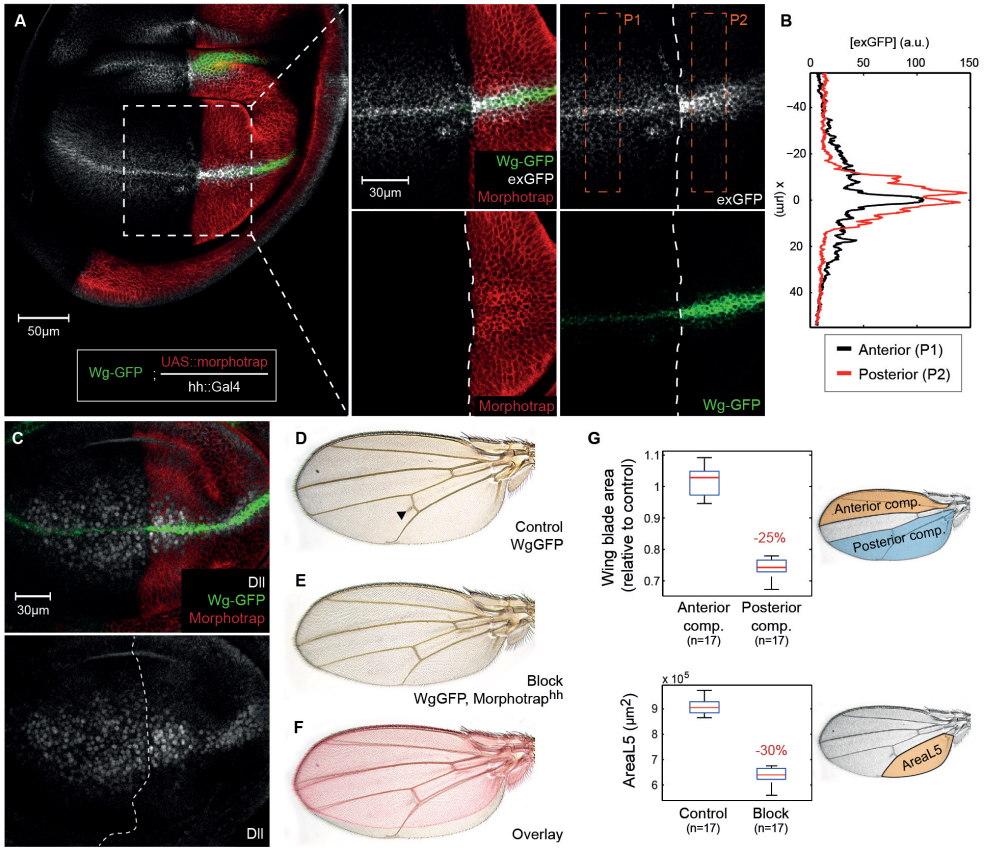

Figure 14: Wg-GFP spreading is not essential for wing development but for proper size control
A, Wing disc of an animal, homozygous for endogenous-tagged Wg-GFP, expressing Morphotrap in the P-compartment (hh::Gal4) stained for extracellular GFP (exGFP). **B**, Quantification of extracellular GFP levels of the regions marked in (**A**). **C**, Distal-less (Dll) expression in a wing disc where posterior Wg-GFP spreading was blocked by Morphotrap. **D-G**, Adult wing phenotypes in the presence or absence of posterior Wg spreading. **D**, Control wing of female homozygous Wg-GFP fly. Most wings (9 of 12) show additional vein tissue at posterior cross-vein (arrow head) **E**, Wing of a homozygous Wg-GFP fly expressing morphotrap in the P-compartment. **F**, Overlay of the wings shown in (**D-E**). Wing with posterior blocked Wg spreading is shown in red. **G**, Quantification of reduction in posterior wing blade area.

4.3.1 ER-retention of Wg-GFP results in strong size and patterning defects

We have shown the power of morphotrap as a tool to immobilize GFP-tagged morphogens and modify their spatial distribution. As shown for both, EGFP::Dpp and Wg-GFP, tethering of the morphogens to producing cells retains their signalling activity, creating a small region (the morphogen source and adjacent cells) that still receives morphogen signalling input. In order to prohibit the signalling activity of immobilized morphogens two approaches are of potential interest: (1) optimizing/modifying morphotrap in a way that bound morphogen cannot (sterically) interact with its receptors any more, or (2) creating a tool that allows to retain the morphogen within producing cells to avoid its signalling activity. Here, I want to provide preliminary

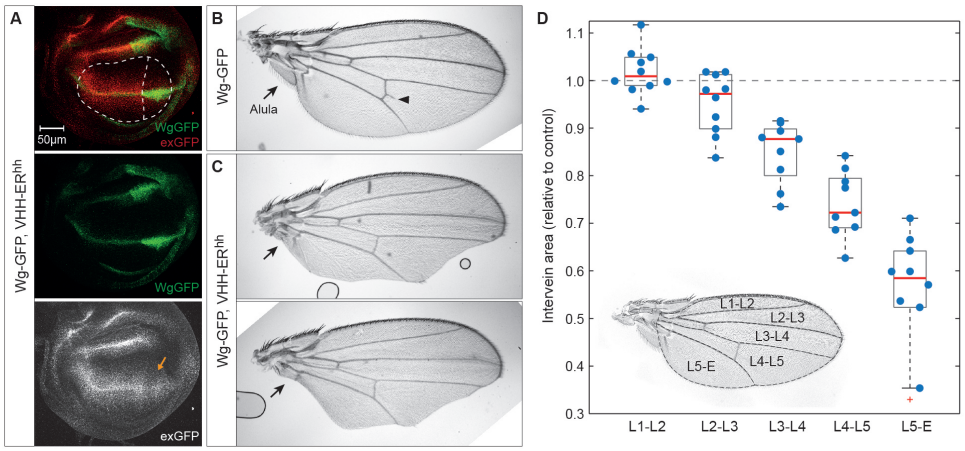

Figure 15: ER-tethering of Wg-GFP results in growth and patterning defects
A, Homozygous Wg-GFP wing disc expressing an ER-localized version of morphotrap in the posterior compartment (*hh::Gal4*), stained for extracellular GFP (exGFP). Strong accumulation of Wg-GFP (green) is observed in posterior Wg source cells (middle). ER-retention of Wg-GFP results in strong growth defects in the posterior pouch. The approximate pouch outlines of the anterior and posterior pouch are marked by dotted lines (top). exGFP signal is reduced in the posterior compartment, suggesting that Wg-GFP secretion is reduced (see arrow, bottom) **B**, Wing of a female Wg-GFP fly (control) **C**, Wings of two female Wg-GFP flies expressing ER-localized morphotrap in posterior cells. Posterior ER-retention of Wg-GFP results in loss of posterior hinge structures (the alula is missing, see arrows in (B) and (C)), the posterior wing margin and growth defects, as quantified in (D). **D**, Quantification of intervein area in Wg-GFP flies expressing posterior ER-morphotrap relative to control flies. (n=10 for each genotype).

results following the second approach, trying to inhibit morphogen signalling via an endoplasmic reticulum (ER) localized morphotrap version.

In order to create a ER-localized morphotrap (VHH-ER), a KDRL sequence, known to retain proteins in the ER [178], was inserted C-terminally to the vhhGFP4 coding sequence. To test the efficiancy of morphogen retention in the ER, we expressed VHH-ER in the posterior compartment of homozygous Wg-GFP flies. While Wg-GFP was normaly secreted from anterior source cells, strong Wg-GFP accumulation was observed in the posterior source cells (Fig.15A). We also observed a reduction in posterior pouch size, suggesting that indeed Wg-GFP is not efficiently secreted any more and that target cells lack Wg signalling. In accordance with this hypothesis, we observed that the posterior extracellular Wg-GFP gradient was reduced, but not absent, upon VHH-ER expression (Fig.15A, bottom). Further experiments are needed to investigate if the residual Wg-GFP observed in the posterior compartment is a result of inefficient ER-capture or results from anterior Wg-GFP dispersal into the posterior compartment. Moreover, the observed growth defects also manifested in the wings of Wg-GFP flies expressing VHH-ER in posterior cells (Fig.15B-D). Reduction of posterior Wg secretion results in a loss of hinge structures and of the posterior wing margin as well as growth defects. We observed that the size of the posterior most wing parts (the area between L5 and the wing edge) were most strongly affected upon

VHH-ER expression (Fig.15D), this is maybe due to the loss of the wing margin. In conclusion, these results suggest that VHH-ER can retain GFP-tagged morphogens in the ER and therefore can be used as a tool to reduce morphogen secretion. Furthermore, these results provide evidence that Wg signalling is necessary for development of the lateral parts of the *Drosophila* wing, while medial parts are not stongly affected by a loss of Wg signalling.

In future experiments, VHH-ER needs to be expressed in all wing disc cells, to characterize the efficiency of ER-retention. Also Wg signalling needs to be investigated by staining for Wg targets, like e.g. Dll. If indeed, VHH-ER can block morphogen secretion in an efficient manner, it could be used together with a temperature-sensitive version of the Gal80 repressor (Gal80ts), to temporally control morphogen secretion. Such experiments would allow to investigate the temporal requirement of Wg and Dpp signalling for wing pouch definition during early development and for wing pouch growth at the larval stages.

5 Discussion and Outlook

We have developed and used morphotrap, a nanobody-based morphogen trapping system, to modify the Dpp gradient *in vivo*. Morphotrap can completely abolish EGFP::Dpp spreading from its central source and thus allowed us to investigate the requirement of Dpp spreading for patterning and growth control. Our major aim was to differentiate between an instructive or a permissive function of Dpp in proliferation control, as suggested by the TRM or the GEM, respectively.

5.1 Cells do not control proliferation by computing temporal Dpp changes

Expression of morphotrap in lateral clones demonstrated that Dpp can disperse over the entire width of the wing disc, hence also control the growth in the lateral region. However, the results we obtained when completely blocking Dpp spreading with morphotrap clearly refute a disc-wide instructive role of Dpp. While we find that Dpp spreading is essential for patterning and growth of the central region of the wing disc, Dpp spreading is dispensable for growth of the lateral region. Hence, our results show that lateral cells do not integrate Dpp signalling levels over time (as suggested by the TRM [126]) to control their proliferation rate, but rather that the proliferation rate in these cells is controlled independent of Dpp (as suggested by the GEM [128, 109]). Importantly, the lateral region experiences high Brk levels and all observed Dpp targets were repressed in our setup, a clear indication for the absence of Dpp signalling, therefore the observed proliferation is neither Dpp-dependent nor arises from Dpp-independent Dpp signalling [125]. According to the TRM, cell proliferation should halt in the absence of Dpp; however, our results show that this is not the case and therefore clearly reject a disc-wide TRM for the control of wing disc growth.

In contrast to the results published by Wartlick *et.al.* [126], we do not observe monotonically increasing EGFP::Dpp levels during wing disc development. We find that in flies rescued with EGFP::Dpp, extracellular EGFP::Dpp (exGFP) levels increase only from 64-91h AEL (Fig.16A); after this period, exGFP levels decrease until the end of larval development (Fig.16B). Importantly, the same behaviour is observed when directly comparing EGFP fluorescence levels (data not shown). This suggests that neither the extracellular EGFP::Dpp gradient (visualized by exGFP staining) nor the overall EGFP::Dpp levels (visualized by GFP fluorescence) monotonically increase during development. These findings show that uniform proliferation and normal development do not depend on increasing EGFP::Dpp levels as suggested by the TRM. The differences observed in temporal EGFP::Dpp transgene expression compared to Wartlick *et.al.* might be due to the different efficiency and stability of the LexA transcriptional activator (TA) we used, compared to the Gal4 TA used by Wartlick *et.al.* However, and in contrast to already published data [164], we observe a constant increase in p-Mad level from 64-112h of larval development in our EGFP::Dpp rescue condition (Fig.16C) and in wild type larvae (data not shown). This observation suggests that the cellular response to Dpp is not strictly linear, and it will be interesting

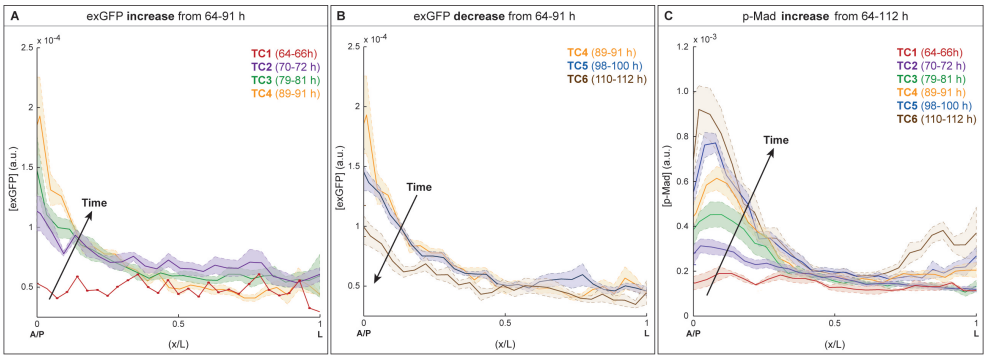

Figure 16: Monotonic increase in p-Mad but not in EGFP::Dpp levels
A, Average extracellular EGFP::Dpp (exGFP) profiles from time classes (TC) 1-4 (64-91h AEL); positions along the x-axis are plotted relative to posterior tissue width L (wheer L corresponds to the posterior edge of the wing disc). In the central region, exGFP levels increase during this time-frame. **B**, For the later TCs, exGFP levels decrease until the end of larval development. **C**, p-Mad levels increase monotonically during the observed time span. The data shown in this figure, and hence sample numbers, are the same as in Extended Data Figure 4c,f of the publication above. The error range shown corresponds to the s.d.

to understand if increasing Dpp signalling levels are required for growth of the medial region of the wing disc.

In summary, our results suggest that Dpp does not directly control the proliferation rate of lateral wing disc cells by computing temporal changes in Dpp, but support the view, that Dpp acts as a permissive modulator of proliferation. We find that Dpp spreading is strictly required for the formation of the medial, but not the lateral region of the wing disc. These observations are in line with the framework of the GEM.

5.2 The GEM can explain the loss of the central domain upon blocking Dpp dispersal

Our observations suggest that two cell populations with different requirements for Dpp signalling exist; while growth of medial cells depends on Dpp signalling, lateral cells grow independent of Dpp. Therefore, when blocking Dpp spreading, the medial region of the target tissue is lost, while the lateral region grows to approximately normal size. Using the multicolour-labelling tool Raeppli, we find that clonal proliferation rates are unaffected in the majority of the posterior tissue upon block of Dpp spreading. However, when Dpp spreading was blocked, we found low numbers of small, one or two cell clones in close proximity of the A/P boundary (however, never in direct contact with Dpp producing cells). The GEM suggests that medial cells depend on the removal of Brk to grow, therefore these small clones are possibly the remnants of the cell population that should have formed the medial region of the wing disc. Since these small clones are observed at varying frequency, and not in all discs, we hypothesized that the majority of "prospective medial cells" undergo apoptosis due to the lack of Dpp signalling (as suggested before [183]). In support of this view,

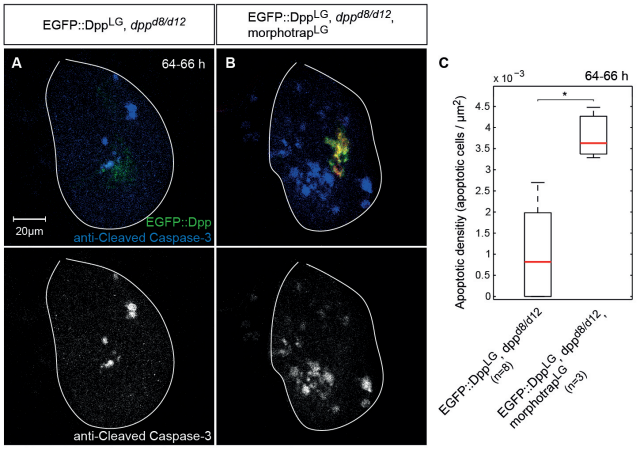

Figure 17: Block of Dpp spreading induces apoptosis in young wing discs
A, Staining for the apoptotic marker Cleaved-Caspase 3 in 64-65 h $dpp^{d8/d12}$ mutant wing discs rescued with EGFP::Dpp. **B**, Block of Dpp spreading by morphotrap results in increased apoptosis during mid-late 2nd instar stage. **C**, Apoptosis rates are significantly increased when Dpp spreading is blocked ($*p<0.05$).

we observe a significant increase in apoptosis in discs with blocked Dpp spreading during mid-late 2nd instar larval stages (Fig.17); during later time points no increase in apoptosis is observed (data not shown). Collectively, these observations suggest that a sub-population of cells, supposedly the ones forming the medial wing disc, depend on Dpp signalling to proliferate and survive.

5.3 How does Dpp spreading control organ size?

Both, the TRM and the GEM suggest a mechanism how graded Dpp levels can result in a uniform proliferation pattern. However, they do not provide an explanation on how the final size of the wing disc is controlled. Our results suggest that the spreading range of Dpp is directly connected to the final size of the wing pouch, the region forming the adult wing blade, but not to the size of the surrounding hinge region (see Fig.18). A range-dependent model for Dpp was proposed by Crickmore *et.al.* to explain organ size control of the *Drosophila* haltere, an organ required for balance during flight [127]. Crickmore *et.al.* suggested that restricting the range of the Dpp gradient results in fewer medial cells exposed to Dpp signalling and hence to a reduction in organ size.

Further investigations are needed to gain a deeper understanding of the connection between Dpp morphogen range and final organ size. Many components are know that affect Dpp spreading and range, e.g. the Dpp receptors [171, 172, 127] and Heparan sulphate proteoglycans (HSPGs) [118, 92, 184], however, all these components are not specific to Dpp but also affect other signalling molecules like Wg or Hh [185, 186, 187]. Therefore, nanobodies provide an excellent opportunity to specifically target Dpp spreading. Future experiments will allow to vary the range of Dpp spreading, by either

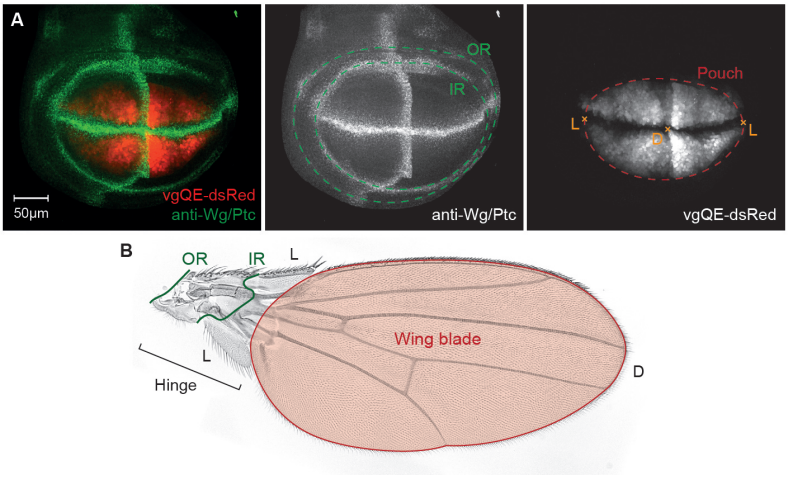

Figure 18: The central wing pouch cells form the adult wing blade
A, Wild type wing disc stained for Vestigial (Vg, red), Wg and Patched (Ptc, both green). Wg is expressed along the D/V boundary and in two rings (inner ring (IR) and outer ring (OR)) surrounding the wing pouch, marked by Vg. During metamorphosis the wing pouch will evaginate, the dorsal cells will fold onto the ventral cells, such that the central region of the wing pouch will form the distal (D) tip of the adult wing. L = lateral. **B**, Wild type wing. The wing blade , forming from the wing pouch, is marked in red. The hinge region, connecting the wing blade to the body wall, forms from the region between the pouch and the outer Wg ring.

modifying the expression levels of morphotrap or by using VHH domains with different binding affinities. Such experiments will shed light on the role of Dpp spreading in controlling the size of the wing pouch.

Another range-dependent recruitment-model has been suggested for wing pouch size control by the Wg morphogen gradient [173, 188, 174], possibly in conjunction with Dpp. Zecca and Struhl suggest that the growth of the wing pouch requires the recruitment of surrounding (non-wing) hinge cells into the wing primordium. According to these studies, new cells are recruited into the wing pouch by a Vg and morphogen-dependent "feed-forward signal", which activates *vg* expression in neighbouring non-wing cells. Interestingly, this model suggests that the range of Wg from the D/V boundary and potentially Dpp from the A/P boundary controls the recruitment of non-wing cells into the wing pouch, and hence the its size.

5.4 Do morphogens need to spread?

However, recently the classical morphogen concept has been questioned by Alexandre *et.al.* They showed that Wg spreading is dispensable for *Drosophila* development [82], by endogenously tethering the Wg protein to the cell surface and thereby abolishing Wg spreading and gradient formation. We sought to reconfirm these results by tethering GFP-Wg to producing cells using morphotrap. In support to the findings made by Alexandre *et.al.*, abolishment of GFP-Wg spreading via morphotrap yields viable adult flies. We also find that upon block of Wg spreading, Wg target gene domains

are strongly decreased in width and that adult wing blade size is reduced to similar extends as reported by Alexandre *et.al.* Interestingly, we find that growth in the absence of Wg spreading is most strongly affected in the very lateral parts of the fly wing, between longitudinal vein 5 and the edge of the wing tissue. In contrast, our data on Dpp spreading suggested that Dpp affects the growth of the medial region of the fly wing. Therefore, these observation suggest that the effect of Dpp more strongly impacts medial wing growth, while the effect of Wg is more prominent in lateral wing growth.

In conclusion, two independent approaches, endogenous protein modification and nanobody-mediated trapping, suggest that a loss of Wg spreading only has minor effects on general fly development. However, and in striking contrast to the facilitative spreading of Wg, we showed that Dpp spreading is required and absolutely crucial for patterning and growth control of the *Drosophila* wing.

Advances in genome modification and development of novel methods, such as morphotrap, will provide a solid framework for future investigations to test if the classical concept of morphogen spreading and concentration gradient formation is the norm or rather the exception during animal development.

Part II

Dissection of Decapentaplegic gradient formation along the apicobasal axis using scaffold-bound nanobodies

---

6 Introduction

Cell fate determination and growth was suggested to be controlled by morphogens, secreted signalling molecules that form concentration gradients in space. How morphogen gradients are established has been studied extensively in the *Drosophila* wing imaginal disc, investigating the Decapentaplegic (Dpp) [24, 79, 109], Hedgehog (Hh) [189] and Wingless (Wg) [190] morphogen gradients. However, due to its mono-layered structure, the wing disc was often simplified as a two dimensional sheet, neglecting its three dimensional composition (see Fig.19A-B). While the two dimensional morphogen distribution and signalling profiles are well studied and extensively quantified (e.g for Dpp see [164, 126]), the role of the three dimensional tissue structure for morphogen dispersal and interpretation is less well understood. Several mechanisms for morphogen dispersal have been suggested [14, 191], however a key component neglected is the sub-cellular localization of the functional morphogen gradient in the wing disc tissue. Moreover, it is not well understood if and how cells in the target tissue respond to the same morphogen ligand presented at different positions along the apicobasal plane and how these signals are integrated.

6.1 The three dimensional structure of the wing disc

The wing disc consists of two contiguous, mono-layered epithelial sheets that form a sac-like structure (Fig.19A-B). One layer is the pseudo-stratified disc proper epithelium (DP), the part of the wing disc forming the wing and the cuticle structures of the notum, forming the flies back. The overlaying structure it the squamous peripodial epithelium (PPE) [192], a structure that is degraded during the pupal stage, but plays an important role during wing disc eversion in metamorphosis [193]. Both epithelia possess a clear apicobasal polarity, in a way that the junctional complexes (septate and adherence junctions) divide the luminal facing apical compartment from the basolateral one [194]. Especially in the DP, the junctions are located close to the apical cell surface of the DP cells, resulting in a rather small apical compartment, compared to the extended basolateral compartment.

If the 3D structure of the wing disc is considered (see Fig.19A-B), then it becomes apparent that morphogen dispersal behaviour might be strongly influenced by the subcellular environment [195]. While molecules secreted along the apical surface into the lumen potentially move freely in space, movement of molecules secreted lateral or basal is restricted by the cell packing and by the interaction partners present on the cell surface and in the extracellular matrix (ECM) (Fig.19C). Therefore, the different subcellular environments potentially influence the dispersal mechanisms and behaviours of morphogens during gradient formation in the wing disc.

6.2 Morphogen gradient formation

The wing disc morphogens are secreted from highly polarized epithelial cells and form gradients along both sides of the disc proper (DP) epithelium. Wg is first secreted apically, then reinternalized and transcytosed to form a long range gradient along the

basolateral compartment of the DP [196, 186, 197, 88]. The Hh morphogen is secreted along the apical and basolateral surface [198, 199, 200], however recent evidence also suggests that apical Hh is transcytosed and that the functional Hh gradient is established along the basolateral side of the DP [201]. Still, the mechanism of Hh dispersal in the wing disc remains controversial; Hh transport along thin, basal cellular extensions called cytonems [202] and movement in extracellular "exo-vesicles" [90] was suggested. In contrast, Dpp localization remains unclear and debated. Formation of long-range gradients in the apical [203] and basolateral [84, 83, 87] space of the wing disc epithelium have been suggested, however, by which mechanisms these different pools of Dpp disperse and how they are sensed at the molecular levels remains unclear.

Formation of the Dpp morphogen gradient was mainly studied using a GFP-tagged Dpp fusion protein (GFP-Dpp) [84, 83]. As shown before, GFP-Dpp can partially rescue the *dpp* disc mutant phenotypes, and served as a valuable surrogate for endogenous Dpp. When expressed in the central stripe source, GFP-Dpp forms steep concentration gradients into the anterior and posterior target tissue. Making use of this GFP-Dpp fusion protein, gradient formation was studied in different genetic backgrounds and several, distinct dispersal mechanisms have been suggested. These mechanisms can be grouped into two classes: (1) diffusion-based mechanisms (free diffusion or restricted diffusion) and (2) active transport mechanisms (via transcytosis or along cytonemes).

Diffusive dispersal of Dpp has been suggested theoretically [117] and recently gained support from a study directly measuring GFP-Dpp diffusion *in vivo* [91]. Zhou *et.al.* used fluorescence correlation spectroscopy (FCS) and by pair correlation func-

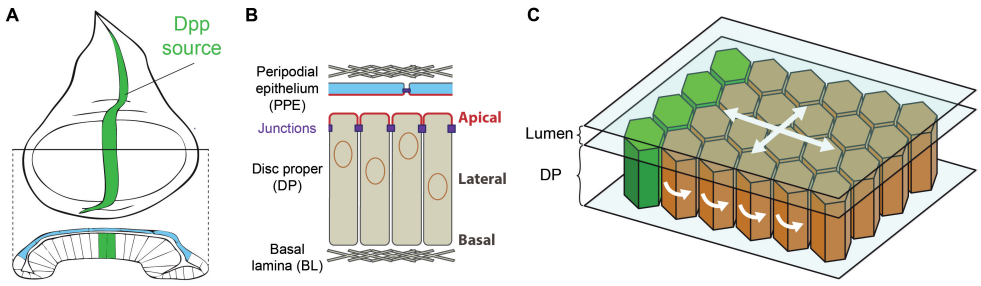

Figure 19: Wing disc morphology and morphogen dispersal
A, Schematic top view (top) and section (bottom) of a wing disc. The section visualizes the sac-like structural organization of the wing disc, consisting of two overlaying, mono-layered epithelial sheets, separated by a luminal cavity. **B**, Schematic drawing of a section trough a wing disc. The wing disc consists of two contiguous epithelial layers with different properties; the pseudo-stratified disc proper (DP) and a squamous epithelium, called the peripodial membrane (PPM, light blue). Both epithelial layers possess a clearly defined polarity, with their apical surface (red) facing the luminal cavity that separates them. Along the opposing surface basal lamina (BL), enveloping the whole wing disc, is deposited. **C**, The sub-cellular environment strongly influences morphogen dispersal. While morphogen movement is less restricted within the luminal cavity, morphogen dispersal within the epithelium is strongly influenced be the epithelial architecture, forcing the morphogen to move around epithelial cells.

tion (pCF) microscopy to directly determine the diffusion coefficient of GFP-Dpp in live wing disc tissue. They found that approximately 65% of GFP-Dpp molecules move rapidly, with a diffusion coefficient consistent with free diffusion, and the other 35% appeared to be immobile or moving very slow. The restricted diffusion model proposes, that morphogen diffusion is hindered by transient interactions with either the receptors or other interaction partners and by the density of the cell packing [191]. It was shown that the levels of the Dpp receptor Tkv modulate the range of Dpp dispersal [127], potentially via receptor mediated uptake and degradation [171]. In addition, Dpp was shown to bind to the two *Drosophila* HSPG Dally and Dally-like protein (Dlp), both needed for gradient formation [204, 205, 206, 118, 92].

One of the proposed active transport mechanisms for Dpp is the transcytosis model. The transcytosis model is based on the observation that GFP-Dpp cannot cross endocytosis-defective clones [83]. The model suggests that Dpp is passed on from one cell to the other via repeated cycles of receptor-mediated endo- and exocytosis [207, 83, 119, 120]. However, theoretical and experimental evidence challenged this model. Lander *et.al.* showed that accumulation of Dpp receptors along endocytosis deficient cells can hinder extracellular Dpp dispersal and explain the observed effect in endocytosis defective clones [117]. Moreover, experiments showed that Dpp signalling is unaffected behind cells defective for endocytosis [118] or mutant for the Dpp receptors *tkv* and *punt* [87]. Thus, the transcytosis model is less favoured by the community.

Yet another model proposes that Dpp is directly transported along thin actin-based cellular protrusions, called cytonemes. Cytonemes have been shown to extend from the apical surface of target cells directed towards the Dpp source stripe [121, 122, 123]. In addition, Tkv was shown to move along these apical protrusions [122]. Functional evidence for Dpp transport along cytonemes exists for cytoneme-mediated transport of Dpp from wing disc cells to the air sac primordium [124] and for Hh gradient formation [208]. However, it remains to be shown if a functional requirement for cytonemes exist for Dpp gradient formation in the wing disc.

Interestingly, most of the suggested transport mechanisms take place in a specific location within the wing disc tissue. While free diffusion can only take place in the wing disc lumen, restricted diffusion must occur in direct contact with either the DP epithelium or the ECM. Dpp cytonemes have been only observed along the apical surface of DP cells. And since transcytosis depends on ligand movement trough cells, it should take place in the plane of the DP epithelium. Hence, investigating the subcellular localization of the functional Dpp gradient can provide information about the respective transport mechanism of Dpp gradient formation.

Therefore, we investigated the subcellular localization of Dpp during gradient formation, in order to obtain a basic understanding about the location of the functional Dpp gradient and the mechanism of Dpp dispersal. We find, that the majority of Dpp is secreted along the basolateral side of source cells and establishes a long-range basolateral morphogen gradient. A much smaller fraction of Dpp is secreted apically into the lumen, where it either disperses along the apical surface of the DP cells or crosses the lumen to PPM cells. In order to understand the function of these

two fractions, we established a novel nanobody-based trapping tool, which allows dissection of the function and the contribution of the specific apicobasal subfractions of the EGFP::Dpp morphogen gradient to patterning and growth control.

6.3 Aim and concept of the project

Here, we want to address a question, that due to technical limitations could not be investigated so far. Namely, we want to understand the contribution of the different subcellular fractions along the apicobasal-axis of the Dpp morphogen gradient for patterning and growth control of the *Drosophila* wing disc. For this purpose we designed novel scaffold-bound nanobodies (SBNs) with specific subcellular localization. In part I of this thesis, we have introduced the use of morphotrap, a SBN that localized unbiased all around the epithelial wing disc cells, and can completely block EGFP::Dpp gradient formation. In the following we want to characterize and use differentially localizing SBNs, that either localize to the apical or the basolateral surface of wing disc cells, or to the basal lamina (BL) (Fig.20A) and only restrict dispersal of specific subfractions of the EGFP::Dpp gradient.

Complementary to the morphotrap approach, differentially localizing SBNs will allow us to restrict or even completely block the spreading of specific subfractions of the Dpp gradient and thereby assess their respective function for patterning and growth control. This approach will allow, for the first time, the modification of specific subfractions of a morphogen gradient and investigate their function. Furthermore, this approach will enable us to investigate, how signalling inputs, presented at different positions along the apicobasal axis are interpreted and translated into target gene expression levels.

In summary, SBNs will allow us to:
(**1**) Investigate the subcellular distribution of EGFP::Dpp during gradient formation
(**2**) Block the dispersal of specific morphogen subfractions along the apicobasal axis
(**3**) Assess the contribution of different subfractions to patterning and growth control.

Moreover, the characterized differentially localized SBNs will provide a novel tool-set for the community to study the dispersal of other morphogens and secreted signalling factors in a novel way.

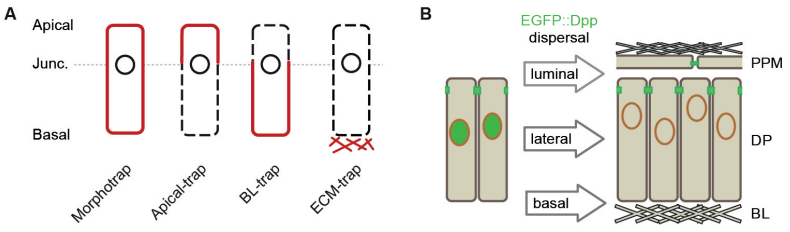

Figure 20: Differentially localized SBNs to dissect the Dpp gradient along the apicobasal axis
A, SBNs with specific subcellular localization. While morphotrap localizes unbiased around epithelial cells, novel SBNs localize either to the apical cell surface (Apical-trap), to the basolateral cell surface (BL-trap) or to the basal lamina (ECM-trap). **B**, Expression of SBNs in either source or target cells will allow to completely block or reduce spreading of specific subcellular fractions of the Dpp gradient. SBNs will allow to specifically block spreading of EGFP::Dpp either in the lumen (Apical-trap), along the basolateral compartment (BL-trap) or along the basal cells surface (ECM-trap).

7 Material and Methods

The general methods are introduced in section 3 of this thesis. In this section, I will only introduce the fly lines and methods specific to this part of my thesis.

7.1 Fly lines

AGir::Gal4	Gal4 driver line that is expressed in PPM cells. 3rd chromosome insertion. [209]
Ubx::Gal4	Gal4 driver line that is expressed in PPM cells. 3rd chromosome insertion. [**?**]
r4::Gal4	Gal4 driver line expressed in the fat body and the salivary gland cells. 3rd chromosome insertion. Bloomington stock center number 33832.
TkvYFP	DGRC 115-298, created by the Cambridge Protein Trap Insertion project [210]

7.2 Cloning of SBNs

The following SBN-constructs were created using standard molecular cloning techniques.

pUASTLOTattB_VHH-GFP4::Nrv1::TagBFP

We inserted the TagBFP (Evrogen) coding sequence between the first and the second exon of the *nervana 1* (Nrv1, FlyBase ID: FBgn0015776) cDNA (BDGP DGC clone LD02379). The vhhGFP4 coding fragment was inserted at the C-terminal end of

Figure 21: VHH-GFP4::Nrv1::TagBFP Sequence

Nrv1::TagBFP. A *Drosophila* Kozak sequence (CAAA) was inserted for higher expression levels and finally, vhhGFP4::Nrv1::TagBFP was cloned into the multiple cloning site (MCS) of the pUASTLOTattB vector. For the construct sequence see Fig.21.

pUASTLOTattB_VHH-GFP4::T48-Baz::mCherry

In a previous study, the *transcript 48* gene (*t48*, FlyBase ID: FBgn0004359) was expressed under UAS control and tagged with an HA-tag [211]. Starting from this construct, we exchanged the HA-tag for the vhhGFP4 fragment. Also, we attached the mCherry coding sequence at the C-terminal end of VHH-GFP4::T48. Unfortunately, this construct did not show good apical localization (data not shown). To improve

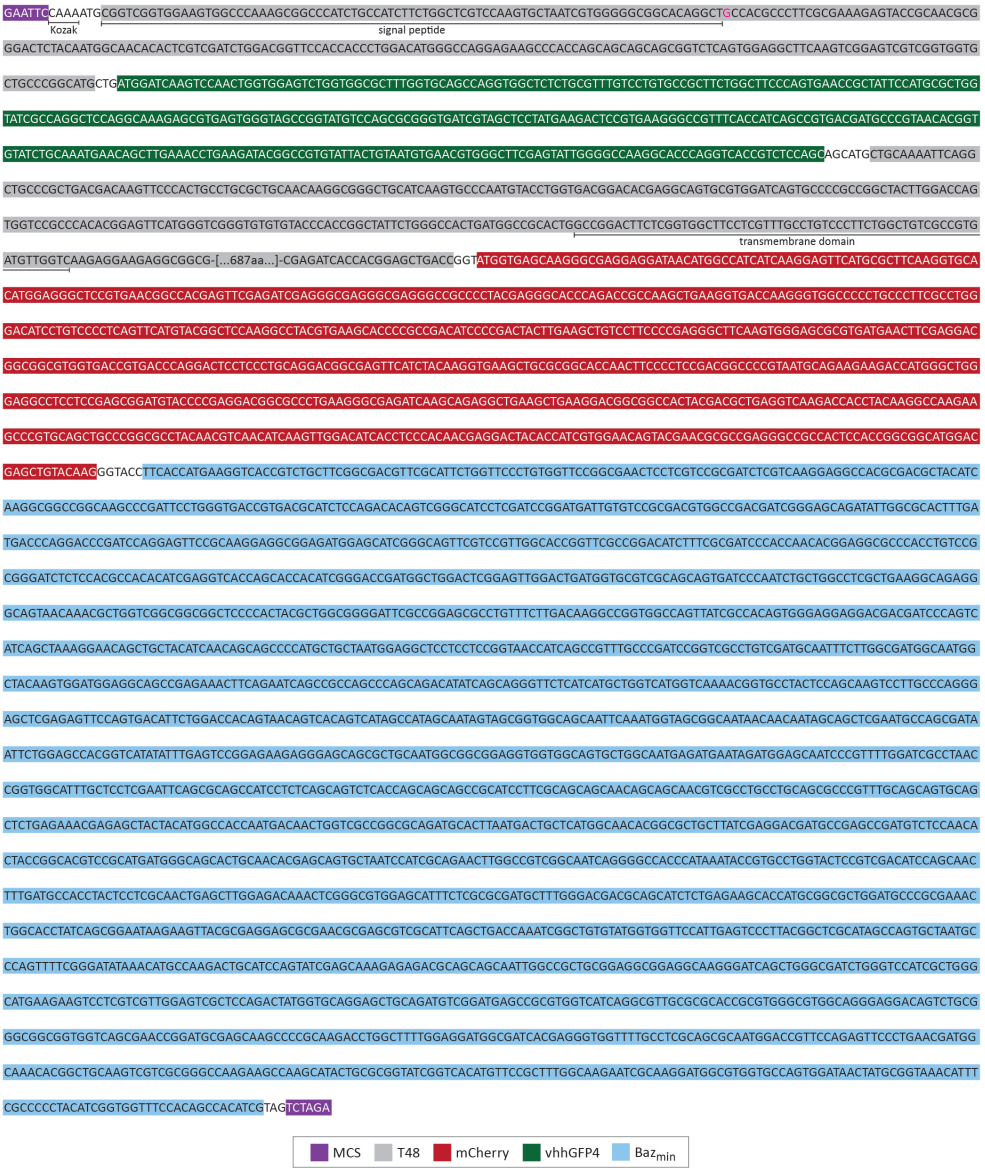

Figure 22: VHH-GFP4::T48-Baz::TagBFP Sequence

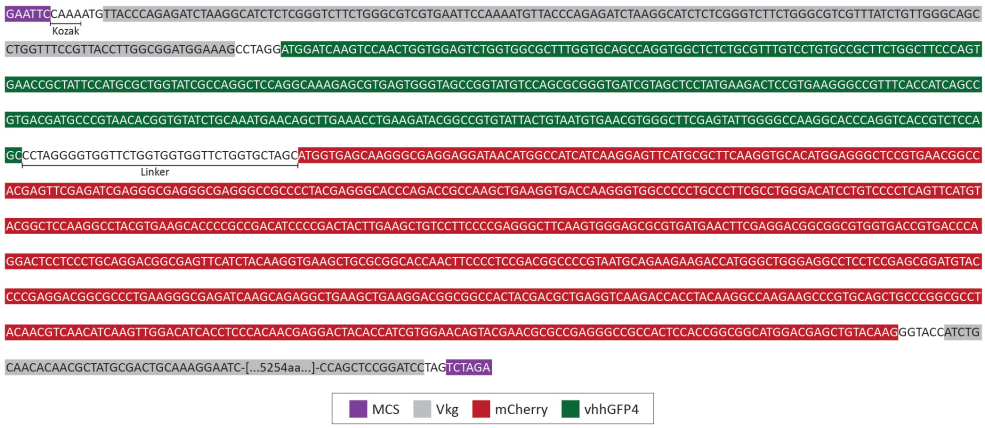

Figure 23: VHH-GFP4::Vkg::mCherry Sequence

apical localization of our VHH-GFP4::T48::mCherry construct, we attached the 2316 base pair (bp) minimal apical localization sequence of Bazooka (Baz_{min}) [212] C-terminally to mCherry. Addition of the Bazooka minimal localization sequence greatly improved apical localization, however could not prevent miss-localization of a small fraction of VHH-GFP4::T48-Baz::mCherry to the baso-lateral domain. Hence, VHH-GFP4::T48-Baz::mCherry does not show an exclusive apical localization, but a strong apically enriched localization. Finally, VHH-GFP4::T48-Baz::mCherry was cloned into the MCS of the pUASTLOTattB vector. The construct sequence is depicted in Fig.22.

pUASTLOTattB_VHH-GFP4::Vkg::mCherry

The Viking $(\text{Vkg})_{\text{full\_length}}$ plasmid was obtained from Hilary L. Ashe [213]. The vhhGFP4 and mCherry coding sequences were inserted between the first and the second exon of the *vkg* gene, separated by a short linker region. We chose this insertion site since a viable GFP-trap line exists, which carries a GFP exon in the endogenous locus between exon one and two [214]. Finally, VHH-GFP4::Vkg::mCherry was cloned into pUASTLOTattB, resulting in the construct sequence shown in Fig.23.

8 Results

This project is still ongoing and the shown results are of preliminary nature. Please consider that some of the shown data might not be conclusively interpretable yet, since further experiments or controls are still ongoing. I will debate the impact of the so far performed experiments in the discussion/outlook section.

8.1 Subcellular localization of the Dpp gradient in the wing disc epithelium

To address the subcellular localization of the Dpp morphogen gradient, we made use of the above introduced EGFP::Dpp fusion protein. Expression of EGFP::Dpp in the central *dpp* source stripe (using the *dpp::LG* LexA driver line [86]) combined with immunostainings against the junctional component Discs large (Dlg) allowed us to assess the relative distribution of EGFP::Dpp in the apical and the basolateral compartment. We find that the vast majority of EGFP::Dpp localizes below the junctions, distributed equally to the basolateral compartment (Fig.24). However, we do not observe extensive EGFP::Dpp signal in the wing disc lumen, as observed before [203]. In contrast, apical EGFP::Dpp is only observed in source cells, but not detectable in the lumen. In addition, we tried to visualize the extracellular fraction of EGFP::Dpp, by trying to optimize the above introduced extracellular staining protocol. However, we did not succeed in obtaining a protocol that robustly labels extracellular luminal antigen (data not shown). In summary, this finding suggests that the EGFP::Dpp gradient mainly forms within the basolateral plain of the DP epithelium.

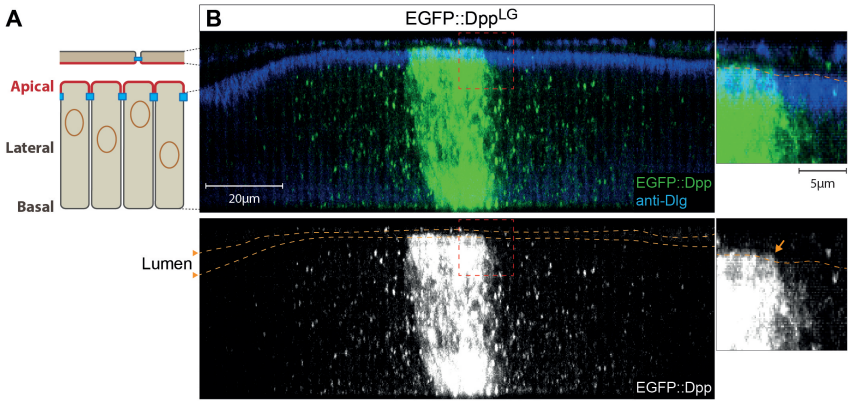

Figure 24: EGFP::Dpp subcellular localization
A, Schematic section of a wing disc. The junctions (blue) are positioned close to the apical surface of the DP, resulting in a relative small apical but extended basolateral compartment. **B**, Section of a wing disc expressing EGFP::Dpp in the central stripe, stained for the junctional marked Dlg. The junctional level is marked by dotted orange lines. EGFP::Dpp signal is mainly observed below the junctions along the basolateral side of the wing disc epithelium. Only in source cells, EGFP signal is observed in the apical compartment above the Dlg staining (see arrow in zoom to the right). In this setup, we do not observe luminal EGFP::Dpp localization.

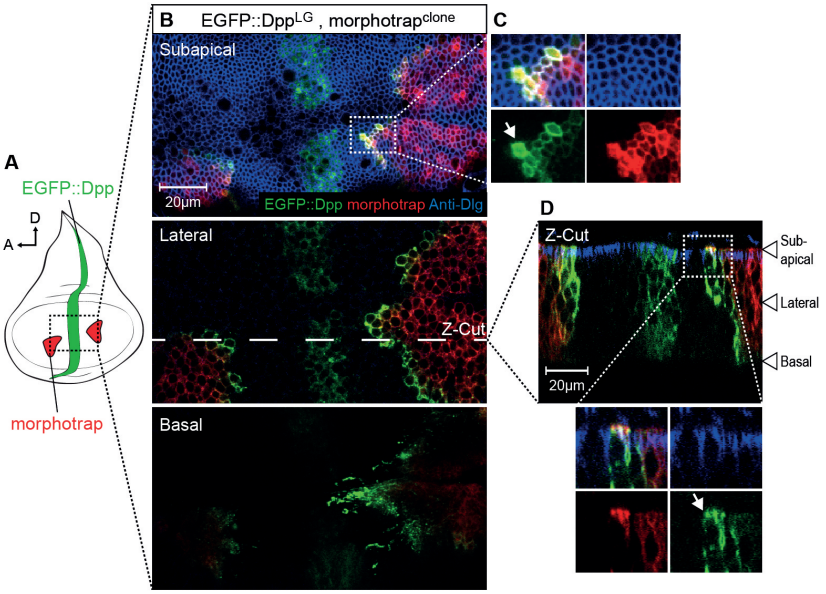

Figure 25: Dpp spreads within the disc proper epithelium and in the luminal cavity
A, EGFP::Dpp is expressed in the central stripe (green, LexA system) and morphotrap in clones (red, Gal4 system). Anterior (A) is facing left, dorsal (D) to the top. **B**, Subapical-apical (top), lateral (middle) and basal (bottom) sections of a wing disc, stained for the junctional marked Discs large (Dlg), carrying two morphotrap clones. **C**, Zoom of the region marked in (B, top). EGFO::Dpp accumulation is observed along the apical surface of morphotrap expressing clones (arrow). **D**, Computed z-section of the disc shown in (B). High amounts of EGFP::Dpp are observed along the basolateral surface of morphotrap clones, facing the Dpp source. However, also along the apical surface, low amounts of EGFP::Dpp can be detected (arrow).

In a further approach, we aimed to use the "accumulation effect" of morphotrap, to visualize even small amounts of EGFP::Dpp morphogen. We therefore expressed EGFP::Dpp in the source stripe (using the LexA system) in a wild type background and morphotrap in small clones (using the Gal4 system), spatially separate from the Dpp expression domain (Fig.25A). In such a situation, clones expressing morphotrap accumulate high levels of EGFP::Dpp on their cell surface [215]. To understand, where along the apicobasal axis EGFP::Dpp is accumulated, we acquired high resolution images along the z-axis of wing discs stained for Dlg (Fig.25B-D). Interestingly, clones expressing morphotrap accumulate high amounts of EGFP::Dpp along their basolateral surface (Fig.25B, middle and D) facing the Dpp source stripe, consistent with the above findings. However, we also observe low level accumulation of EGFP::Dpp along the apical compartment, above the Dlg staining (Fig.25B, top and C). These findings support the view, that the majority of the EGFP::Dpp gradient forms along the basolateral compartment, but also suggest, that low amounts of EGFP::Dpp are secreted apically and disperses within the wing disc lumen or along the apical surface of DP cells. Furthermore, we observe cytonemes, emanating from the morphotrap expressing clones directed towards the Dpp source, that accumulate EGFP::Dpp on

their surface. In summary, these experiments show that different pools of EGFP::Dpp disperse in the apical as well as in the lateral and the basal compartments of the wing disc. In the following we will dissect the respective role of these different fractions to understand the subcellular localization of the functional Dpp gradient.

8.2 Differentially localized scaffold-bound nanobodies

In order to interfere with specific subfractions of the EGFP::Dpp during gradient formation *in vivo*, we designed novel SBNs that localize to specific subregions along the apicobasal axis. These novel SBNs consist of fusions between vhhGFP4 and proteins known to localize to e.g. the apical or the basolateral cell surface or the ECM. Therefore, the localization of the "scaffold protein" determines the localization

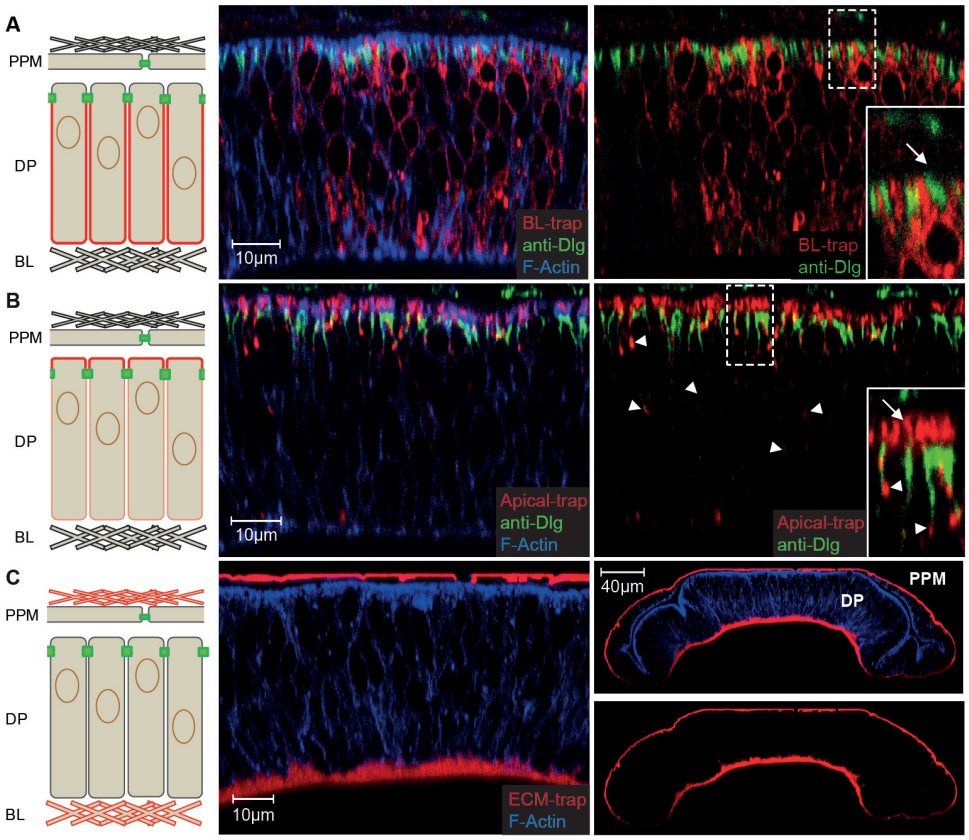

Figure 26: Differentially localized SBNs to study morphogen gradient formation along the apicobasal axis
A, Basal-trap (red) localizes exclusively to the basolateral side of DP cells. The cell outlines are visualized by F-actin (middle). While F-actin signal is observed below (basolateral) and above (apical) of the junctions, marked by Dlg (green), BL-trap does not localize apical to the junctions (see arrow in insert, right). B, Apical-trap (red) preferentially localizes to the apical side of DP cells (see arrow in insert, rigth). However, a small fraction of Apical-trap miss-localizes to the basolateral region (arrowheads). C, ECM-trap is secreted from fat body cells and is inserted into the larval ECM. In the wing disc ECM-trap exclusively localizes to the BL, while it is not observed in the DP epithelium or the disc lumen.

of the vhhGFP4 morphogen trap, and hence the site were the specific SBNs interfere with EGFP::Dpp dispersal.

Since we observed that the majority of EGFP::Dpp potentially disperses within the basolateral DP epithelium, we wanted to create a tool that can specifically interfere with EGFP::Dpp dispersal in this area. For this purpose, we created the basolateral-trap (BL-trap), a SBN that localizes exclusively to the basolateral compartment of wing disc cells (Fig.26A). BL-trap consists of a fusion between the vhhGFP4 nanobody to the extracellular domain of the transmembrane protein Nrv1 and mCherry (for details on the cloning see 7.2). Nrv1 is a subunit of the Na^+/K^+ ATPase [216, 217], and was choosen because is localizes to the basolateral compartment, even when expressed ectopically in the wing disc [218, 219].

For specifically interfering with dispersal along the apical surface or within the wing disc lumen, we created a SBN that localizes preferentially to the apical compartment of the wing disc (referred to as Apical-trap). Our Apical-trap preferential, but not exclusively localizes to the apical surface of epithelial cells (Fig.26B). Furst we used the transmembrane protein Transcript 48 (T48) as a backbone for Apical trap, since T48 was shown to localize to the apical membrane when expressed in *Drosophila* embryos [211]. However, a fusion protein between vhhGFP4, T48 and mCherry did not result in specific apical localization (data not shown). In order to improve apical localization, we introduced the minimal localization domain of Bazooka (Baz) [212], a component of the apical protein complex, into the Apical-trap construct. The addition of the Baz apical-localiaztion domain resulted in improved apical localization of Apical-trap. However, we could only observe a preferential, not an exclusive, apical localization of Apical-trap (Fig.26B, arrows).

Finally, to address the importance of EGFP::Dpp dispersal along or within the basal lamina, we designed an ECM-trap, that localizes to the BL of the wing disc. For this we inserted the vhhGFP4 and the mCherry fragments into the coding sequence of Viking, a type IV collagen [220, 213]. Expressed in the larval fat body (using *r4::Gal4*), ECM-trap is secreted into the hemolymph, distributes in the larvae and is incorporated into the ECM of the wing disc's BL (Fig.26C). These three novel morphotraps will allow to specifically interfere with EGFP::Dpp gradient formation in the apical, basal and basolateral compartments.

8.3 Fractional block of Dpp spreading using SBNs

In a next step we wanted to understand, if the different SBNs capture EGFP::Dpp only in the desired subcellular compartment. We therefore expressed EGFP::Dpp in its central stripe source (*dpp::LexA*) and the different SBNs either in the posterior compartment if membraneous or in the case of ECM-trap in fat body cells (using *hh::Gal4* or *r4::Gal4*, respectively). In a control condition, where no SBN is expressed, EGFP::Dpp is secreted from central source cells and spreads to form concentration gradients in the target tissue; no EGFP::Dpp accumulation is observed either luminal or in the plane of the epithelium (Fig.27A).

In a next step we expressed morphotrap in the posterior compartment (*hh::Gal4*).

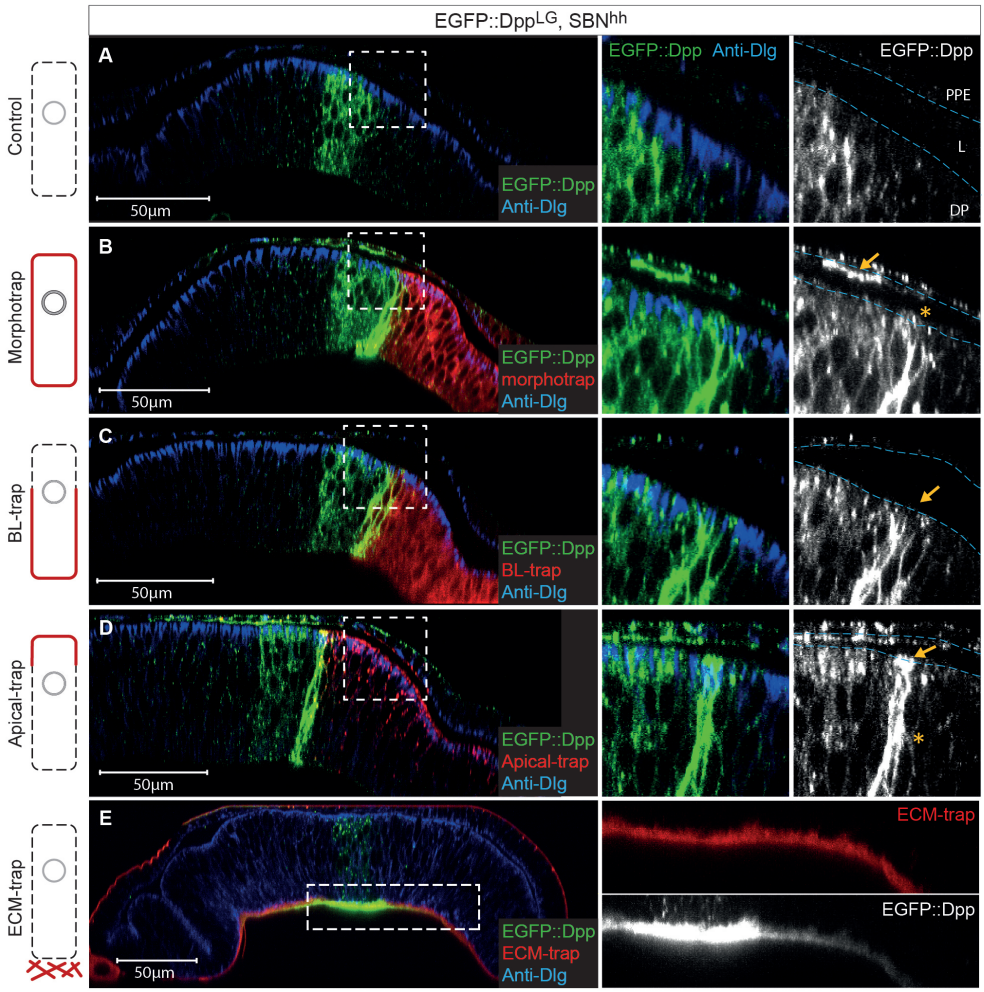

Figure 27: Restricting basolateral EGFP::Dpp spreading using SBNs
Sections of wing discs that expressing EGFP::Dpp (green) in the central stripe source (dpp:LexA) and a SBN (red) either in the posterior compartment (hh::Gal4, B-D) or in the fat body (r4::Gal4, E). The position of the cell junctions is visualized by staining for Dlg (blue). The site of EGFP::Dpp immobilization and hence the impairment of the dispersal range depends on the localization of the capturing construct (the SBNs). **A**, In control discs only expressing EGFP::Dpp , no apical or basolateral accumulation is observed, hence dispersal is normal. **B**, When morphotrap is expressed in posterior cells, strong EGFP::Dpp accumulation is observed basolateral and apical in DP (asterisk, right) and PPM (arrow, right) cells. **C**, BL-trap immobilizes EGFP::Dpp only along the basolateral compartment, not apically. **D**, Posterior expression of Apical-trap results in accumulation of EGFP::Dpp along the apical surface of DP and PPM cells, but also along the basolateral surface (due to construct mislocalization). **E**, ECM-trap expressed in the fat body localizes to the BL, where high amounts of EGFP::Dpp are immobilized direct below the stripe source and graded laterally (right, bottom).

As shown above, morphotrap localizes unbiased around the epithelial DP cells, and hence should be able to restrict apical and basolateral EGFP::Dpp dispersal. Indeed, when we express morphotrap in posterior cells, we observe strong accumulation of EGFP::Dpp along the basolateral side of the wing disc epithelium, as observed in clones. We also observe low EGFP::Dpp accumulation along the apical surface of morphotrap expressing cells in the DP (asterisk in Fig.27B, right). Furthermore, since the *hh::Gal4* driver line is as well expressed in posterior PPM cells, we observe strong accumulation of EGFP::Dpp in the PPM cells that overlay the Dpp stripe source (arrow in Fig.27B, right). These findings support our previous observation, that low amounts of EGFP::Dpp are secreted apically and disperse freely within the luminal cavity.

In accordance, when we expressed BL-trap in posterior cells, we only observed accumulation and reduction of EGFP::Dpp spreading in the basolateral compartment (Fig.27C). Importantly, no apical accumulation was observed, neither along the apical surface of DP cells or in the PPM cells overlaying the DP source. These findings support (1) the exclusive basolateral localization of BL-trap and (2) that therefore BL-trap solely affects basolateral dispersal of EGFP::Dpp.

In a next step, we expressed Apical-trap in the posterior compartment to interfere with the dispersal of the apical fraction of EGFP::Dpp. However, posterior expression of Apical-trap did not result in EGFP::Dpp accumulation exclusively along the apical surface of expressing cells (see arrow in Fig.27D, right), but also resulted in extensive immobilization along the basolateral compartment (see asterisk in Fig.27D, right). Therefore, is seems that even low amounts of mislocalized SBN (as observed above, see Fig.26B) can result in extensive accumulation of EGFP::Dpp by the non-apical localized fraction of the SBN. Based on this observation, we conclude that Apical-trap is not suitable to specifically reduce apical morphogen dispersal and hence we will not make use of this construct in the following.

In a last setup, we tested if ECM-trap, expressed in the fat body and localized to the BL of the wing disc, can immobilize EGFP::Dpp that is secreted along the basal surface of producing cells and disperses within the BL. Indeed, we find that ECM-trap immobilizes maximum levels of EGFP::Dpp right below the Dpp source and decreasing levels with laterally increasing distance to the source (Fig.27E). This observation suggests that a big fraction of EGFP::Dpp is (1) secreted along the basal surface of source cells and (2) that a certain fraction of EGFP::Dpp dispersing within the plane of the DP epithelium leaves the DP epithelium dispersing towards or within the BL. It will be of interest to further investigate if EGFP::Dpp leaving the DP epithelium finally contributions to wing disc growth and patterning or is lost for wing disc development.

In summary,we have shown that a novel tool-set of differentially localized SBNs can interfere with EGFP::Dpp gradient formation in specific subcellular localizations, and hence will allow us in the following to investigate and understand the function of the different EGFP::Dpp fractions for wing disc development.

8.4 Posterior block of basolateral Dpp dispersal strongly impairs patterning and growth

In a next step, we wanted to investigate the role of the basolateral EGFP::Dpp gradient on patterning and growth of the wing disc. For this we compared Dpp signalling (patterning) and pouch size (growth) in wing discs with normal or reduced Dpp spreading (Fig.28). First we compared $dpp^{d8/d12}$ wing discs expressing EGFP::Dpp in the central stripe (normal spreading) with $dpp^{d8/d12}$ wing discs expressing EGFP::Dpp in the stripe and morphotrap in the posterior compartment (*hh::Gal4*, posterior spreading reduced) (Fig.28A-B). Morphotrap localizes to the basolateral and apical surface of posterior cells and therefore affects apical and basolateral EGFP::Dpp spreading, as shown before (Fig.27B and [215]). As expected, upon reducing EGFP::Dpp dispersal into the posterior compartment, the range of the posterior p-Mad gradient is strongly restricted. Moreover, posterior reduction of EGFP::Dpp spreading by morphotrap also results in a significant reduction of posterior wing pouch size, as marked by Distal-less (Dll) expression (Fig.28E-G). These results show that morphotrap indeed can interfere with the fraction of the EGFP::Dpp gradient required for patterning and growth control.

In a next step, we specifically reduced dispersal in the basolateral compartment by posterior expression of BL-trap (Fig.28C). Strikingly, reduction of basolateral dispersal of EGFP::Dpp into the posterior compartment had similar effects on patterning (compare graphs in 28B and C) and growth (Fig.28E,H) as blocking apical and basolateral dispersal by morphotrap. These results show that EGFP::Dpp dispersing along the basolateral compartment is required for wing disc patterning and growth.

In order to understand what role basally secreted and dispersing EGFP::Dpp plays, we expressed ECM-trap in the fat body of $dpp^{d8/d12}$ flies rescued by EGFP::Dpp. ECM-trap localizes to the BL of the wing disc and immobilizes basolaterally secreted and dispersing EGFP::Dpp as shown before (see Fig.27E). When restricting basal EGFP::Dpp dispersal, peak p-Mad signalling levels were reduced especially in the centre of the disc, and the overall p-Mad range and the posterior pouch area were reduced (Fig.28D-E,I). These findings show that EGFP::Dpp secreted along the basal surface is required for proper adjustment of p-Mad signalling levels and is also influencing pouch size control, although to a lesser extend than the lateral fraction.

The Dpp gradient and p-Mad signalling profiled were shown to expand proportionally to the expanding tissue size during growth [126, 164], a phenomenon called scaling. The concept of scaling suggests that a certain read-out "scales", if the readouts concentration profiles keep its relative shape during individual development and between individuals of a population. In order to understand role of lateral and basal EGFP::Dpp spreading for the scaling of Dpp signalling output, represented by p-Mad, we plotted the obtained p-Mad concentration profiles normalized to tissue size along the x-axis (Fig.29). In the case that scaling is not affected, the normalized p-Mad profiles should collapse onto each other. In contrast, in a situation when scaling is disrupted, e.g. by complete block of EGFP::Dpp spreading by morphotrap (Fig.29A), the average p-Mad profiles differ in their relative shape. In a situation where only

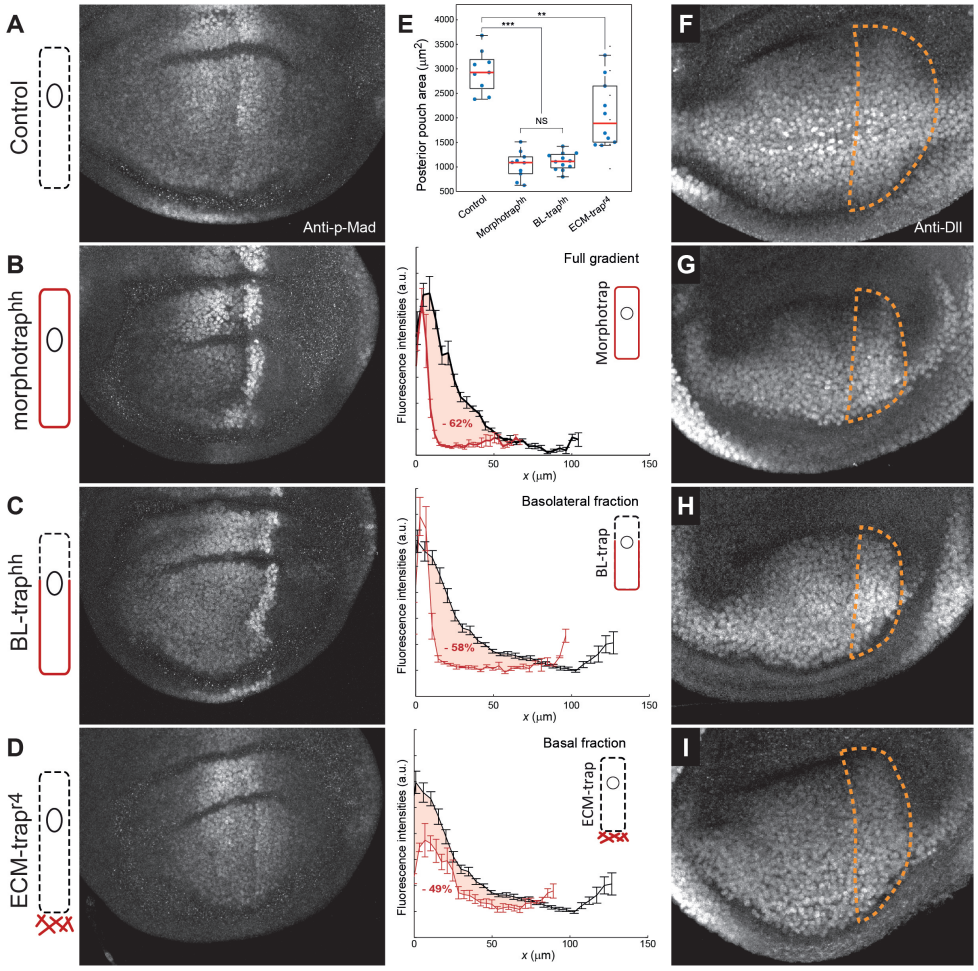

Figure 28: p-Mad range and wing pouch size is strongly impaired when blocking basolateral Dpp spreading

A-D, 98-100h old Wing discs stained for p-Mad of of $dpp^{d8/d12}$ flies rescued by EGFP::Dpp (**A**), $dpp^{d8/d12}$ flies rescued by EGFP::Dpp expressing either morphotrap (**B**) or BL-trap (**C**) in the posterior compartment (*hh::Gal4*) and $dpp^{d8/d12}$ flies rescued by EGFP::Dpp expressing ECM-trap in the fat body (**D**, *r4::Gal4*). Average p-Mad concentration profiles of control (black) and the respective nanobody condition (red) are shown to the right (98-100h, measured 30%D). The reduction in area under the graph is given relative to the control profile (n > 5). **E**, Quantification of posterior wing pouch area as shown by dotted orange lines in (F-I) (n > 9). **F-I**, 98-100h old wing discs of the genotypes indicated parallel in (A-D), stained for the wing pouch marked Dll. The region of the posterior wing pouch is marked by a dotted orange line.

basolateral spreading is affected (Fig.29B), we observe a similar effect on scaling as observed when completely blocking EGFP::Dpp spreading by morphotrap. This observation suggests that the basolateral EGFP::Dpp gradient is crucial for scaling of the Dpp signalling profile. However, reducing basal dispersal via ECM-trap (Fig.29C) did only mildly affect the scaling of the Dpp signalling profile. In the ECM-trap condition, p-Mad levels in the central part were reduced, but overall scaling, especially in the lateral regions was unaffected. Therefore these results suggest that the lateral portion of the EGFP::Dpp gradient is required for the scaling of the Dpp signalling profile, while short range basal spreading of EGFP::Dpp seem to be required for central peak p-Mad levels.

In summary, we have shown that basolateral EGFP::Dpp dispersal is required for patterning and growth control of the wing disc. The results obtained when sequentially blocking dispersal of Dpp gradient subfractions suggest that EGFP::Dpp dispersal within the epithelial/lateral plane of the wing disc is of critical importance for patterning, scaling and growth control of the wing disc. Moreover, our data suggests that EGFP::Dpp secreted along the basal surface of producing cells or EGFP::Dpp leaving the DP epithelium to disperse within the BL layer is not lost for wing disc development, but is required for adjusting maximum p-Mad levels and proper disc size.

8.5 Ongoing approaches to block apical Dpp dispersal

Since the function of the apical fraction of EGFP::Dpp remains unkown, it is important to develop a setup that allows the modification of apical/luminal EGFP::Dpp dispersal. Considering that our first approach, using apical-trap, was unsuccessful

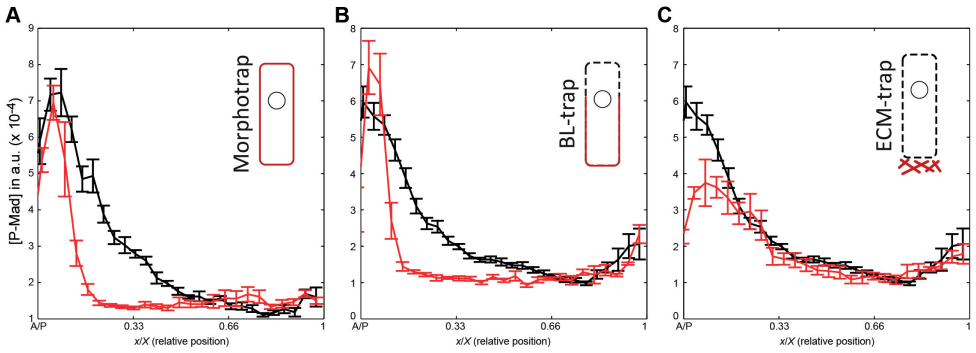

Figure 29: Reducing lateral, not basal dispersal disrupts scaling of Dpp signalling
Average posterior p-Mad profiles from Fig.28 B-C plotted normalized to tissue size along the x-axis. Proflies of controls, $dpp^{d8/d12}$ wing discs expressing EGFP::Dpp in the stripe, are shown in black. Conditions in which apical and basolateral (**A**, morphotrap), basolateral (**B**, bL-trap) or basal (**C**, ECM-trap) dispersal were reduced by SBN expression are plotted in red. Profiles were extracted from 98-100h old wing discs with 30% offset in the dorsal compartment.

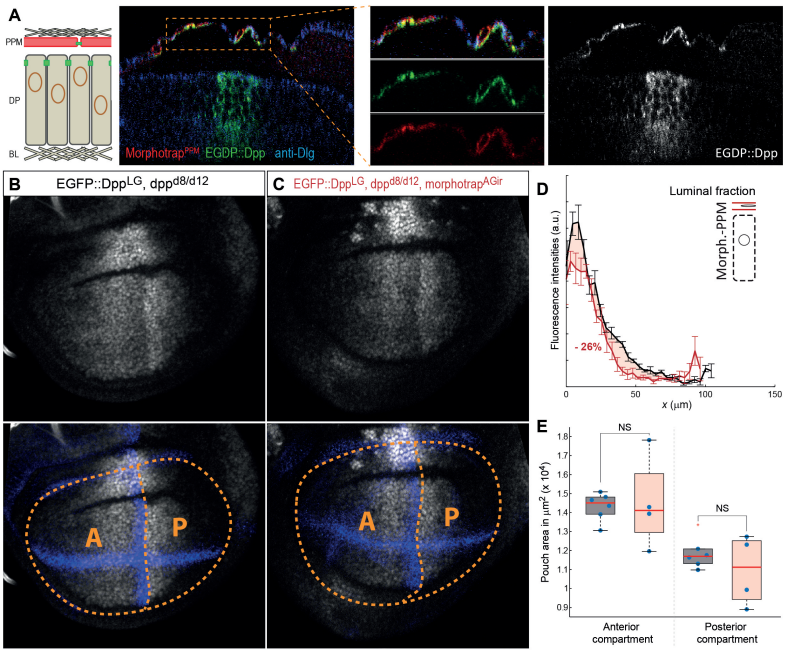

Figure 30: Peripodial expression of morphotrap does not disturb disc development
A, Section of a $dpp^{d8/d12}$ mutant wing disc rescued with EGFP::Dpp (green), expressing morphotrap (red) in the PPM controlled by *AGir::Gal4* [209], stained for the junctional marked Dlg (blue). **B-C**, Representative 98-100h old wing discs stained for P-Mad (white) and Wg/Ptc (blue) of $dpp^{d8/d12}$mutants rescued by EGFP::Dpp (B) and $dpp^{d8/d12}$mutants rescued by EGFP::Dpp expressing morphotrap in the PPM (C). The anterior (A) and posterior (A) pouch area was defined by the Wg/Ptc pattern and is marked by dotted orange lines. **D**, Average posterior p-Mad concentration profiles of control (black, n=6) flies and flies expressing morphotrap in the PPM (red, n=5). **E**, Anterior and posterior pouch area, as marked in (B-C) of control (grey, n=6) and morphotrap (red, n=6) flies.

---

in specifically modifying apical EGFP::Dpp dispersal, we had to develop an alternative approach to interfere with the apical fraction of EGFP::Dpp. We therefore expressed morphotrap in PPM cells (using *AGir::Gal4*, Fig.30A). Similar to expression of morphotrap in the posterior compartment, expression of morphotrap in PPM cells resulted in immobilization and accumulation of EGFP::Dpp in the PPM cells that cover the Dpp source (Fig.30, middle). Interfering with apical dispersal by PPM expression of morphotrap showed no significant effect neither on Dpp signalling (Fig.30B-D) nor on wing disc growth control (Fig.30E). Further investigations are needed to clarify if EGFP::Dpp dispersal in the lumen is truly dispensable for patterning and growth control, or if PPM expression of morphotrap cannot modify the functional apical fraction of EGFP::Dpp.

8.6 Adult wing phenotypes support the importance of lateral Dpp spreading for patterning

In order to better understand the role of different subfractions of the EGFP::Dpp gradient for patterning and growth, we studied the adult wing phenotypes upon gradient disruption. $dpp^{d8/d12}$ mutant flies rescued by the expression of EGFP::Dpp have troubles to emerge from the pupal case. However, low numbers of animals succeed in hatching and unfold their wings, allowing us to study the effect of SBN-mediated morphogen trapping on wing development.

Expression of EGFP::Dpp in $dpp^{d8/d12}$ mutant flies results in a rescue of the $dpp^{d8/d12}$ mutant phenotype to a reasonable extend (Fig.31A-B and [215]). Rescued flies show normal wing shape and the wing veins are located properly. The only caveat is, that for unknown reasons, longitudinal vein 4 does not form completely and is shorter than in wild type flies. We have shown before, that co-expression of morphotrap and EGFP::Dpp in the central stripe source results in a drastic reduction of wing blade area (Fig.31C and [215]). Strikingly, co-expression of EGFP::Dpp and BL-trap in the $dpp^{d8/d12}$ mutant background results in wings that are much bigger than the ones obtained from EGFP::Dpp and morphotrap co-expression (Fig.31D). Interestingly, EGFP::Dpp and BL-trap co-expression wings have a well defined wing margin, however patterning is affected since the number of longitudinal veins (LV) is reduced from five to three. It is well known that Dpp signalling is required for positioning of LV 2 in the anterior and LV 5 in the posterior compartment, while vein

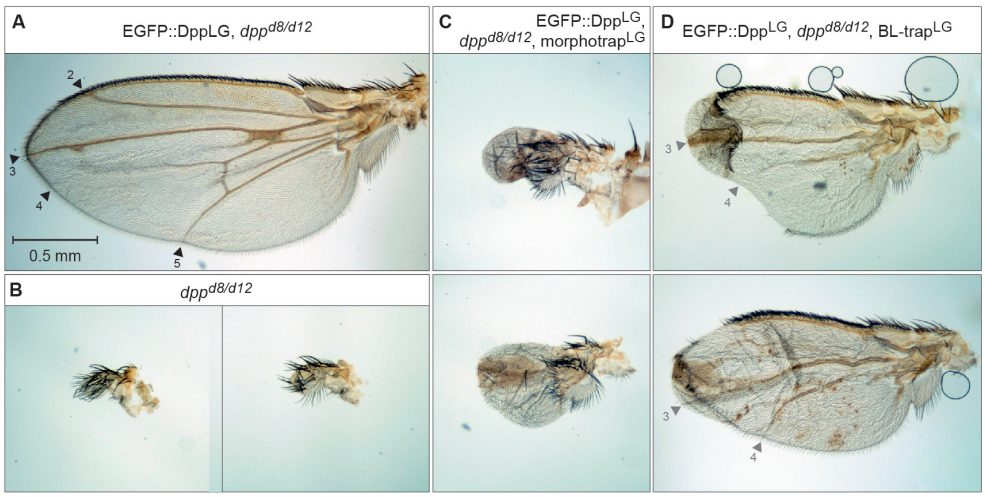

Figure 31: Co-expression of BL-trap and EGFP::Dpp results in a loss of patterning but not growth
A, Wing of a $dpp^{d8/d12}$ mutant fly rescued by EGFP::Dpp expression. LVs 2-5 are marked by arrowheads. **B**, Wing structures developed by $dpp^{d8/d12}$ mutant flies. **C**, Wing of $dpp^{d8/d12}$ mutant flies rescued by EGFP::Dpp, co-expressing morphotrap in the EGFP::Dpp source stripe. **D**, Wings of $dpp^{d8/d12}$ mutant flies rescued by EGFP::Dpp, co-expressing BL-trap in the EGFP::Dpp source stripe. All images are show at the same magnification, scale bar is shown in (A).

LV3 and LV4 are positioned independent of Dpp. Therefore, we hypothesise that the loss of basolateral Dpp signalling causes the loss of LV2 and LV5. Despite blocking basolateral EGFP::Dpp spreading, wing growth is not completely disrupted as observed in the morphotrap condition. This finding suggests that in the EGFP::Dpp BL-trap co-expression condition, a functional subfraction of the EGFP::Dpp gradient, potentially the apical one, forms and promotes the growth of the wing pouch. In summary these findings suggests that (1) basolateral EGFP::Dpp spreading is crucial to execute the patterning function of Dpp, but also that (2) proper growth control requires the input from basolateral and apical EGFP::Dpp.

Moreover, the adult wing phenotypes from posterior compartment and fat body expression of SBNs highlight that the lateral fraction is responsible for the patterning function of the Dpp gradient, while the apical/luminal and basal fractions seem to be involved in growth control. Before, we have shown that expression of morphotrap in the PPM cells can immobilize luminal EGFP::Dpp, however has no effect on patterning and growth (see Fig.30). In accordance, the wings of $dpp^{d8/d12}$ mutant flies rescued by EGFP::Dpp and expressing morphotrap in the PPM cells do not show a patterning or growth defect (Fig.32A-B). Also wings of $dpp^{d8/d12}$ mutant flies rescued by EGFP::Dpp and expressing ECM-trap in the fat body cells form wings with all 5 LVs (Fig.32C). However, all of these wings (n=5) show mild to strong reduction in wing blade size (compare Fig.32C left and right). Posterior expression of morphotrap (Fig.32D) and BL-trap (Fig.32E) in $dpp^{d8/d12}$ mutant flies rescued by EGFP::Dpp, in both cases, resulted in a loss of LV5 and a consistent strong reduction in wing blade area. Consistent with the morphotrap/BL-trap EGFP::Dpp co-expression wing phenotypes, wings of flies expressing BL-trap in the posterior compartment are bigger than the ones expressing morphotrap (compare Fig.32D and E). In summary, these results suggest that indeed lateral EGFP::Dpp spreading is crucial for Dpp-mediated patterning, since LV5 is only affected in conditions where lateral dispersal of EGFP::Dpp was affected. Moreover, we find evidence that the size of the wing blade is controlled by the basolateral and apical EGFP::Dpp gradients. Further experiments and proper quantification will help to understand the respective impact of the apical and basolateral fraction of EGFP::Dpp on wing growth control.

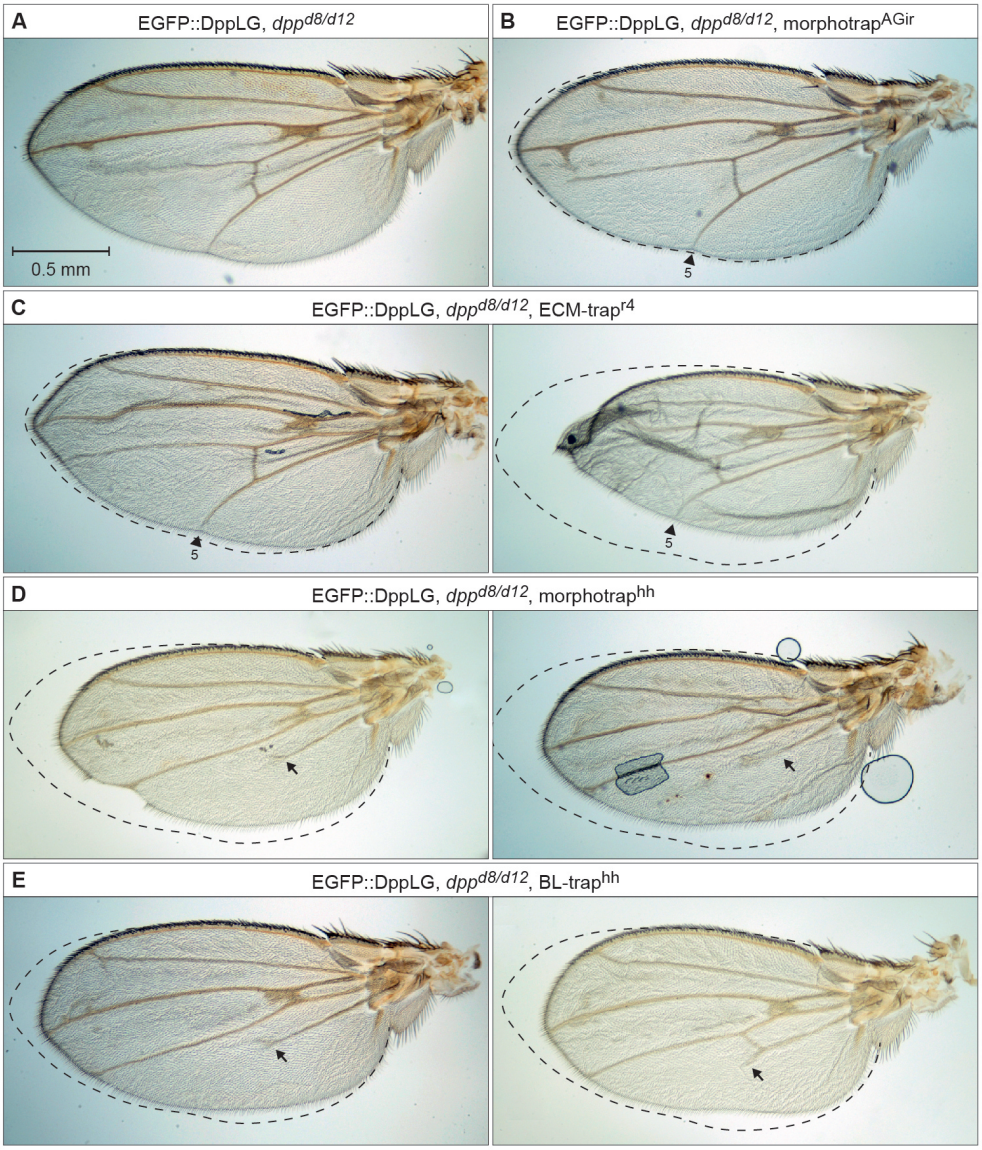

Figure 32: The lateral Dpp gradient instructs the patterning of the wing disc
A, Wing of a $dpp^{d8/d12}$ mutant fly rescued by EGFP::Dpp expression. **B**, Wing of a $dpp^{d8/d12}$ mutant fly rescued by EGFP::Dpp, expressing morphotrap in the PPM. LV5 is properly defined (arrowhead) and wing blade size is simmilar to control wings. The shape of the control wing shown in (A) is marked by a dotted black line. **C**, Wing of a $dpp^{d8/d12}$ mutant fly rescued by EGFP::Dpp, expressing ECM-trap in the fat body (*r4::Gal4*). Reducing basal EGFP::Dpp dispersal does not affect patterning (LV5 is present) but results in reduced wing blade size. **D**, Wing of $dpp^{d8/d12}$ mutant flies rescued by EGFP::Dpp, expressing morphotrap in the posterior compartment (*hh::Gal4*). LV5 is lost (see arrows) and wing blade size is strongly reduced. **E**, Wings of $dpp^{d8/d12}$ mutant flies rescued by EGFP::Dpp, expressing BL-trap in posterior cells. Also here, LV5 is affected, however wing blade area is less strongly reduced than in (D). All images are show at the same magnification, scale bar is shown in (A).

8.7 The Dpp receptor Tkv localizes basolateral and can be mislocalized using SBNs

The data shown before suggests that the basolateral pool of Dpp is of high importance for patterning and growth control of the wing disc. Since we aim to understand the role of morphogen dispersal and perception along the apicobasal axis, we also investigated the subcellular localization of the Dpp type I receptor Tkv. For this purpose we used a Tkv-YFP protein-trap line [210] that carries a Yellow fluorescent protein (YFP)-cassette flanked by splice acceptor sites at the endogenous *tkv* locus, such that the YFP is include in the mature Tkv protein.

The Tkv-YFP protein-trap line recapitulates the expected Tkv expression profile along the A-P axis, with low central Tkv levels and gradually increasing levels towards the lateral edges of the disc (Fig.33A). Interestingly, when we investigate the subcelllar

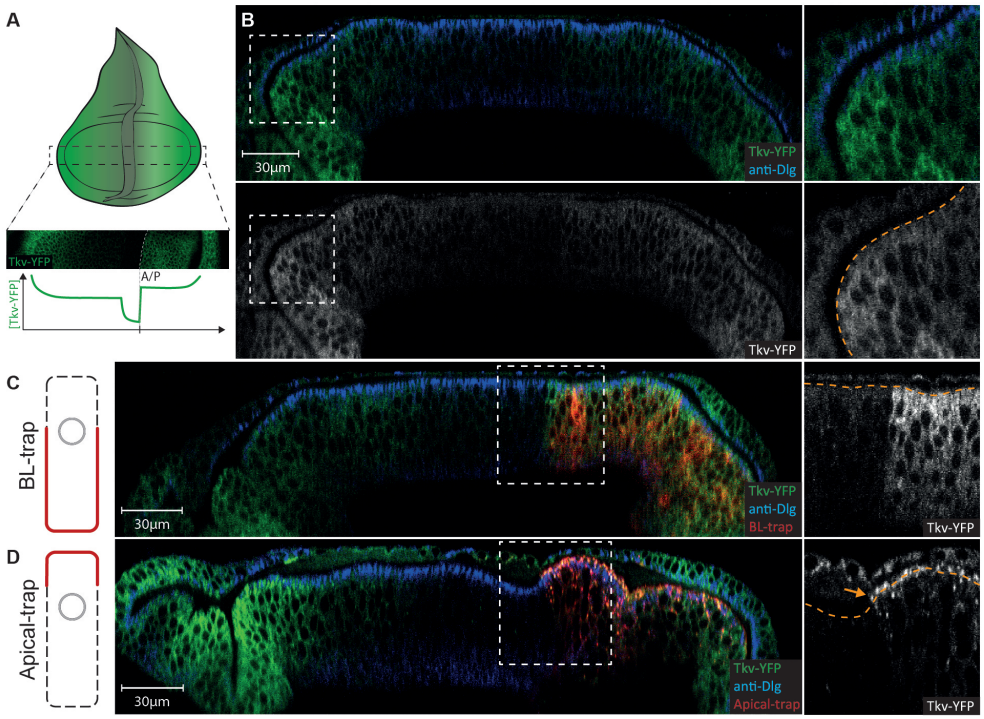

Figure 33: Tkv localizes to the basolateral compartment and can be mislocalized by SBNs
A, TkvYFP (green) protein levels along the A-P axis. **B**, Cross-section of a TkvYFP heterozygous wing disc stained for Dlg. The marked regions are enlarged to the right. The level of the junctions, marked by Dlg (blue), is drawn with a dotted orange line. No YFP signal is observed above the junctions, also not in the lateral region where TkvYFP levels are highest. **C**, Cross-section of a TkvYFP heterozygous wing disc expressing BL-trap (red) in the posterior compartment (*hh::Gal4*) stained for Dlg. BL-trap expression results in stabilization of TkvYFP along the basolateral compartment. D, Cross-section of a TkvYFP heterozygous wing disc expressing Apical-trap (red) in the posterior compartment (*hh::Gal4*) stained for Dlg. Apical-trap partially mislocalizes TkvYFP to the apical surface of DP cells (arrow).

localization of Tkv-YFP, we find that it localizes to the basolateral compartment of the wing disc exclusively, with no visual apical fraction (Fig.33B). Basolateral localization of the BMP-II receptors was also observed in mammalian cell culture [221].

In order to better understand the role of polarized receptor localization, we wanted to test if SBNs are potential tools to mislocalize transmembrane proteins, such as Tkv-YFP, along the apicobasal axis. Since Tkv-YFP carries the YFP-tag in the extracellular domain, YFP might be accessible to the vhhGFP4 domain of the SBNs. To test if the SBNs can interact with Tkv-YFP, we first expressed BL-trap in the posterior compartment (*hh:Gal4*) of Tkv-YFP heterozygous flies (Fig.33C). Expression of BL-trap resulted in increased YFP signal along the basolateral side of the posterior compartment. Interestingly, expression of Apical-trap in posterior cells of Tkv-YFP heterozygous flies resulted in a partial mislocalization of Tkv-YFP to the apical compartment (Fig.33D). These findings suggest that SBNs can interact with GFP/YFP-tagged transmembrane proteins and induce a localization bias along the apicobasal axis. Therefore SBNs are potential tools to disturb protein localization along the apicobasal axis and investigate the function of proteins with polarized localization. It will be interesting to see if future experiments using SBNs can help to understanding the role of basolateral Tkv localization.

9 Discussion and Outlook

Here we studied the subcellular localization of EGFP::Dpp gradient formation in the *Drosophila* wing imaginal disc using SBNs. We find that the EGFP::Dpp gradient consists of two fractions of different concentrations, a small apical/luminal one and a large basolateral one. In order to investigate the respective contributions to pattering and growth of these two fractions, we created and characterized SBNs that localize to specific subcellular regions along the apicobasal axis of the wing disc. SBNs allow us to reduce or block the dispersal of specific gradient subfractions and assess their contribution to wing development. We find evidence that the pattering function of the Dpp gradient is executed by Dpp dispersing in the lateral plane of the wing disc epithelium. In contrast, we find that the growth of the wing disc is influenced by EGFP::Dpp spreading in the lateral plane, as well as in the disc lumen and in the BL.

We find evidence that patterning strictly depends on the formation of the lateral EGFP::Dpp gradient within the epithelial plane. This conclusion is based on three findings: (1) The co-expression of EGFP::Dpp and BL-trap results in the loss of two LVs, presumably LVs 2 and 5 which are positioned by Dpp. (2) Reducing basolateral spreading in the posterior compartment by BL-trap results in a loss of LV 5. And (3) the block of basal EGFP::Dpp spreading using ECM-trap does not affect the positioning of the LVs and hence the patterning. However, there are two caveats we did not yet investigate, but that will be addressed in further experimental setups. First, we have not shown that BL-trap indeed completely blocks the release of basolateral EGFP::Dpp from source cells. And second, we cannot say if EGFP::Dpp is still secreted along the apical surface when BL-trap is expressed in source cells. These points can be investigated by co-expression of EGFP::Dpp and BL-trap in source cells and expression of morphotrap in clones (analogous to what we have done before to investigate the efficiency of morphotrap [215]). In such a situation, morphotrap clones should not accumulate EGFP::Dpp along their basolateral surface, but exclusively trap EGFP:Dpp on their lumen facing apical surface.

In striking contrast to patterning, we obtained evidence, that growth of the wing pouch and the adult wing blade is controlled by both, the apical and basolateral fractions of EGFP::Dpp. This suggestion is mainly based on the finding that the co-expression of EGFP::Dpp with BL-trap results in significantly increased wing blade area compared to morphotrap expression (Fig.31C and D). While in the morphotrap co-expression condition, the release of basolateral and apical EGFP::Dpp is blocked, co-expression of EGFP::Dpp with BL-trap should not interfere with the apical fraction of EGFP::Dpp. These results suggest that the increase in wing blade area observed, might be due to a growth promoting function of apical/luminal EGFP::Dpp. However, this hypothesis is not supported by the observations (1) that PPM expression of morphotrap does not affect wing disc growth and (2) that the Dpp receptors localize to the basolateral side of the DP epithelium. For this reason, it will be crucial to test if PPM expression of morphotrap effectively blocks luminal EGFP::Dpp dispersal. To do so, the same approach suggested as for BL-trap can be used. PPM expression of

morphotrap and additional expression of morphotrap in clones can be used to ask if PPM expression of morphotrap affects the apical accumulation of EGFP::Dpp in DP cells. If this is not the case, other setups to specifically target apical EGFP::Dpp dispersal will need to be established. Alternative approaches include the co-expression of Apical-trap in Dpp source cells and optimization of Apical-trap localization, e.g. by using other scaffold-proteins. Zona pellucida proteins for example are well known transmembrane proteins that localize to the apical cell surface [222] and therefore are potential scaffold alternatives.

Another contradictory finding is that the Dpp type-I receptor Tkv localizes to the basolateral compartment. In addition to Tkv, also the type-II receptor Punt was observed to localize to the basolateral compartment (personal communication with I. Alborelli). This raises the question, how an apical fraction of Dpp could be sensed by DP cells. One possibility is that Tkv and Punt mainly reside along the basolateral surface, and apically localized Tkv and Punt is re-internalized at fast rates. Experiments in which endocytosis is blocked in clones (e.g. *shibire* mutant clones [83]) should provide evidence, if Tkv and Punt accumulate along the apical surface of such clones. Another explanation could be that apical EGFP::Dpp is transcytosed to the basal surface in a glypican-dependent manner, as it was suggested for Wg [186]. In support of this hypothesis, the glypicals Dally and Dlp both are enriched along the apical surface of DP cells (personal communication with I. Alborelli and S. Matsuda). Further investigations are needed to understand the role of receptor localization for Dpp spreading and perception.

One of our major findings is that Dpp spreading is not restricted to a single subcellular environment, but that different pools of Dpp disperse in different environments and potentially by different mechanisms. We find that morphotrap expression in the posterior compartment results in high EGFP::Dpp accumulation in PPM cells, but very low accumulation along the apical surface of DP cells located adjacent to the source. These findings clearly suggests that Dpp disperses in the lumen via free diffusion, since restricted diffusion and transport along cytonemes should take place along the apical surface and hence not result in high PPM accumulation. In contrast, the EGFP::Dpp accumulation pattern in the ECM-trap experiments suggest that low amounts of EGFP::Dpp leave the DP epithelium to disperse within the BL, an observation not consistent with transport along basal cytonemes (as observed in Fig.25).

In summary, our observations suggest that the majority of EGFP::Dpp disperses within the lateral plane of the wing disc epithelium. Moreover, we have shown that the lateral fraction of EGFP::Dpp carries the patterning function of the Dpp gradient. Especially for the patterning process morphogen levels have to be measured and interpreted precisely by target cells. In addition, it seems that robust gradient formation and scaling is the foundation for proper appendage development. Therefore, we tempt to speculate that dispersal within the epithelial plane is a necessity to allow robust gradient formation, since the dispersal properties are precisely controlled by adjusting cell shape, receptors and interaction partner levels.

10 Appendix

10.1 Further publications

Reprint from Cytokine Growth Factor Rev, Vol.27, S. Matsuda, et al., BMP morphogen gradients in flies, pg.119-127, (2015), http://dx.doi.org/ 10.1016/j.cytogfr.2015.11.003 with permission from Elsevier.

G Model
CGFR 897 No. of Pages 9

ARTICLE IN PRESS

Cytokine & Growth Factor Reviews xxx (2015) xxx–xxx

Contents lists available at ScienceDirect

Cytokine & Growth Factor Reviews

journal homepage: www.elsevier.com/locate/cytogfr

Mini review

BMP morphogen gradients in flies

Shinya Matsuda, Stefan Harmansa, Markus Affolter*

Biozentrum der Universität Basel, Klingelbergstrasse 50/70, CH-4053 Basel, Switzerland

ARTICLE INFO

Article history:
Received 19 November 2015
Accepted 20 November 2015
Available online xxx

Keywords:
Morphogen
Dpp
Growth and patterning
Nanobody
Genome engineering

ABSTRACT

Bone morphogenetic proteins (BMPs) act as morphogens to control patterning and growth in a variety of developing tissues in different species. How BMP morphogen gradients are established and interpreted in the target tissues has been extensively studied in *Drosophila melanogaster*. In *Drosophila*, Decapentaplegic (Dpp), a homologue of vertebrate BMP2/4, acts as a morphogen to control dorsal–ventral patterning of the early embryo and anterior–posterior patterning and growth of the wing imaginal disc. Despite intensive efforts over the last twenty years, how the Dpp morphogen gradient in the wing imaginal disc forms remains controversial, while gradient formation in the early embryo is well understood. In this review, we first focus on the current models of Dpp morphogen gradient formation in these two tissues, and then discuss new strategies using genome engineering and nanobodies to tackle open questions.

1. Introduction

Morphogens are secreted molecules controlling the patterning of tissues and organs in a concentration-dependent manner. From their region of production (the source), morphogens form concentration gradients into the adjacent target tissue. Cells in the target tissue acquire positional information by reading the local morphogen concentration (or other morphogen parameters), and regulate target gene expression according to thresholds [1]. Thereby, morphogens can subdivide tissues into defined subdomains with distinct cell fates (French flag model) [2].

Bone morphogenetic proteins (BMPs) belong to one of the best-studied family of morphogens. In *Drosophila*, there are three BMP-type ligands, Decapentaplegic (Dpp), Screw (Scw), and Glass bottom boat (Gbb) [3–5]. Dpp is the *Drosophila* homolog of vertebrate BMP2/4, Gbb is the homolog of BMP5/6/7/8, and Scw is a distant relative of the BMP5/6/7/8 subclass, with no clear vertebrate ortholog. BMP-type ligands act as homo- or heterodimers and bind to type I receptors Thickveins (Tkv) and Saxophone (Sax). Dpp preferentially binds to Tkv, while Gbb preferentially signals via binding to Sax [6]. Upon Dpp binding, the Type II receptor Punt phosphorylates and thereby activates Tkv. Mothers against dpp (Mad) is then phosphorylated by Tkv, and the phosphorylated Mad (pMad) translocates to the nucleus together with the Smad4 homolog Medea, and regulates expression of target genes [7–9].

Among the three BMP-type ligands, mutants lacking Dpp show the most dramatic phenotype affecting all fifteen imaginal discs of the *Drosophila* larvae [10]. Importantly, Dpp represents the first validated secreted morphogen [11–13]. An important criteria showing that Dpp indeed acts as a bona fide morphogen was that a constitutively active form of the Dpp receptor Tkv acts cell autonomously, while the Dpp ligand acts through its receptors Tkv and Punt on surrounding cells in a non-cell autonomous manner. This excluded the possibility that long-range action of Dpp was mediated via a relay mechanism that involves secondary signals downstream of BMP signaling, and showed that Dpp acted directly at the level of its receptors in distant cells [12].

Since there is no good Dpp antibody, the Dpp morphogen gradient has been visualized by overexpression of tagged Dpp or genomic tagged Dpp capable to rescue to some degree the mutant phenotype [14–17]. The mechanisms of gradient formation have been intensively studied using these tools, especially in dorsal–ventral patterning of the early embryo and in anterior–posterior patterning of the larval wing imaginal disc. Although Dpp acts as a morphogen in both tissues, the shape and the timescale of the activity of the morphogen gradient differ largely. For example, during embryonic development, *dpp* is uniformly expressed at the dorsal side of the embryo and a sharp morphogen gradient is established within the *dpp* expression domain in 30–40 min [18]. In contrast, in the larval wing disc, *dpp* is expressed in a stripe of anterior cells at the anterior–posterior compartment boundary. A shallow Dpp morphogen gradient is established in the adjacent target tissue, outside the *dpp* expression domain, during much of the four days of larval development. Furthermore, while cells in the embryonic target field do not proliferate during Dpp gradient

* Corresponding author.
E-mail address: markus.affolter@unibas.ch (M. Affolter).

http://dx.doi.org/10.1016/j.cytogfr.2015.11.003
1359-6101/

formation, the cells in the wing disc are highly proliferative, leading to a continuous increase of the size of the target tissue.

In line with these differences, past studies have indeed shown that different molecular mechanisms operate to establish the Dpp morphogen gradient in the embryo and in the wing imaginal disc. While the Dpp morphogen gradient is established by an active transport mechanism in the embryo [18], several models have been proposed for Dpp dispersal in the wing imaginal disc. In this review, we summarize the current understanding on how the Dpp morphogen gradient is established in these two developmental processes, and discuss new approaches, which might allow to better study morphogen dispersal and its effects on patterning and growth of the wing imaginal disc.

2. Dpp morphogen gradient formation in the embryo

In the early *Drosophila* embryo, Dpp is uniformly expressed in the dorsal side of the embryo. At the early blastoderm stage, Dpp signaling is uniform and low along the dorsal side. During cellularization, a sharp Dpp signaling profile becomes evident at the dorsal midline of the embryo (Fig. 1A). High levels of Dpp signaling in the dorsal midline region specify the extraembryonic amnioserosa, while lower levels of Dpp signaling in the more lateral cells specify the dorsal ectoderm (Fig. 1C) [11,19].

Two studies successfully visualized the Dpp morphogen gradient in the early embryo [16,17]. Shimmi et al . utilized a genomic construct containing all Dpp coding exons fused to three HA-tags under the control of an embryonic enhancer that can rescue the embryonic lethality of *dpp* mutants. Using available anti-HA antibodies, this approach revealed that Dpp-HA is initially uniformly distributed along the dorsal surface of the early blastoderm embryo, and subsequently accumulates at the dorsal midline during cellularization, when pMad levels also rise (Fig. 1B). In another study, Wang and Ferguson injected an anti-GFP antibody into the perivitelline space in order to detect the extracellular fraction of GFP-tagged Dpp (GFP-Dpp). Although GFP-Dpp was ectopically expressed under the control of the *even-skipped* stripe 2 (*eve-st2*) enhancer, Dpp was redistributed to the dorsal midline (Fig. 1B). This observation suggests that Dpp is redistributed by an active transport mechanism.

Dpp morphogen gradient formation in the embryo depends on the extracellular proteins Short gastrulation (Sog), Twisted gastrulation (Tsg), Tolloid (Tld), and Screw (Scw) [5,20–22]. Biochemical studies revealed the molecular function of these

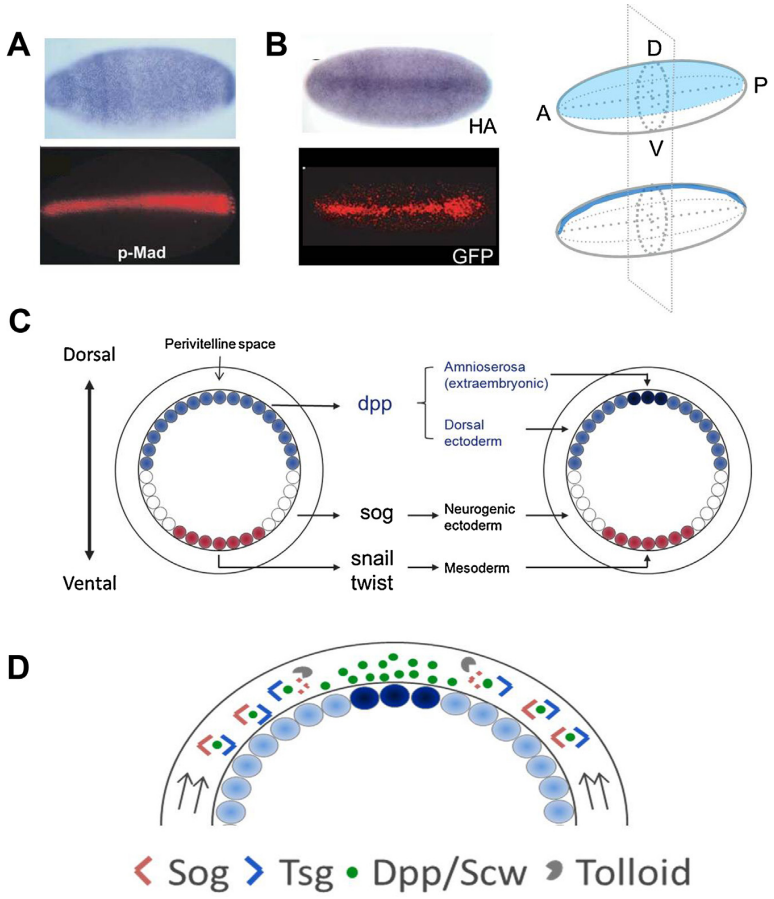

Fig. 1. (A) Uniform Dpp expression along the dorsal side of the early embryo and a sharp pMad gradient at the dorsal midline (images from [16]). (B) Dpp-HA and GFP-Dpp accumulation in the dorsal midline of the embryo (images from [16,17]). Schematic view of the embryo showing *dpp* expression (light blue) and accumulation (blue). (C) Schematic cross-section of the early embryo. Dpp acts as a morphogen to specify the extraembryonic amnioserosa and the dorsal ectoderm. (D) A proposed active Dpp transport model. Dpp/Scw heterodimers bind to Sog/Tsg, this complex cannot bind to the receptor but is transported toward the dorsal midline promoted by the graded ventral–dorsal Sog concentration. Dpp/Scw heterodimers are released at the dorsal midline by Tld-mediated Sog processing.

Please cite this article in press as: S. Matsuda, et al., BMP morphogen gradients in flies, Cytokine Growth Factor Rev (2015), http://dx.doi.org/10.1016/j.cytogfr.2015.11.003

proteins; Sog and Tsg are BMP inhibitors that prevent Dpp binding to its receptor [22], while Tld is a metalloprotease that processes Sog [23]. Sog, Tsg, and Tld are evolutionarily conserved [24–28].

How do these players regulate the formation of the Dpp morphogen gradient? Sog is produced in the ventral–lateral regions of the embryo and forms a concentration gradient towards the dorsal side [29]. Based on the biochemical function of Sog as a BMP inhibitor, it was suggested that Sog could be involved in generating the inverse dorsal–ventral Dpp activity gradient via its repressive function. However, this model only provided an explanation for the lateral refinement of decreasing Dpp signaling level, but failed to account for the intensification of Dpp signaling at the dorsal midline. Interestingly, the pMad signaling gradient fails to intensify at the dorsal midline in *sog* and *tsg* mutants, accompanied by a loss of amnioserosa markers [20,22]. These observations could not be explained by a purely inhibitory action of Sog. Thus, how the increase of BMP signaling required for dorsal midline development could be brought about by the BMP inhibitors Sog and Tsg remained an open question. A model explaining this paradoxical situation suggested that Sog and Tsg not only act as inhibitors but can also shuttle BMP-type ligands towards the dorsal midline [30] (Fig. 1D). In line with this proposal, long-range enhancement of BMP signaling by Sog has indeed been reported [31–33].

The active transport mechanism was directly tested by visualization of Dpp redistribution in the early embryo [16,17]. These studies revealed that Dpp is indeed redistributed toward the dorsal midline and that this redistribution requires Sog and Tsg. Collectively, these data suggest that Sog and Tsg form a complex together with Dpp, and that this complex is shuttled toward the dorsal midline. The direction of Dpp transport is determined by high ventral–lateral expression of Sog [29]. To activate Dpp signaling at the dorsal midline, Dpp needs to be released by the metalloprotease Tolloid (Tld), which mediates Sog processing [21,23].

Another BMP type ligand Scw is also involved in the dorsal–ventral patterning of the embryo [5]. In contrast to Dpp homodimers, Scw homodimers have a very weak signaling activity in vitro . For a long time, it was not clear how these two BMP-type ligands with different signaling activity contributed to the dorsal–ventral patterning of the early embryo. Interestingly, biochemical studies showed that Dpp and Scw form heterodimers and that Dpp/Scw heterodimers show a higher signaling activity than Dpp homodimers. Furthermore, Dpp/Scw heterodimers interact with Sog/Tsg and induce Tld-mediated Sog processing more effectively than Dpp homodimer in vitro [16]. Thus it is likely that Dpp/Scw heterodimers are the primary ligands transported by Sog/Tsg, while Dpp homodimers mainly contribute to the short-range signal in the dorsal–lateral region of the embryo. Consistent with this interpretation, the dorsal accumulation of Dpp was lost in *scw* mutants [16,17]. The critical role of BMP heterodimeric ligands in the establishment of BMP gradients was also proposed in the vertebrate embryo [34,35].

In addition to the active extracellular Dpp transport mechanism, a positive feedback mechanism through yet unknown transcriptional targets was found to be involved in Dpp gradient formation in the early embryo [17]. Injecting mRNA encoding the constitutively active form of Tkv (but not the injection of wild type Tkv mRNA) results in accumulation of GFP-Dpp at the site of injection in embryos expressing GFP-Dpp under the control of the *even-skipped* stripe 2 (*eve-st2*) enhancer. Furthermore, Dpp redistribution toward the dorsal midline was lost in *medea* mutants. These observations indicate that Dpp signaling promotes interaction between Dpp and Tkv through unknown downstream target genes. A similar positive feedback mechanism was also proposed for wing vein specification in the pupal wing [36]. Recent

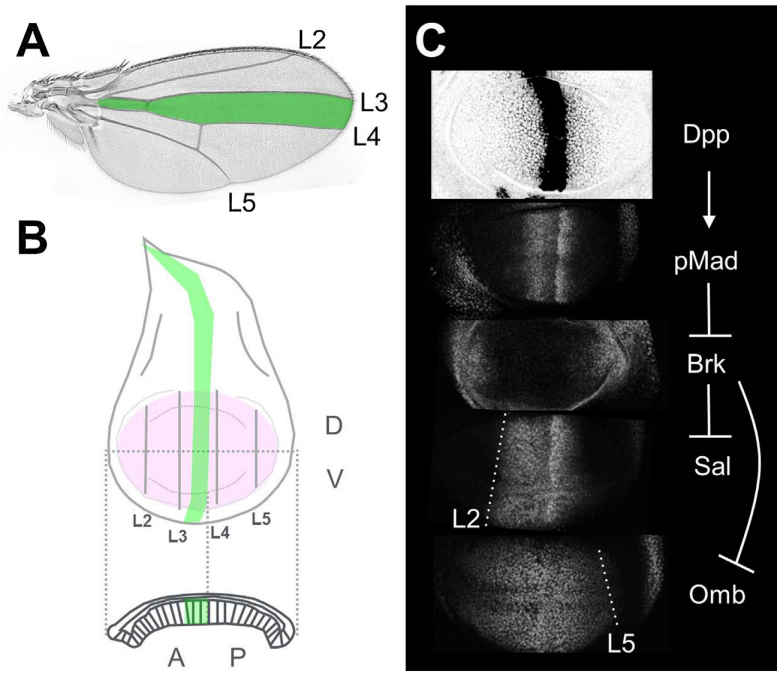

Fig. 2. (A) Wild type adult *Drosophila* wing. Wing veins (L2–L5) are patterned along the anterior–posterior axis. (B) Schematic view of the wing imaginal disc. *dpp* is expressed at the border of the anterior–posterior boundary (green). The future wing vein positions are specified along the anterior–posterior axis in the wing pouch (pink). (C) The Dpp morphogen gradient visualized by overexpression of GFP-Dpp by dpp-Gal4 (dpp > GFP-Dpp), its activity gradient (pMad), and downstream gene expression of Dpp targets (*brk*,*sal* and *omb*).

Please cite this article in press as: S. Matsuda, et al., BMP morphogen gradients in flies, Cytokine Growth Factor Rev (2015), http://dx.doi.org/10.1016/j.cytogfr.2015.11.003

studies indeed identified Dpp target genes required for enhanced Dpp signaling [37,38]. The *Drosophila* tumor necrosis factor α homolog Eiger (Egr) promotes Dpp signaling through the Jun N-terminal kinase (JNK) pathway. However, it remains unclear how the JNK pathway promotes enhanced Dpp signaling and whether it is involved in the positive feedback mechanism, which promotes Dpp–Tkv interaction in the early embryo [38]. It has also been shown recently that integrin signaling promotes Dpp signaling and that an α-integrin subunit is a Dpp target gene [37]. It will be interesting to test if Dpp–Tkv interaction is affected in these mutants.

All the components required for Dpp transport in the early fly embryo, i.e., Sog, Tsg, and Tld, are evolutionarily conserved [24–28], and active transport mechanism for BMP-type ligands are also involved in dorsal-ventral patterning of early embryos of other species such as *Xenopus* and *Tribolium* ([39,40], reviewed in [41]). Furthermore, an active Dpp transport mechanism is also used in other *Drosophila* tissues, e.g., in the pupal wing during specification of the posterior crossvein, where Dpp is transported from the longitudinal veins to the posterior crossvein territory by Sog and the Tsg paralog Crossveinless and released by Tolloid-related (Tlr) [36,42,43].

Heparan sulfate proteoglycans (HSPGs) play a critical role in morphogen gradient formation in a variety of contexts. In *Drosophila*, for example, the HSPGs *dally* and *dally-like* are critical for Dpp morphogen gradient formation in the wing imaginal disc [44–47]. However, the function of HSPGs seems to be inverse in the embryo as compared to the wing (see below), since heparin inhibits Dpp signaling during dorsal–ventral patterning of the embryo. In the early embryo, HSPGs are suppressed by delayed translation of mRNAs encoding enzymes essential for HSPG synthesis, thus facilitating BMP transport at this developmental stage [48]. The critical role of ECM proteins of the type IV Collagen, Vkg and Cg25c, has recently been reported in Dpp morphogen gradient formation in the embryo. Dpp binds to Type IV collagens and Type IV collagens are required for Dpp gradient formation, for Dpp signaling activity, and thereby also for target gene expression [49]. Biochemical data suggest that Collagen IV acts as a scaffold to assemble the Dpp/Scw/Sog/Tsg complex, which is critical for Dpp gradient formation [50].Collagen IV has been shown to have an additional function to potentiate Dpp signaling. Collagen IV binds its receptor integrin, thereby activating integrin signaling which is necessary for the dorsal peak of Dpp signaling in the embryo through interaction with Tkv [37].

3. Dpp morphogen gradient formation in the wing imaginal disc

In the wing imaginal disc, Dpp is expressed in a stripe of anterior cells adjacent to the anterior–posterior compartment boundary (Fig. 2). From this source, Dpp forms concentration gradients into both the anterior and the posterior compartment, controlling a number of aspects of patterning and growth of the wing imaginal disc, particularly in the wing pouch. Visualization of the BMP activity gradient using an antibody specific for pMad revealed that Dpp signaling is relatively weak in the Dpp source cells but high adjacent to it and then graded towards the peripheral region of the wing pouch [51]. Dpp signaling activity inhibits the expression of the transcriptional repressor Brinker (Brk), resulting in a gradient of Brk inverse in shape to the Dpp activity gradient [52,53]. The relative levels of Dpp signaling and Brk are translated into the nested expression patterns of target genes such as *daugthers against dpp (dad)*, *spalt* (*sal*), and *optomotor blind* (*omb*) [7,54–56] (Fig. 2C). A consequence of the Dpp/Brk-mediated patterning is the positioning of wing vein 2 (L2), which is induced at the border of *sal* expression in the anterior compartment, and wing vein 5 (L5), which is induced at the posterior border of *omb* and *brk* expression (Fig. 2) [7,57,58]. BMP signaling was also shown to be important for regulating the growth of the wing imaginal disc, in particular the wing pouch. *dpp* mutants lacking the enhancer required for *dpp* expression in the imaginal disc show significantly reduced adult wing size [10,59], while ectopic

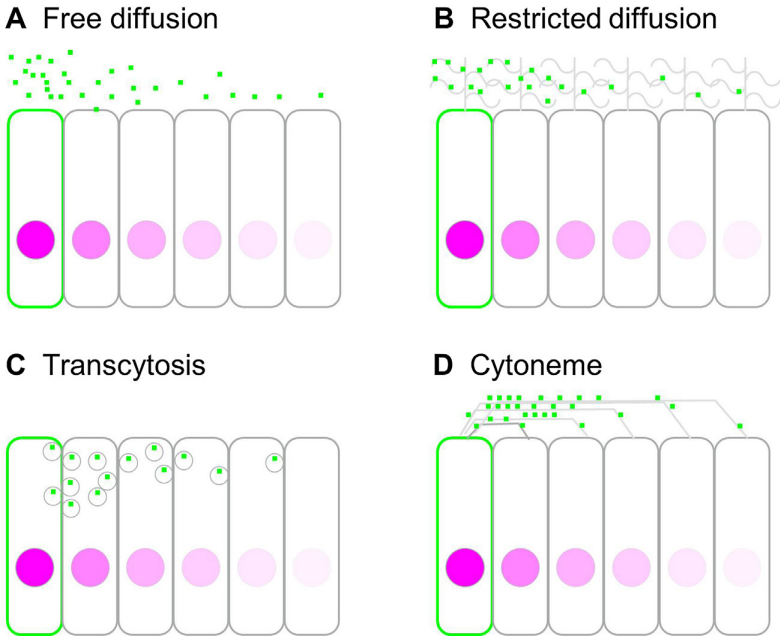

Fig. 3. Schematic representation of Dpp dispersal mechanisms in the wing disc. For simplicity the dispersal mechanisms are depicted along the apical surface of the wing disc, however Dpp dispersal could also take place along the basal surface or within the wing disc epithelium. (A) Free diffusion model. Dpp dispersals via free diffusion in the extracellular space. (B) Restricted diffusion model. Dpp dispersal requires interaction of Dpp with HSPGs. (C) Transcytosis model. Dpp dispersal requires repeated endocytosis and exocytosis. (D) Cytoneme model. Dpp dispersal requires actin-based fibers to connect Dpp producing cells to receiving cells.

Please cite this article in press as: S. Matsuda, et al., BMP morphogen gradients in flies, Cytokine Growth Factor Rev (2015), http://dx.doi.org/10.1016/j.cytogfr.2015.11.003

activation of Dpp signaling induces overgrowth of the imaginal disc [60–62]. In addition, the hox gene Ultrabithorax (Ubx) was shown to control differences in organ size between the wing imaginal disc and the haltere disc in part through differential regulation of Dpp transcription and Dpp mobility [63].

The Dpp morphogen gradient has been visualized via the expression of a GFP-tagged Dpp fusion protein [14,15] that can partially rescue the growth and patterning defects of *dpp* disc mutants (Fig. 2C). GFP-Dpp forms steep gradients along the anterior–posterior axis when expressed in the centrally located stripe source. Using GFP-Dpp fusion proteins and characterizing their properties in different genetic backgrounds, a variety of mechanisms have been proposed to be involved in establishing the morphogen gradient. The current models involve (1) diffusion-based mechanisms (free or restricted diffusion) and (2) active transport mechanisms (transcytosis or cytonemes) (Fig. 3).

3.1. Free diffusion model

The simplest mechanism, which could account for the formation of a morphogen gradient, is free extracellular diffusion and receptor-mediated degradation (Fig. 3A). In such a case, the diffusion coefficient of morphogen dispersal should be in the range of a similarly sized molecule diffusing in water (50–100 $\mu m^2 s^{-1}$). However, the diffusion coefficient of GFP-Dpp measured by fluorescence recovery after photobleaching (FRAP) assays was measured to be two orders of magnitude lower than expected for free diffusion ($0.1 \pm 0.05\ \mu m^2 s^{-1}$) [64], arguing against a free diffusion model.

However, and in support of free diffusion, a recent study argued that the slow recovery of GFP-Dpp observed in FRAP experiments does not necessarily arise from a slow diffusion process. In a scenario, in which only a small amount of morphogen is mobile and disperses via fast free diffusion, coupled with slow immobilization (e.g., via receptor or ECM binding) and/or slow degradation of the ligand, the GFP-Dpp recovery observed by FRAP would be governed by the later, slower processes [65]. Therefore, the FRAP kinetics yield little information about ligand transport; it might thus be difficult to distinguish between slow and fast diffusing molecules by using FRAP analyses. To directly measure the diffusion coefficient of GFP-Dpp in vivo, single molecules of Dpp were directly followed by fluorescence correlation spectroscopy (FCS) and by pair correlation function (pCF) microscopy. These measurements revealed that 65% of the Dpp ligands diffuse rapidly ($D = 21 \pm 3\ \mu m^2 s^{-1}$ for DppDendra2, $D = 10 \pm 1\ \mu m^2 s^{-1}$ for Dpp-GFP), and 35% of ligands diffuse slowly ($D = 0.03 \pm 0.006\ \mu m^2 s^{-1}$ for DppDendra2, $D = 0.08 \pm 0.01\ \mu m^2 s^{-1}$ for DppGFP). The fast diffusion coefficient is consistent with free diffusion, and the slow diffusion coefficient is consistent with Dpp bound to receptors or glypicans [65]. It remains to be tested whether the fast diffusing fraction of Dpp indeed plays a critical role in the formation of the Dpp gradient, and what the role of the slow diffusing fraction is.

3.2. Restricted diffusion model

The restricted diffusion model postulates that extracellular diffusion of a morphogen is hindered by the geometry of cell packing (tortuosity) and and/or by transient interactions with receptors or ECM proteins [66] (Fig. 3B). In the case of Dpp, it has been proposed that Tkv impedes Dpp dispersal through receptor-mediated uptake and degradation [51,67]. Dpp was also shown to bind to the HSPGs *dally* and *dally-like*, which are required for Dpp morphogen gradient formation [44–47,68,69]. Dpp cannot accumulate and activate Dpp signaling behind *dally*, *dlp* double mutant clones, consistent with a role of HSPGs in Dpp transport. However, it remains unclear whether HSPGs are indeed required for Dpp transport and/or for Dpp stabilization downstream of the diffusion processes. To distinguish this, it would be important to know whether Dpp can disperse but fails to signal or whether Dpp dispersal itself is impaired in the absence of *dally* and *dlp*.

3.3. Transcytosis model

Transport via transcytosis, involving repeated receptor-mediated endocytosis and subsequent exocytosis of the ligand, has also been proposed as a mechanism by which Dpp disperses in the wing imaginal disc tissue [15,64,70,71] (Fig. 3C). This model is based on the observation that Dpp cannot accumulate across clones mutant for *shibire* (*shi*), which encodes a Dynamin GTPase required for endocytosis [15]. However, theoretical and experimental evidence challenging the transcytosis model has been reported [65,72,73]. Theoretically, Lander et al. showed that accumulation of the Dpp receptor Tkv in endocytosis defective cells can inhibit extracellular Dpp diffusion and cause the observed defect in Dpp dispersal behind *shi* mutant clones [72]. Experimentally, extracellular staining of GFP-Dpp showed that Dpp was able to accumulate over *shi* mutant clones, and that Dpp signaling was unaffected behind *shi* single mutant or *tkv*, *brk* double mutant clones [69,73].

3.4. Cytoneme model

Other studies on the wing imaginal disc have proposed that Dpp is directly transported to the target cells along actin-based filopodia, called cytonemes (Fig. 3D). Cytonemes extend from the apical surface of Dpp responding cells and directly contact Dpp producing cells [74–78]. It remains unknown whether formation of the Dpp morphogen gradient depends on cytonemes, but a link between cytonemes and Dpp signaling has been reported. First, apical cytonemes were found to be oriented towards the anterior–posterior compartment boundary, where Dpp is produced. The direct contact of Dpp producing cells and responding cells was more recently shown by the GRASP technique, although it is not clear where the contact is formed along the apical-basal axis [78]. Second, Dpp is required for and sufficient to extend and maintain cytonemes. Third, Tkv moves along apical cytonemes [75]. Although the functional impact of cytonemes on Dpp morphogen gradient formation in the wing disc remains to be addressed, a recent study showed that cells in the air sac primordium, which is associated with the wing imaginal disc, extend basal cytonemes towards Dpp producing cells in the wing disc proper, and Dpp transport was observed along these cytonemes [78]. Importantly, factors required for cytoneme formation were identified. *diaphanous* (*dia*) and *neuroglian* (*nrg*) are required for cytoneme formation and *capricious* (*caps*) is required for contact formation of air sac cytonemes with Dpp producing cells. Loss of function of these factors in the air sac primordium affects Dpp signaling, thus showing a functional link between cytonemes and Dpp signaling. It would be interesting to test whether these factors are also critical for the apical cytonemes formed by the epithelial cells of the wing imaginal disc, and, if yes, whether these cytonemes are required for Dpp morphogen gradient formation and/or readout. Although difficult to visualize, recent studies were able to visualize cytonemes required for Hh dispersal more robustly by expressing factors stabilizing cytonemes [79]. This strategy may help to visualize and analyze the role of cytonemes in Dpp transport.

4. Novel approaches to study morphogen gradient formation

Despite intensive studies over the last twenty years, it remains unclear how the Dpp morphogen gradient is established and regulates patterning and growth of the wing imaginal disc. In order to differentiate between some of the proposed mechanisms, new

Please cite this article in press as: S. Matsuda, et al., BMP morphogen gradients in flies, Cytokine Growth Factor Rev (2015), http://dx.doi.org/10.1016/j.cytogfr.2015.11.003

approaches that specifically modify defined properties of the Dpp morphogen gradient or components proposed to be involved in Dpp dispersal are desirable.

4.1. Nanobodies: emerging new tools to study morphogen function

Engineered single-domain antibodies derived from Camelid heavy chain antibodies, so called nanobodies, have emerged as potential tools to manipulate protein function in vivo . Due to their single domain nature, they can easily be "functionalized" by fusing them to a protein domain with a specific function, and expressed in cells ([80,81]; reviewed in [82,83]). For example, an anti-GFP nanobody fused to a subunit of the ubiquitination machinery was shown to specifically degrade GFP-tagged proteins [81].

Recently, a nanobody-based morphogen trapping system called morphotrap was developed. Morphotrap consists of a GFP nanobody fused to the extracellular domain of the mouse CD8 transmembrane protein (Fig. 4A) [84]. Morphotrap was implemented as a Gal4-responsive transgene; therefore, the temporal and spatial expression pattern can be controlled by the combination of morphotrap with various Gal4 lines. In the wing disc, morphotrap can successfully retain secreted EGFP::Dpp on the cell surface of the source cells or in the target tissue via binding of GFP-Dpp to the GFP nanobody.

Using morphotrap, two models proposing how Dpp controls the growth of the wing disc were tested. The growth-equalization model (GEM) suggests that the role of Dpp is to remove the growth suppressor Brk from the medial region of the disc to allow growth, and that cells in the lateral region grow independent of Dpp signaling [85,86]. In contrast, according to the temporal rule model (TRM), all the cells in the wing disc integrate Dpp signaling levels over time and divide when Dpp signaling increased by roughly 50% [87]. Thus Dpp has an instructive role on growth in the TRM, while it acts permissive and only locally according to the GEM. A key experimental setup to discriminate between these two modes of Dpp action is to block Dpp dispersal into the target tissue to prevent a temporal increase in Dpp signaling. This was achieved by the expression of morphotrap in the Dpp source stripe of *dpp* mutant wing discs rescued by a GFP-Dpp transgene. Under these conditions, Dpp signaling was only observed in source cells and in the cells adjacent to and contacting source cells (Fig. 4B). Accordingly, the expression domains of Dpp target genes collapsed onto the source region and the adjacent cells, clearly demonstrating that Dpp dispersal is indispensable for the patterning function of Dpp. In contrast, while cell proliferation in the medial region of the wing disc (in particular in the wing pouch area) was affected, lateral cells continued to proliferate at normal levels. Thus, the lateral region of the wing disc can grow in the absence of Dpp, and thus independently of Dpp spreading. These results are inconsistent with an instructive role of Dpp for the proliferation control of the entire wing disc, as proposed in the TRM, but are in line with the GEM, in which Dpp acts preferentially in medial cells.

4.2. Genome engineering

Another approach to study morphogen function is to apply emerging genome engineering methods to manipulate gene function at the endogenous locus. Using the CRISPR technique, the *dpp* coding region was successfully flanked with FRT sites [88]. This allows excision of the corresponding fragment from the genome, thereby allowing to select the time point, at which the *dpp* gene is inactivated, as well as the cells, in which inactivation is achieved (Fig. 4C). As expected, removing Dpp from the stripe of cells at the anterior–posterior compartment boundary severely affected patterning. However, and rather surprisingly, this removal had almost no effect on growth. In contrast, growth was affected when Dpp was removed from the whole anterior compartment but not upon removal from the posterior compartment (Fig. 4D). These results appear to indicate that Dpp from the stripe regulates patterning, and a not-yet characterized source of Dpp in the

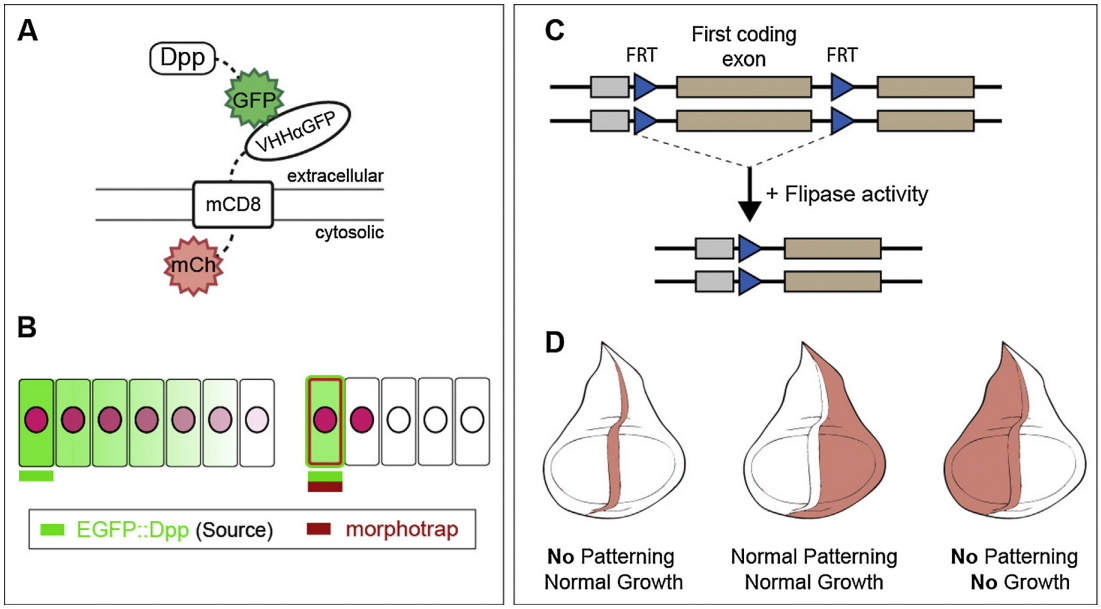

Fig. 4. (A) Schematic representation of morphotrap. The anti-GFP nanobody presented along the cell surface can immobilize EGFP::Dpp or other GFP-fusion proteins. (B) EGFP::Dpp morphogen levels (green) and Dpp signaling levels (pink) decrease with increasing distance from the morphogen source (green bar). When morphotrap is expressed in Dpp source cells (red bar), EGFP::Dpp is immobilized on source cells, hence gradient formation blocked. Only source cells and adjacent cells experience Dpp signaling. (C) Schematic representation of the inducible conditional null allele. The first coding exon of dpp is flanked by FRT sites. Flipase activity results in excision of the FRT-flanked exon and a null allele. (D) Overview over resulting patterning and growth phenotypes obtained, when FRT recombination is induced in the red marked regions of the wing disc.

Please cite this article in press as: S. Matsuda, et al., BMP morphogen gradients in flies, Cytokine Growth Factor Rev (2015), http://dx.doi.org/10.1016/j.cytogfr.2015.11.003

anterior compartment regulates growth of the wing imaginal disc. It is not clear how Dpp from different sources would be sensed by the target tissue in order to control distinct functions. In addition, Dpp expression in anterior cells distinct from the source has not been described yet. Clearly, further experiments are needed to better understand and interpret these recent observations.

5. Conclusions and future perspectives

While the active transport mechanism for Dpp morphogen gradient formation in the dorsal–ventral patterning of the early embryo is supported by a wealth of experimental evidence and is well accepted by current investigators [18], formation of the Dpp gradient in the wing imaginal disc remains controversial and highly debated. Fundamentally different mechanisms have been proposed, ranging from diffusion mechanisms (free diffusion or restricted diffusion) to active transport mechanisms (transcytosis or cytonemes) (see [66,89] for a more detailed discussion of these models.)

Due to the lack of good antibodies to detect Dpp in *Drosophila* tissue, the Dpp gradient has been visualized and quantified by the expression of GFP tagged Dpp. However, overexpression of the GFP-Dpp fusion protein might result in artifacts and non-physiological gradients. It should be also noted that GFP was inserted after the final Furin processing site in one study [14], but was inserted between two Furin processing sites in another study [15]. Thus GFP-Dpp derived from the latter study may be cleaved from the mature Dpp ligand, and therefore the GFP signal may not exclusively reflect Dpp behavior. This may be one reason why different models for gradient formation and growth control have been proposed.

It is possible that several mechanisms contribute to Dpp morphogen gradient formation. In this case, figuring out to which extent each mechanism contributes to the Dpp spreading will be a major challenge in the future. To tackle this issue, two major approaches of high potential are currently emerging: visualization and modification of the endogenous Dpp morphogen gradient.

Recent advances in genome engineering such as the availability of CRISPR technology already allowed the generation of an inducible null allele of Dpp [88]. Further applications of this approach might allow tagging Dpp at the endogenous locus. Tagging of Dpp with a fluorescent protein, such as GFP, would allow visualizing endogenous Dpp distribution, either by antibody staining or by live imaging. Furthermore, such an endogenous GFP-Dpp morphogen gradient could be manipulated by morphotrap. If a small tag is preferred to avoid changing the physical properties of the morphogen, the gradient may be manipulated by a single chain antibody against such a tag. In addition, using antibodies against the tag might allow characterizing (and manipulating) the intrinsic property of the Dpp morphogen gradient, such as production, dispersal, and degradation, under more physiologically relevant conditions.

The power of endogenous protein modification has recently been demonstrated by the group of J.P. Vincent. Alexandre et al. succeeded in modifying another morphogen, Wingless (Wg), at its endogenous locus, such that all Wg is tethered to the cell surface of Wg producing cells [90]. This approach demonstrated that long-range spreading of Wg is dispensable for patterning and, to some extent, also for growth of the fly wing. Furthermore, this approach allowed to express tethered Wg in specific tissues only, in order to sort out the role of long range signal of Wg derived from different sources on tissue growth and patterning. Tethering of all the endogenous Dpp to the surface of producing cells would most likely results in embryonic lethality, but the generation of conditional alleles might circumvent this problem.

Manipulation of endogenous morphogen dispersal by nanobodies or protein binders represents an alternative approach to the generation of conditional null alleles or conditionally membrane tethered versions of the morphogen, since morphotrap expression can be tightly controlled in a spatial-temporal manner. It is worth noting that generation of conditional null alleles or switching alleles via Flp mediated recombination depends on mRNA and protein stability itself. In contrast, nanobodies or other protein binders allow direct manipulation at the protein level, and thus these methods do not depend on mRNA and protein stability but become effective as soon as the modifiers are expressed. In the future, several variations of morphotrap are possible. By combining the GFP nanobody with a protein that localizes to specific subcellular compartments of the plasma membrane, e.g., the apical or the basolateral surface, the subcellular localization of morphotrap can be controlled. Such tools would allow dissecting the function of sub-fractions of the endogenous Dpp or Wg gradient along the apico-basal axis. Nanobodies localized to the ER might retain the morphogen in the ER, thereby blocking secretion and signaling also in source cells.

Nanobody-based approaches or approaches based on other protein binders [91], in combination with CRISPR-based genome engineering techniques, will allow direct manipulation of Dpp secretion, dispersal, and degradation, the characteristic features of morphogen gradients. This will allow testing the impact of each parameter on patterning and on growth. Importantly, this approach does not depend on the identification and modification of genes required for setting each parameter, but allows to *directly* modify the parameter itself. In addition, in order to get a more complete view of morphogen dispersal and function, it will be important to compare the results obtained from direct manipulation of the Dpp morphogen gradient with previously reported results obtained in various mutant backgrounds. Combining the new approaches with the increasing possibilities of genetic manipulations in *Drosophila* might allow a comprehensive understanding of how morphogen gradients are established and control patterning and growth of developing tissues.

Acknowledgement

We would like to acknowledge the follwoing funding sources: S. H. was supported by the 'Fellowships for Excellence' International PhD Program in Molecular Life Sciences of the Biozentrum, University of Basel and from the SystemsX.ch initiative within the framework of the MorphogenetiX projects. The work in the laboratory of M.A. was supported by grants from Cantons Basel-Stadt and Basel-Land, from the SNSF and from SystemsX.ch.

References

[1] K.W. Rogers, A.F. Schier, Morphogen gradients: from generation to interpretation, Ann. Rev. Cell Dev. Biol. 27 (2011) 377–407.
[2] L. Wolpert, Positional information and the spatial pattern of cellular differentiation, J. Theor. Biol. 25 (1) (1969) 1–47.
[3] R.W. Padgett, R.D. St Johnston, W.M. Gelbart, A transcript from a *Drosophila* pattern gene predicts a protein homologous to the transforming growth factor-beta family, Nature 325 (6099) (1987) 81–84.
[4] J.S. Doctor, et al., Sequence, biochemical characterization, and developmental expression of a new member of the TGF-beta superfamily in *Drosophila melanogaster*, Dev. Biol. 151 (2) (1992) 491–505.
[5] K. Arora, M.S. Levine, M.B. O'Connor, The screw gene encodes a ubiquitously expressed member of the TGF-beta family required for specification of dorsal cell fates in the Drosophila embryo, Genes Dev. 8 (21) (1994) 2588–2601.
[6] T.E. Haerry, et al., Synergistic signaling by two BMP ligands through the SAX and TKV receptors controls wing growth and patterning in *Drosophila*, Development 125 (20) (1998) 3977–3987.
[7] M. Affolter, K. Basler, The Decapentaplegic morphogen gradient: from pattern formation to growth regulation, Nat. Rev. Genet. 8 (9) (2007) 663–674.
[8] A. Moustakas, C.H. Heldin, The regulation of TGFbeta signal transduction, Development 136 (22) (2009) 3699–3714.

Please cite this article in press as: S. Matsuda, et al., BMP morphogen gradients in flies, Cytokine Growth Factor Rev (2015), http://dx.doi.org/10.1016/j.cytogfr.2015.11.003

[9] A.J. Peterson, M.B. O'Connor, Strategies for exploring TGF-beta signaling in *Drosophila*, Methods 68 (1) (2014) 183–193.
[10] F.A. Spencer, F.M. Hoffmann, W.M. Gelbart, Decapentaplegic: a gene complex affecting morphogenesis in *Drosophila melanogaster*, Cell 28 (3) (1982) 451–461.
[11] E.L. Ferguson, K.V. Anderson, Decapentaplegic acts as a morphogen to organize dorsal–ventral pattern in the *Drosophila* embryo, Cell 71 (3) (1992) 451–461.
[12] D. Nellen, et al., Direct and long-range action of a DPP morphogen gradient, Cell 85 (3) (1996) 357–368.
[13] T. Lecuit, et al., Two distinct mechanisms for long-range patterning by Decapentaplegic in the *Drosophila* wing, Nature 381 (6581) (1996) 387–393.
[14] A.A. Teleman, S.M. Cohen, Dpp gradient formation in the *Drosophila* wing imaginal disc, Cell 103 (6) (2000) 971–980.
[15] E.V.A. Entchev Schwabedissen, M. Gonzalez-Gaitan, Gradient formation of the TGF-beta homolog *Dpp*, Cell 103 (6) (2000) 981–991.
[16] O. Shimmi, et al., Facilitated transport of a Dpp/Scw heterodimer by Sog/Tsg leads to robust patterning of the *Drosophila blastoderm* embryo, Cell 120 (6) (2005) 873–886.
[17] Y.C. Wang, E.L. Ferguson, Spatial bistability of Dpp-receptor interactions during Drosophila dorsal–ventral patterning, Nature 434 (7030) (2005) 229–234.
[18] M.B. O'Connor, et al., Shaping BMP morphogen gradients in the *Drosophila* embryo and pupal wing, Development 133 (2) (2006) 183–193.
[19] K.A. Wharton, R.P. Ray, W.M. Gelbart, An activity gradient of decapentaplegic is necessary for the specification of dorsal pattern elements in the *Drosophila* embryo, Development 117 (2) (1993) 807–822.
[20] V. Francois, et al., Dorsal–ventral patterning of the *Drosophila* embryo depends on a putative negative growth factor encoded by the short gastrulation gene, Genes Dev. 8 (21) (1994) 2602–2616.
[21] M.J. Shimell, et al., The Drosophila dorsal–ventral patterning gene tolloid is related to human bone morphogenetic protein 1, Cell 67 (3) (1991) 469–481.
[22] J.J. Ross, et al., Twisted gastrulation is a conserved extracellular BMP antagonist, Nature 410 (6827) (2001) 479–483.
[23] G. Marques, et al., Production of a DPP activity gradient in the early Drosophila embryo through the opposing actions of the SOG and TLD proteins, Cell 91 (3) (1997) 417–426.
[24] P. Blader, et al., Cleavage of the BMP-4 antagonist chordin by zebrafish tolloid, Science 278 (5345) (1997) 1937–1940.
[25] C. Chang, et al., Twisted gastrulation can function as a BMP antagonist, Nature 410 (6827) (2001) 483–487.
[26] S. Piccolo, et al., Cleavage of Chordin by Xolloid metalloprotease suggests a role for proteolytic processing in the regulation of Spemann organizer activity, Cell 91 (3) (1997) 407–416.
[27] Y. Sasai, et al., Xenopus chordin: a novel dorsalizing factor activated by organizer-specific homeobox genes, Cell 79 (5) (1994) 779–790.
[28] I.C. Scott, et al., Homologues of twisted gastrulation are extracellular cofactors in antagonism of BMP signalling, Nature 410 (6827) (2001) 475–478.
[29] S. Srinivasan, K.E. Rashka, E. Bier, Creation of a Sog morphogen gradient in the *Drosophila* embryo, Dev. Cell 2 (1) (2002) 91–101.
[30] S.A. Holley, et al., The Xenopus dorsalizing factor noggin ventralizes *Drosophila* embryos by preventing DPP from activating its receptor, Cell 86 (4) (1996) 607–617.
[31] H.L. Ashe, M. Levine, Local inhibition and long-range enhancement of Dpp signal transduction by Sog, Nature 398 (6726) (1999) 427–431.
[32] E. Decotto, E.L. Ferguson, A positive role for Short gastrulation in modulating BMP signaling during dorsoventral patterning in the *Drosophila* embryo, Development 128 (19) (2001) 3831–3841.
[33] A. Eldar, et al., Robustness of the BMP morphogen gradient in *Drosophila* embryonic patterning, Nature 419 (6904) (2002) 304–308.
[34] B. Schmid, et al., Equivalent genetic roles for bmp7/snailhouse and bmp2b/swirl in dorsoventral pattern formation, Development 127 (5) (2000) 957–967.
[35] S.C. Little, M.C. Mullins, Bone morphogenetic protein heterodimers assemble heteromeric type I receptor complexes to pattern the dorsoventral axis, Nat. Cell Biol. 11 (5) (2009) 637–643.
[36] S. Matsuda, O. Shimmi, Directional transport and active retention of Dpp/BMP create wing vein patterns in *Drosophila*, Dev. Biol. 366 (2) (2012) 153–162.
[37] A. Sawala, et al., Peak BMP responses in the *Drosophila* embryo are dependent on the activation of integrin signaling, Cell Rep. 12 (10) (2015) 1584–1593.
[38] J. Gavin-Smyth, et al., A genetic network conferring canalization to a bistable patterning system in *Drosophila*, Curr. Biol. 23 (22) (2013) 2296–2302.
[39] M. van der Zee, et al., Sog/Chordin is required for ventral-to-dorsal Dpp/BMP transport and head formation in a short germ insect, Proc. Natl. Acad. Sci. U. S. A. 103 (44) (2006) 16307–16312.
[40] D. Ben-Zvi, et al., Scaling of the BMP activation gradient in *Xenopus* embryos, Nature 453 (7199) (2008) 1205–1211.
[41] E. Bier, E.M. De Robertis, Embryo development. BMP gradients: a paradigm for morphogen-mediated developmental patterning, Science 348 (6242) (2015) aaa5838.
[42] O. Shimmi, et al., The crossveinless gene encodes a new member of the twisted gastrulation family of BMP-binding proteins which, with short gastrulation, promotes BMP signaling in the crossveins of the *Drosophila* wing, Dev. Biol. 282 (1) (2005) 70–83.
[43] S. Matsuda, et al, Dpp/BMP transport mechanism is required for wing venation in the sawfly *Athalia rosae*, Insect Biochem. Mol. Biol. 43 (5) (2013) 466–473.
[44] D.J. Bornemann, et al., Abrogation of heparan sulfate synthesis in *Drosophila* disrupts the Wingless, Hedgehog and Decapentaplegic signaling pathways, Development 131 (9) (2004) 1927–1938.
[45] M. Fujise, et al., Dally regulates Dpp morphogen gradient formation in the *Drosophila* wing, Development 130 (8) (2003) 1515–1522.
[46] C. Han, et al., Distinct and collaborative roles of *Drosophila* EXT family proteins in morphogen signalling and gradient formation, Development 131 (7) (2004) 1563–1575.
[47] Y. Takei, et al., Three *Drosophila* EXT genes shape morphogen gradients through synthesis of heparan sulfate proteoglycans, Development 131 (1) (2004) 73–82.
[48] D.J. Bornemann, et al., A translational block to HSPG synthesis permits BMP signaling in the early *Drosophila* embryo, Development 135 (6) (2008) 1039–1047.
[49] X. Wang, et al., Type IV collagens regulate BMP signalling in *Drosophila*, Nature 455 (7209) (2008) 72–77.
[50] A. Sawala, C. Sutcliffe, H.L. Ashe, Multistep molecular mechanism for bone morphogenetic protein extracellular transport in the *Drosophila* embryo, Proc. Natl. Acad. Sci. U. S. A. 109 (28) (2012) 11222–11227.
[51] H. Tanimoto, et al., Hedgehog creates a gradient of DPP activity in *Drosophila* wing imaginal discs, Mol. Cell 5 (1) (2000) 59–71.
[52] B. Muller, et al., Conversion of an extracellular Dpp/BMP morphogen gradient into an inverse transcriptional gradient, Cell 113 (2) (2003) 221–233.
[53] G. Pyrowolakis, et al., A simple molecular complex mediates widespread BMP-induced repression during *Drosophila* development, Dev. Cell 7 (2) (2004) 229–240.
[54] A. Weiss, et al., A conserved activation element in BMP signaling during Drosophila development, Nat. Struct. Mol. Biol. 17 (1) (2010) 69–76.
[55] R. Barrio, J.F. de Celis, Regulation of spalt expression in the *Drosophila* wing blade in response to the Decapentaplegic signaling pathway, Proc. Natl. Acad. Sci. U. S. A. 101 (16) (2004) 6021–6026.
[56] R. Sivasankaran, et al., Direct transcriptional control of the Dpp target omb by the DNA binding protein Brinker, EMBO J. 19 (22) (2000) 6162–6172.
[57] J.F. De Celis, Pattern formation in the *Drosophila* wing: the development of the veins, Bioessays 25 (5) (2003) 443–451.
[58] S.S. Blair, Wing vein patterning in *Drosophila* and the analysis of intercellular signaling, Ann. Rev. Cell Dev. Biol. 23 (2007) 293–319.
[59] M. Zecca, K. Basler, G. Struhl, Sequential organizing activities of engrailed: hedgehog and decapentaplegic in the *Drosophila* wing, Development 121 (8) (1995) 2265–2278.
[60] R. Burke, K. Basler, Dpp receptors are autonomously required for cell proliferation in the entire developing *Drosophila* wing, Development 122 (7) (1996) 2261–2269.
[61] J. Capdevila, I. Guerrero, Targeted expression of the signaling molecule decapentaplegic induces pattern duplications and growth alterations in *Drosophila* wings, EMBO J. 13 (19) (1994) 4459–4468.
[62] C. Martin-Castellanos, B.A. Edgar, A characterization of the effects of Dpp signaling on cell growth and proliferation in the *Drosophila* wing, Development 129 (4) (2002) 1003–1013.
[63] M.A. Crickmore, R.S. Mann, Hox control of organ size by regulation of morphogen production and mobility, Science 313 (5783) (2006) 63–68.
[64] A. Kicheva, et al., Kinetics of morphogen gradient formation, Science 315 (5811) (2007) 521–525.
[65] S. Zhou, et al., Free extracellular diffusion creates the Dpp morphogen gradient of the *Drosophila* wing disc, Curr. Biol. 22 (8) (2012) 668–675.
[66] P. Muller, et al., Morphogen transport, Development 140 (8) (2013) 1621–1638.
[67] T. Lecuit, S.M. Cohen, Dpp receptor levels contribute to shaping the Dpp morphogen gradient in the *Drosophila* wing imaginal disc, Development 125 (24) (1998) 4901–4907.
[68] T. Akiyama, et al., Dally regulates Dpp morphogen gradient formation by stabilizing Dpp on the cell surface, Dev. Biol. 313 (1) (2008) 408–419.
[69] T.Y. Belenkaya, et al., Drosophila Dpp morphogen movement is independent of dynamin-mediated endocytosis but regulated by the glypican members of heparan sulfate proteoglycans, Cell 119 (2) (2004) 231–244.
[70] M. Gonzalez-Gaitan, H. Jackle, The range of spalt-activating Dpp signalling is reduced in endocytosis-defective *Drosophila* wing discs, Mech. Dev. 87 (1–2) (1999) 143–151.
[71] K. Kruse, et al., Dpp gradient formation by dynamin-dependent endocytosis: receptor trafficking and the diffusion model, Development 131 (19) (2004) 4843–4856.
[72] A.D. Lander, Q. Nie, F.Y. Wan, Do morphogen gradients arise by diffusion ? Dev. Cell 2 (6) (2002) 785–796.
[73] G. Schwank, et al., Formation of the long range Dpp morphogen gradient, PLoS Biol. 9 (7) (2011) e1001111.
[74] F.A. Ramirez-Weber, T.B. Kornberg, Cytonemes cellular processes that project to the principal signaling center in *Drosophila* imaginal discs, Cell 97 (5) (1999) 599–607.
[75] F. Hsiung, et al., Dependence of *Drosophila* wing imaginal disc cytonemes on Decapentaplegic, Nature 437 (7058) (2005) 560–563.
[76] S. Roy, T.B. Kornberg, Direct delivery mechanisms of morphogen dispersion, Sci. Signal. 4 (200) (2011) pt8.
[77] S. Roy, F. Hsiung, T.B. Kornberg, Specificity of *Drosophila* cytonemes for distinct signaling pathways, Science 332 (6027) (2011) 354–358.
[78] S. Roy, et al., Cytoneme-mediated contact-dependent transport of the *Drosophila* decapentaplegic signaling protein, Science 343 (6173) (2014) 1244624.

Please cite this article in press as: S. Matsuda, et al., BMP morphogen gradients in flies, Cytokine Growth Factor Rev (2015), http://dx.doi.org/10.1016/j.cytogfr.2015.11.003

[79] M. Bischoff, et al., Cytonemes are required for the establishment of a normal Hedgehog morphogen gradient in *Drosophila* epithelia, Nat. Cell Biol. 15 (11) (2013) 1269–1281.
[80] J. Maier, B. Traenkle, U. Rothbauer, Real-time analysis of epithelial-mesenchymal transition using fluorescent single-domain antibodies, Sci. Rep. 5 (2015) 13402.
[81] E. Caussinus, O. Kanca, M. Affolter, Fluorescent fusion protein knockout mediated by anti-GFP nanobody, Nat. Struct. Mol. Biol. 19 (1) (2012) 117–121.
[82] P.D. Kaiser, et al., Recent progress in generating intracellular functional antibody fragments to target and trace cellular components in living cells, Biochim. Biophys. Acta 1844 (11) (2014) 1933–1942.
[83] J. Helma, et al., Nanobodies and recombinant binders in cell biology, J. Cell Biol. 209 (5) (2015) 633–644.
[84] S. Harmansa, et al., Dpp spreading is required for medial but not for lateral wing disc growth, Nature (2015) .
[85] G. Schwank, S. Restrepo, K. Basler, Growth regulation by Dpp: an essential role for Brinker and a non-essential role for graded signaling levels, Development 135 (24) (2008) 4003–4013.
[86] G. Schwank, et al., Antagonistic growth regulation by Dpp and fat drives uniform cell proliferation, Dev. Cell 20 (1) (2011) 123–130.
[87] O. Wartlick, et al., Dynamics of Dpp signaling and proliferation control, Science 331 (6021) (2011) 1154–1159.
[88] T. Akiyama, M.C. Gibson, Decapentaplegic and growth control in the developing *Drosophila* wing, Nature (2015) .
[89] S. Restrepo, J.J. Zartman, K. Basler, Coordination of patterning and growth by the morphogen DPP, Curr. Biol. 24 (6) (2014) R245–R255.
[90] C. Alexandre, A. Baena-Lopez, J.P. Vincent, Patterning and growth control by membrane-tethered Wingless, Nature 505 (7482) (2014) 180–185.
[91] M. Brauchle, et al., Protein interference applications in cellular and developmental biology using DARPins that recognize GFP and mCherry, Biol. Open 3 (12) (2014) 1252–1261.

Shinya Matsuda is a postdoc in the Affolter lab, and is interested in manipulating endogenous Dpp morphogen gradients to better understand the morphogen function. He completed his bachelor and master degree at the University of Tokyo, and received his Ph.D at the University of Helsinki. Outside the lab, he enjoys playing mölkky and is a founding member of the Japan mölkky association (www.molkky.jp/).

Stefan Harmansa is a PhD student in the laboratory of Markus Affolter. He studies the dispersal properties of Dpp during gradient formation and the impact of gradient shape on growth control of the *Drosophila* wing disc.

Markus Affolter is professor for Developmental Biology at the Biozentrum of the University of Basel. His lab is interested in morphogenesis, in particular in how morphogens control organ formation and how branching morphogenesis leads to the formation of complex, branched organs. More recently, his lab pioneered the use of protein binders in multicellular organisms.

Please cite this article in press as: S. Matsuda, et al., BMP morphogen gradients in flies, Cytokine Growth Factor Rev (2015), http://dx.doi.org/10.1016/j.cytogfr.2015.11.003

10.2 List of Abbreviations

α	Anti
aa	Amino acid
Ab	Antibody
AE	Activator element
A/P	Anterior/posterior
Ap	Apterous
AEL	After egg laying
Bl	Blistered
BL	Basal lamina
BMP	Bone morphogenetic protein
Brk	Brinker
CDR	Complementarity determining region
Ci	Cubitus interruptus
Co-Smad	Common-mediator Smad
CRE-DOG	Cre-recombinase dependent on GFP
CyO	"Curly of Oster"
Dad	Daughters against dpp
Daw	Dawdle
deGradFP	degrade Green Fluorescent Protein
Dll	Distal-less
Dll	Distal-less
D/V	Dorsal/ventral
Dpp	Decapentaplegic
ECM	Extracellular matrix
EGF	Epidemal growth factor
EGFP	enhanced GFP
En	Engrailed
FGF	Fibroblast growth factor
Gbb	Glas bottom boat
GDF	Growth and differentiation factor
GEM	Growth Equalization Model
GFP	Green fluorescent protein
gp	Guinea pig
HA	Hemagglutinin
HCAb	Heavy chains antibody
Hh	Hedgehog
I-Smad	Inhibitory-Smad
LV	Longitudinal vein
Mad	Mothers against dpp
Mav	Maverick
mCh	mCherry

MCS	Multiple cloning site
Myo	Myoglianin
Nrv1	Nervana 1
p-Mad	Phospho-Mothers against Dpp
Ptc	Patched (receptor of Hh)
Put	Punt
RNAi	RNA interference
r-Smad	Receptor-Smad
RT	Room temperature
Sax	Saxophone
SBN	Scaffold-bound nanobody
Scw	Screw
s.d.	Standard deviation
SE	Silencer element
Shn	Schnurri
T48	Transcript 48
TA	Transcriptional activator
T-DDOG	Transcription device dependent on GFP
TGF	Transforming growth factor
Tkv	Thickveins
TRM	Temporal Rule Model
UAS	Upstream activation sequence
Vg	Vestigal
VH	Variable heavy chain
VHH	Variable heavy chain of heavy chain-only antibodies
Vkg	Viking
VL	Variable light chain
Wg	Wingless
Wnt	Wingless-related integration site
YFP	Yellow fluorescent protein

References

[1] Hans Driesch. Entwicklungsmechanische Studien. *Zeitschrift für wissenschaftliche Zoologie*, 53, 1891. Translated as "The Potency of the First Two Cleavage Cells in Echinoderm Development. Experimental Production of Partial and Double Formations." In *Foundations of Experimental Embryology*, eds. Benjamin H. Willier and Jane M. Oppenheimer, 38-50. New York: Hafner Press, 1964.

[2] Edward M. De Robertis. Spemann's organizer and self- regulation in amphibian embryos. *Nature Reviews Molecular Cell Biology*, 7:102–108, 2006. DOI:10.1038/nrm1855.

[3] Hans Spemann. *Embryonic Development and Induction*. Yale Univ. New Haven, 1938.

[4] Hans Spemann and Hilde Mangold. Über Induktion von Embryoanlagen durch Implantation artfremder Organisatoren. *Roux's Arch. Entw. Mech.*, (100):599–638, 1924.

[5] Ortrud Wartlick, Anna Kicheva, and Marcos González-Gaitán. Morphogen gradient formation. *Cold Spring Harbor Perspectives in Biology*, 1(3):a001255, September 2009. DOI: 10.1101/cshperspect.a001255.

[6] A. M. Turing. The Chemical Basis of Morphogenesis. *Philosophical Transactions of the Royal Society of London*, 237(641):37–72, 1951.

[7] Meinhardt H. *Models of biological pattern formation.* London, UK: Academic Press, 1982.

[8] James D. Murray. How the leopard gets its spots. *Scientific American*, (258):80–87, 1988. DOI:10.1038/scientificamerican0388-80.

[9] R.T. Liu, S.S. Liaw, and P.K. Maini. Two-stage turing model for generating pigment patterns on the leopard and the jaguar. *Phys. Rev. Nonlinear Soft Matter Phys.*, (74), Jul 2006.

[10] Akiko Nakamasu, Go Takahashi, Akio Kanbe, and Shigeru Kondo. Interactions between zebrafish pigment cells responsible for the generation of Turing patterns. *PNAS*, 106(21):8429–8434, 2009. DOI: 10.1073/pnas.0808622106.

[11] Masakatsu Watanabe and Shigeru Kondo. Is pigment patterning in fish skin determined by the Turing mechanism? *Trends in Genetics*, 31(2):88–96, February 2015. DOI: http://dx.doi.org/10.1016/j.tig.2014.11.005.

[12] Kimberly L. Cooper. Self-organization in the limb : a Turing mechanism for digit development. *Current Opinion in Genetics & Development*, 32:92–97, 2015. DOI: 10.1016/j.gde.2015.02.001.

[13] Albert Dalcq. *Form and causality in early development.* Cambridge [England] University Press, 1938.

[14] Katherine W. Rogers and Alexander F. Schier. Morphogen gradients: from generation to interpretation. *Annual Review of Cell and Developmental Biology*, 27:377–407, November 2011. DOI: 10.1146/annurev-cellbio-092910-154148.

[15] Lewis Wolpert. Positional information and the spatial pattern of cellular differentiation. *Journal of Theoretical Biology*, 25(1):1–47, October 1969.

[16] Lewis Wolpert. Positional information and patterning revisited. *Journal of Theoretical Biology*, 269(1):359–65, January 2011. DOI: 10.1016/j.jtbi.2010.10.034.

[17] A. Gierer and H. Meinhardt. A Theory of Biological Pattern Formation. *Kybernetik*, (12):30–39, 1972.

[18] Francis Crick. Diffusion in embryogenesis. *Nature*, (225):420–422, January 1970. doi:10.1038/225420a0.

[19] W. Driever and C. Nüsslein-Volhard. A gradient of *bicoid* protein in *Drosophila* embryos. *Cell*, 54(1):83–93, July 1988. DOI: 10.1016/0092-8674(88)90182-1.

[20] W. Driever and C. Nüsslein-Volhard. The *bicoid* protein determines position in the *Drosophila* embryo in a concentration-dependent manner. *Cell*, 54(1):95–104, July 1988. DOI: 10.1016/0092-8674(88)90183-3.

[21] Gary Struhl, Kevin Struhl, and Paul M. Macdonald. The Gradient Morphogen *bicoid* is a Concentration-Dependent Transcriptional Activator. *Cell*, 57(7):1259–1273, June 1989. DOI: 10.1016/0092-8674(89)90062-7.

[22] D. Nellen, R. Burke, G. Struhl, and K. Basler. Direct and long-range action of a DPP morphogen gradient. *Cell*, 85(3):357–68, May 1996. DOI: 10.1016/S0092-8674(00)81114-9.

[23] T. Lecuit, W.J. Brook, M. Ng, M. Calleja, H. Sun, and S.M. Cohen. Two distinct mechanisms for long-range patterning by Decapentaplegic in the *Drosophila* wing. *Nature*, 381:378–393, May 1996. DOI: 10.1038/381387a0.

[24] Markus Affolter and Konrad Basler. The Decapentaplegic morphogen gradient: from pattern formation to growth regulation. *Nature Reviews Genetics*, 8(9):663–74, September 2007. DOI: 10.1038/nrg2166.

[25] E. Bier and E. M. De Robertis. BMP gradients: A paradigm for morphogen-mediated developmental patterning. *Science*, 348(6242):aaa5838–aaa5838, June 2015. DOI: 10.1126/science.aaa5838.

[26] J.B. Gurdon and P.Y. Bourillot. Morphogen gradient interpretation. *Nature*, 413:797–803, 2001. DOI: 10.1038/35101500.

[27] Hilary L. Ashe and James Briscoe. The interpretation of morphogen gradients. *Development (Cambridge, England)*, 133(3):385–94, February 2006. DOI: 10.1242/dev.02238.

[28] Christian Bökel and Michael Brand. Generation and interpretation of FGF morphogen gradients in vertebrates. *Current opinion in genetics & development*, 23(4):415–22, August 2013. DOI: 10.1016/j.gde.2013.03.002.

[29] V. Duboc, E. Röttinger, L. Besnardeau, and T. Lepage. Nodal and BMP2/4 Signaling Organizes the Oral-Aboral Axis of the Sea Urchin Embryo. *Developmental Cell*, 6(3):397–410, March 2004. DOI: 10.1016/S1534-5807(04)00056-5.

[30] Michael M. Shen. Nodal signaling: developmental roles and regulation. *Development (Cambridge, England)*, 134(6):1023–34, March 2007. DOI: 10.1242/dev.000166.

[31] Alexander F. Schier. Nodal morphogens. *Cold Spring Harbor perspectives in biology*, 1(5):a003459, November 2009. DOI: 10.1101/cshperspect.a003459.

[32] Sebastian J. Arnold and Elizabeth J. Robertson. Making a commitment: cell lineage allocation and axis patterning in the early mouse embryo. *Nature Reviews Molecular Cell Biology*, 10(2):91–103, February 2009. DOI: 10.1038/nrm2618.

[33] J. Raspopovic, L. Marcon, L. Russo, and J. Sharpe. Digit patterning is controlled by a Bmp-Sox9-Wnt Turing network modulated by morphogen gradients. *Science*, 345(6196):566–571, 2014. DOI: 10.5061/dryad.jm6pj.

[34] Javier Lopez-Rios, Amandine Duchesne, Dario Speziale, Guillaume Andrey, Kevin a Peterson, Philipp Germann, Erkan Unal, Jing Liu, Sandrine Floriot, Sarah Barbey, Yves Gallard, Magdalena Müller-Gerbl, Andrew D Courtney, Christophe Klopp, Sabrina Rodriguez, Robert Ivanek, Christian Beisel, Carol Wicking, Dagmar Iber, Benoit Robert, Andrew P McMahon, Denis Duboule, and Rolf Zeller. Attenuated sensing of SHH by Ptch1 underlies evolution of bovine limbs. *Nature*, 511(7507):46–51, July 2014. DOI: 10.1038/nature13289.

[35] Aimée Zuniga. Next generation limb development and evolution: old questions, new perspectives. *Development (Cambridge, England)*, 142(22):3810–3820, November 2015. DOI: 10.1242/dev.125757.

[36] M. Cohen, J. Briscoe, and R. Blassberg. Morphogen interpretation: the transcriptional logic of neural tube patterning. *Current Opinion in Genetics & Development*, 23(4):423–428, Aug 2013. DOI: 10.1016/j.gde.2013.04.003.

[37] J. Briscoe and S. Small. Morphogen rules: design principles of gradient-mediated embryo patterning. *Development*, 142(23):3996–4009, Dec 2015. DOI: 10.1242/dev.129452.

[38] Jeremy P. Brockes and Anoop Kumar. Comparative aspects of animal regeneration. *Annual review of cell and developmental biology*, 24:525–49, January 2008. DOI: 10.1146/annurev.cellbio.24.110707.175336.

[39] Alexander Weiss and Liliana Attisano. The TGFbeta Superfamily Signaling Pathway. *Wiley Interdisciplinary Reviews: Developmental Biology*, 2(1):47–63, January 2013. DOI: 10.1002/wdev.86.

[40] Joan Massagué. TGFbeta signalling in context. *Nature Reviews Molecular Cell Biology*, 13(10):616–30, October 2012. DOI: 10.1038/nrm3434.

[41] Joan Massagué and Qiaoran Xi. TGF-beta control of stem cell differentiation genes. *FEBS letters*, 586(14):1953–8, July 2012. DOI: 10.1016/j.febslet.2012.03.023.

[42] Kelly J. Gordon and Gerard C. Blobe. Role of transforming growth factor-beta superfamily signaling pathways in human disease. *Biochimica et biophysica acta*, 1782(4):197–228, April 2008. DOI: 10.1016/j.bbadis.2008.01.006.

[43] Hiroaki Ikushima and Kohei Miyazono. TGFbeta signalling: a complex web in cancer progression. *Nature Reviews Cancer*, 10(6):415–24, June 2010. DOI: 10.1038/nrc2853.

[44] Joan Massagué. TGFbeta in Cancer. *Cell*, 134(2):215–30, July 2008. DOI: 10.1016/j.cell.2008.07.001.

[45] Craig A. Harrison, Sara L. Al-Musawi, and Kelly L. Walton. Prodomains regulate the synthesis, extracellular localisation and activity of TGF-beta superfamily ligands. *Growth Factors (Chur, Switzerland)*, 29(5):174–86, October 2011. DOI: 10.3109/08977194.2011.608666.

[46] A. Galat. Common structural traits for cystine knot domain of the TGFbeta superfamily of proteins and three-fingered ectodomain of their cellular receptors. *Cellular and molecular life sciences : CMLS*, 68(20):3437–51, October 2011. DOI: 10.1007/s00018-011-0643-4.

[47] Richard W. Padgett, R. Daniel St. Johnston, and William M. Gelbart. A transcript from a *Drosophila* pattern gene predicts a protein homologous to the transforming growth factor-beta family. *Nature*, 325(6099):81–84, July 1987. DOI: 10.1038/325081a0.

[48] J.S. Doctor, P.D. Jackson, K.E. Rashka, M. Visalli, and F.M. Hoffmann. Sequence, biochemical characterization, and developmental expression of a new member of the TGF-beta superfamily in *Drosophila melanogaster*. *Dev. Biol.*, 151(2):491–505, 1992.

[49] K. Arora, M.S. Levine, and M.B. O'Connor. The *screw* gene encodes a ubiquitously expressed member of the TGF-beta family required for specification of dorsal cell fates in the *Drosophila* embryo. *Genes & development*, 8(21):2588–2601, December 1994. DOI: 10.1101/gad.8.21.2588.

[50] Denise Nellen, Markus Affolter, and Konrad Basler. Receptor serine/threonine kinases implicated in the control of *Drosophila* body pattern by *decapentaplegic*. *Cell*, 78(2):225–237, July 1994. DOI: 10.1016/0092-8674(94)90293-3.

[51] T.E. Haerry, Ongkar Khalsa, M.B. O'Connor, and K.A. Wharton. Synergistic signaling by two BMP ligands through the SAX and TKV receptors controls

wing growth and patterning in *Drosophila*. *Development*, 125(20):3977–3987, November 1998.

[52] Esther Ruberte, Thomas Marty, Denise Nellen, Markus Affolter, and Konrad Basler. An Absolute Requirement for Both the Type II and Type I Receptors, Punt and Thick Veins, for DPP Signaling In Vivo. *Cell*, 80(6):889–897, March 1995. DOI: 10.1016/0092-8674(95)90292-9.

[53] Yuto Kamiya, Kohei Miyazono, and Keiji Miyazawa. Specificity of the inhibitory effects of Dad on TGF-beta family type I receptors, Thickveins, Saxophone, and Baboon in *Drosophila*. *FEBS letters*, 582(17):2496–500, July 2008. DOI: 10.1016/j.febslet.2008.05.052.

[54] Michael Bate and Alfonso Martinez-Arias. The embryonic origin of imaginal discs in *Drosophila*. *Development*, 112(3):755–761, August 1991.

[55] Claude Desplan, James Theis, and P.H. O'Farrell. The *Drosophila* developmental gene, *engrailed*, encodes a sequence-specific DNA binding activity. *Nature*, 318(6047):630–635, December 1985. DOI: 10.1038/318630a0.

[56] Claude Desplan, Jim Theis, and P.H. O'Farrell. The sequence specificity of homeodomain-DNA interaction. *Cell*, 54(7):1081–1090, September 1988. DOI: 10.1016/0092-8674(88)90123-7.

[57] Francisco A. Martin and Ginés Morata. Compartments and the control of growth in the *Drosophila* wing imaginal disc. *Development (Cambridge, England)*, 133(22):4421–6, November 2006. DOI: 10.1242/dev.02618.

[58] M.M. Madhavan and H.A. Schneidermann. Histological analysis of the dynamics of growth of imaginal discs and histoblast nests during the larval development of *Drosophila melanogaster*. *W Roux's Arch.*, 183:269–305, 1977.

[59] P.J. Bryant and Levinson P. Intrinsic growth control in the imaginal primordia of *Drosophila*, and the autonomous action of a lethal mutation causing overgrowth. *Developmental Biology*, 107(2):355–363, February 1985. DOI: 10.1016/0012-1606(85)90317-3.

[60] M. Milán, S. Campuzano, and A. Garcia-Bellido. Cell cycling and patterned cell proliferation in the wing primordium of *Drosophila*. *PNAS*, 93(2):640–645, January 1996.

[61] M. Zecca, K. Basler, and G. Struhl. Sequential organizing activities of engrailed, hedgehog and decapentaplegic in the *Drosophila* wing. *Development (Cambridge, England)*, 121(8):2265–78, August 1995.

[62] Myriam Zecca, Konrad Basler, and Gary Struhl. Direct and Long-Range Action of a Wingless Morphogen Gradient. *Cell*, 87(5):833–844, November 1996. DOI: 10.1016/S0092-8674(00)81991-1.

[63] C.J. Neumann and S.M. Cohen. Long-range action of Wingless organizes the dorsal-ventral axis of the *Drosophila* wing. *Development*, 124(4):871–880, March 1997.

[64] F. A. Spencer, F. M. Hoffmann, and W. M. Gelbart. Decapentaplegic: a gene complex affecting morphogenesis in drosophila melanogaster. *Cell*, 28(3):451–461, March 1982. DOI: 10.1016/0092-8674(82)90199-4.

[65] J.P. Couso and M. Gonzáles-Gaitán. Embryonic limb development in *Drosophila*. *Trends Genet.*, 9(11):371–373, November 1993. DOI: http://dx.doi.org/10.1016/0168-9525(93)90125-2.

[66] J.A. Williams, S.W. Paddock, and S.B. Carroll. Pattern formation in a secondary field: a hierarchy of regulatory genes subdivides the developing *Drosophila* wing disc into discrete subregions. *Development*, 117(2):571–584, March 1993.

[67] Jr. Lewis I. Held. *Imaginal Discs - The Genetic and Cellular Logic of Pattern Formation.* Cambridge University Press, 2005. DOI: 10.2277/0521018358.

[68] Scott F. Gilbert. *Developmental Biology, Ninth Edition*. Sinauer Associates, Inc., Sunderland, Massachusetts USA, 2010.

[69] A. Garcia-Bellido. Genetic control of wing disc development in *Drosophila*. *Ciba Found. Symp.*, pages 161–82, 1975.

[70] R.S. Mann and G. Morata. The developmental and molecular biology of genes that subdivide the body of *Drosophila*. *Annual review of cell and developmental biology*, 16:243–71, November 2000. DOI: 10.1146/annurev.cellbio.16.1.243.

[71] Fernando J. Diaz-Benjumea and Stephen M. Cohen. Interaction between dorsal and ventral cells in the imaginal disc directs wing development in *Drosophila*. *Cell*, 75(4):741–752, November 1993. DOI: http://dx.doi.org/10.1016/0092-8674(93)90494-B.

[72] Konrad Basler and Gary Struhl. Compartment boundaries and the control of *Drosophila* limb pattern by *hedgehog* protein. *Nature*, 368:208–214, March 1994. DOI: 10.1038/368208a0.

[73] Tetsuya Tabata and Thomas B. Kornberg. Hedgehog Is a Signaling Protein with a Key Role in Patterning *Drosophila* lmaginal Discs. *Cell*, 76(1):89–102, January 1994. DOI: 10.1016/0092-8674(94)90175-9.

[74] J Capdevila and I Guerrero. Targeted expression of the signaling molecule decapentaplegic induces pattern duplications and growth alterations in Drosophila wings. *The EMBO journal*, 13(19):4459–68, October 1994.

[75] Jill Heemskerk and Stephen DiNardo. *Drosophila hedgehog* acts as a morphogen in cellular patterning. *Cell*, 76(3):449–460, February 1994. DOI: 10.1016/0092-8674(94)90110-4.

[76] Isabel Guillén, J.L. Mullor, J. Capdevila, E. Sánchez-Herrero, G. Morata, and I. Guerrero. The function of engrailed and the specification of Drosophila wing pattern. *Development*, 121:3447–3456, 1995.

[77] S. Eaton and T. B. Kornberg. Repression of ci-D in posterior compartments of *Drosophila* by engrailed. *Genes*, 4(6):1068–1077, July 1990. DOI: 10.1101/gad.4.6.1068.

[78] Seth S. Blair. Engrailed expression in the anterior lineage compartment of the developing wing blade of *Drosophila*. *Development*, 115:21–33, 1992.

[79] Fisun Hamaratoglu, Markus Affolter, and George Pyrowolakis. Dpp/BMP signaling in flies: From molecules to biology. *Seminars in Cell & Developmental Biology*, 32:128–36, August 2014. DOI: 10.1016/j.semcdb.2014.04.036.

[80] J. Kim, K. D. Irvine, and S. B. Carroll. Cell recognition, signal induction, and symmetrical gene activation at the dorsal-ventral boundary of the developing *Drosophila* wing. *Cell*, 82(5):795–802, September 1995. DOI: http://dx.doi.org/10.1016/0092-8674(95)90476-X.

[81] E. J. Rulifson and S. S. Blair. Notch regulates wingless expression and is not required for reception of the paracrine wingless signal during wing margin neurogenesis in *Drosophila*. *Development*, 121:2813–24, 1995.

[82] Cyrille Alexandre, Alberto Baena-Lopez, and Jean-Paul Vincent. Patterning and growth control by membrane-tethered Wingless. *Nature*, 505(7482):180–5, January 2014. DOI: 10.1038/nature12879.

[83] E. V. Entchev, A. Schwabedissen, and M. González-Gaitán. Gradient formation of the TGF-beta homolog Dpp. *Cell*, 103(6):981–91, December 2000. DOI: 10.1016/S0092-8674(00)00200-2.

[84] Aurelio A. Teleman and Stephen M. Cohen. Dpp Gradient Formation in the *Drosophila* Wing Imaginal Disc. *Cell*, 103(6):971–980, December 2000. DOI: http://dx.doi.org/10.1016/S0092-8674(00)00199-9.

[85] Andrea H. Brand and Norbert Perrimon. Targeted gene expression as a means of altering cell fates and generating dominant phenotypes. *Development*, 118:401–415, 1993.

[86] Ryohei Yagi, Franz Mayer, and Konrad Basler. Refined LexA transactivators and their use in combination with the *Drosophila* Gal4 system. *PNAS*, 107(37):16166–16171, August 2010. DOI: 10.1073/pnas.1005957107.

[87] Gerald Schwank, Sascha Dalessi, Schu-Fee Yang, Ryohei Yagi, Aitana Morton de Lachapelle, Markus Affolter, Sven Bergmann, and Konrad Basler. Formation of the long range Dpp morphogen gradient. *PLoS biology*, 9(7):e1001111, July 2011. DOI: 10.1371/journal.pbio.1001111.

[88] M. Strigini and S.M. Cohen. Wingless gradient formation in the *Drosophila* wing. *Current Biology*, 10(6):293–300, March 2000. DOI: 10.1016/S0960-9822(00)00378-X.

[89] Luis Alberto Baena-Lopez, Xavier Franch-Marro, and Jean-Paul Vincent. Wingless promotes proliferative growth in a gradient-independent manner. *Science signaling*, 2(91):ra60, January 2009. DOI: 10.1126/scisignal.2000360.

[90] Tamás Matusek, Franz Wendler, Sophie Polès, Sandrine Pizette, Gisela D'Angelo, Maximilian Fürthauer, and Pascal P. Thérond. The ESCRT machinery regulates the secretion and long-range activity of Hedgehog. *Nature*, 516(7529):99–103, December 2014. DOI: 10.1038/nature13847.

[91] Shaohua Zhou, Wing-Cheong Lo, Jeffrey L. Suhalim, Michelle A. Digman, Enrico Gratton, Qing Nie, and Arthur D. Lander. Free Extracellular Diffusion Creates the Dpp Morphogen Gradient of the *Drosophila* Wing Disc. *Current Biology*, 22(8):668–675, April 2012. DOI: http://dx.doi.org/10.1016/j.cub.2012.02.065.

[92] T. Akiyama, K. Kamimura, C. Firkus, Takeo. S., O. Shimmi, and H. Nakato. Dally Regulates Dpp Morphogen Gradient Formation by Stabilizing Dpp on the Cell Surface. *Developmental Biology*, 313(1):408–419, 2008. DOI: 10.1016/j.ydbio.2007.10.035.

[93] Bruno Müller, Britta Hartmann, George Pyrowolakis, Markus Affolter, and Konrad Basler. Conversion of an extracellular Dpp/BMP morphogen gradient into an inverse transcriptional gradient. *Cell*, 113(2):221–33, April 2003. DOI: 10.1016/S0092-8674(03)00241-1.

[94] Yoko Funakoshi, Maki Minami, and Tetsuya Tabata. mtv shapes the activity gradient of the Dpp morphogen through regulation of thickveins. *Development*, 128:67–74, 2001.

[95] G. Pyrowolakis, B. Hartmann, B. Muller, K. Basler, and M. Affolter. A simple molecular complex mediates widespread BMP-induced repression during *Drosophila* development. *Dev. Cell*, 7(2):229–240, August 2004. DOI: 10.1016/j.devcel.2004.07.008.

[96] S. Gao, J. Steffen, and A. Laughon. Dpp-responsive Silencers Are Bound by a Trimeric Mad-Medea Complex. *JBC*, 280:36158–36164, August 2005. DOI: 10.1074/jbc.M506882200.

[97] K. Arora, H. Dai, S.G. Kazuko, J. Jamal, M.B. O'Connor, A. Letsou, and R. Warrior. The *Drosophila schnurri* gene acts in the Dpp/TGFbeta signaling pathway and encodes a transcription factor homologous to the human MBP family. *Cell*, 81(5):781–790, June 1995. DOI: 10.1016/0092-8674(95)90539-1.

[98] T. Marty, B. Müller, K. Basler, and M. Affolter. Schnurri mediates DPP-dependent repression of *brinker* transcription. *Nature Cell Biology*, 2:69–76, 2000. DOI: 10.1038/35036383.

[99] J. Torres-Vazgues, R. Warrior, and K. Arora. *schnurri* is required for DPP-dependent patterning of the *Drosophila* wing. *Development*, 227(2):388–402, 2000. DOI: 10.1006/dbio.2000.9900.

[100] G. Campbell and A. Tomlinson. Transducing the Dpp morphogen gradient in the wing of *Drosophila*: regulation of Dpp targets by brinker. *Cell*, 96(4):553–62, February 1999. DOI: 10.1016/S0092-8674(00)80659-5.

[101] A. Jazwinska, N. Kirov, E. Wieschaus, S. Roth, and C. Rushlow. The Drosophila gene *brinker* reveals a novel mechanism of Dpp target gene regulation. *Cell*, 96(4):563–73, February 1999. DOI: 10.1016/S0092-8674(00)80660-1.

[102] M. Minami, N. Kinoshita, Y. Kamoshida, H. Tanimoto, and T. Tabata. *brinker* is a target of DPP in *Drosophila* that negatively regulates DPP-dependent genes. *Nature*, 398:242–246, March 1999. DOI: 10.1038/18451.

[103] K. Tsuneizumi, T. Nakayama, Y. Kamoshida, T.B. Kornberg, J.L. Christian, and T. Tabata. *Daughters against dpp* modulates *dpp* organizing activity in *Drosophila* wing development. *Nature*, 389:627–631, October 1997. DOI: 10.1038/39362.

[104] A. Weiss, E. Charbonnier, E. Ellertsdóttir, A. Tsirigos, C. Wolf, R. Schuh, G. Pyrowolakis, and M. Affolter. A conserved activation element in BMP signaling during *Drosophila* development. *Nature Structural & Molecular Biology*, 17:69–76, December 2010. DOI: 10.1038/nsmb.1715.

[105] Rosa Barrio and J.F. de Celis. Regulation of *spalt* expression in the *Drosophila* wing blade in response to the Decapentaplegic signaling pathway. *Proceedings of the National Academy of Sciences of the United States of America*, 101(16):6021–6, April 2004. DOI. 10.1073/pnas.0401590101.

[106] G.O. Pflugfelder, H. Schwarz, H. Roth, B. Poeck, A. Sigl, S. Kerscher, B. Jonschker, W.L. Pak, and M. Heisenberg. Genetic and molecular characterization of the optomotor-blind gene locus in *Drosophila melanogaster*. *Genetics*, 126(1):91–104, September 1990.

[107] Stefan Grimm and Gert O. Pflugfelder. Control of the Gene *optomotor-blind* in *Drosophila* Wing Development by *decapentaplegic* and itwingless. *Science*, 271(5255):1601–1604, March 1996. DOI: 10.1126/science.271.5255.1601.

[108] R. Sivasankaran, M. A. Vigano, B. Müller, M. Affolter, and K. Basler. Direct transcriptional control of the Dpp target *omb* by the DNA binding protein Brinker. *EMBO Journal*, 19(22):6162–72, 2000. DOI 10.1093/emboj/19.22.6162.

[109] Simon Restrepo, Jeremiah J. Zartman, and Konrad Basler. Coordination of Patterning and Growth by the Morphogen DPP. *Current biology*, 24(6):R245–R255, March 2014. DOI: 10.1016/j.cub.2014.01.055.

[110] Jose F. DeCelis. Pattern formation in the *Drosophila* wing: the development of the veins. *BioEssays*, 25(5):443–451, April 2003. DOI: 10.1002/bies.10258.

[111] Seth S. Blair. Wing Vein Patterning in *Drosophila* and the Analysis of Intercellular Signaling. *Annu. Rev. Cell Dev. Biol.*, 23:293–319, June 2007. DOI: 10.1146/annurev.cellbio.23.090506.123606.

[112] Jose F. DeCelis and Rosa Barrio. Function of the *spalt/spalt-related* gene complex in positioning the veins in the *Drosophila* wing. *Mechanisms of Development*, 91(1-2):31–41, March 2000. DOI: 10.1016/S0925-4773(99)00261-0.

[113] M.A. Sturtevant, B. Biehs, E. Marin, and Bier E. The *spalt* gene links the A/P compartment boundary to a linear adult structure in the *Drosophila* wing. *Development*, 124(1):21–32, 1997.

[114] K. Lunde, B. Biehs, U. Nauber, and Bier E. The *knirps* and *knirps-related* genes organize development of the second wing vein in *Drosophila*. *Development*, 125:4145–4154, 1998.

[115] O. Cook, B. Biehs, and E. Bier. *brinker* and *optomotor-blind* act coordinately to initiate development of the L5 wing vein primordium in *Drosophila*. *Development*, 131:2113–2124, January 2004. DOI: 10.1242/dev.01100.

[116] J. F. DeCelis, R. Barrio, and F. C. Kafatos. A gene complex acting downstream of *dpp* in *Drosophila* wing morphogenesis. *Nature*, 381:421–424, May 1996. DOI: 10.1038/381421a0.

[117] Arthur D. Lander, Q. Nie, and Frederic Y.M. Wan. Do morphogen gradients arise by diffusion? *Dev. Cell*, 2:785–796, June 2002. DOI: 10.1016/S1534-5807(02)00179-X.

[118] Tatyana Y. Belenkaya, Chun Han, Dong Yan, Robert J. Opoka, Marat Khodoun, Hongzhu Liu, and Xinhua Lin. *Drosophila* Dpp Morphogen Movement Is Independent of Dynamin-Mediated Endocytosis but Regulated by the Glypican Members of Heparan Sulfate Proteoglycans. *Cell*, 119(2):231–244, October 2004. DOI: 10.1016/j.cell.2004.09.031.

[119] Karsten Kruse, Periklis Pantazis, Tobias Bollenbach, Frank Jülicher, and Marco González-Gaitán. Dpp gradient formation by dynamin-dependent endocytosis: receptor trafficking and the diffusion model. *Development (Cambridge, England)*, 131(19):4843–56, October 2004. DOI: 10.1242/dev.01335.

[120] Anna Kicheva, Periklis Pantazis, Tobias Bollenbach, Yannis Kalaidzidis, Thomas Bittig, Frank Jülicher, and Marcos González-Gaitán. Kinetics of morphogen gradient formation. *Science*, 315(5811):521–525, January 2007. DOI: 10.1126/science.1135774.

[121] Felipe-Andrés Ramírez-Weber and Thomas B. Kornberg. Cytonemes: Cellular Processes that Project to the Principal Signaling Center in *Drosophila* Imaginal Discs. *Cell*, 97(5):599–607, May 19999.

[122] F. Hsiung, Felipe-Andrès Ramirez-Weber, D. David Iwaki, and Thomas B. Kornberg. Dependence of *Drosophila* wing imaginal disc cytonemes on Decapentaplegic. *Nature*, 437:560–563, September 2005. DOI: 10.1038/nature03951.

[123] Sougata Roy, Frank Hsiung, and Thomas B. Kornberg. Specificity of *Drosophila* Cytonemes for Distinct Signaling Pathways. *Science*, 332(6027):354–358, April 2011. DOI: 10.1126/science.1198949.

[124] Sougata Roy, Hai Huang, Songmei Liu, and Thomas B Kornberg. Cytoneme-mediated contact-dependent transport of the *Drosophila decapentaplegic* signaling protein. *Science*, 343(6173):1244624, February 2014. DOI: 10.1126/science.1244624.

[125] O. Wartlick, F. Julicher, and M. Gonzalez-Gaitan. Growth control by a moving morphogen gradient during *Drosophila* eye development. *Development*, 141(9):1884–1893, April 2014. DOI: 10.1242/dev.105650.

[126] O. Wartlick, P. Mumcu, A. Kicheva, T. Bittig, C. Seum, F. Jülicher, and M. González-Gaitán. Dynamics of Dpp signaling and proliferation control. *Science*, 331(6021):1154–9, March 2011. DOI: 10.1126/science.1200037.

[127] Michael A. Crickmore and Richard S. Mann. Hox Control of Organ Size by Regulation of Morphogen Production and Mobility. *Science*, 313(5783):63–68, June 2006. DOI: 10.1126/science.1128650.

[128] Gerald Schwank, Simon Restrepo, and Konrad Basler. Growth regulation by Dpp: an essential role for Brinker and a non-essential role for graded signaling levels. *Development (Cambridge, England)*, 135(24):4003–13, December 2008. DOI: 10.1242/dev.025635.

[129] Gerald Schwank, Schu-Fee Yang, Simon Restrepo, and Konrad Basler. Comment on "Dynamics of Dpp Signaling and Proliferation Control". *Science*, 335(6067):401, January 2012. DOI: 10.1126/science.1210997.

[130] C. Hamers-Casterman, T. Atarhouch, S. Muyldermans, G. Robinson, C. Hammers, E. Bajyana Songa, N. Bendahman, and R. Hammers. Naturally occurring antibodies devoid of light chains. *Nature*, 363:446–448, June 1993. DOI: 10.1038/363446a0.

[131] V.K. Nguyen, R. Hamers, L. Wyns, and S. Muyldermans. Loss of splice consensus signal is responsible for the removal of the entire CH1 domain of the functional camel IGG2A heavy-chain antibodies1. *Molecular Immunology*, 36(8):515–524, June 1999.

[132] S. Muyldermans, T.N. Barala, V. Cortez Retamozzoa, P. De Baetseliera, E. De Gensta, J. Kinnec, H. Leonhardt, S. Magez, V.K. Nguyen, H. Revets,

U. Rothbauer, B. Stijlemans, S. Tillib, U. Wernery, L. Wyns, G. Hassanzadeh-Ghassabeh, and D. Saerens. Camelid immunoglobulins and nanobody technology. *Veterinary Immunology and Immunopathology*, 128(1-3):178–183, March 2009. DOI: 10.1016/j.vetimm.2008.10.299.

[133] Marta H. Kubala, Oleksiy Kovtun, Kirill Alexandrov, and Brett M. Collins. Structural and thermodynamic analysis of the GFP:GFP-nanobody complex. *Protein Science*, 19(12):2389–2401, December 2010. DOI: 10.1002/pro.519.

[134] E. De Genst, K. Silence, K. Decanniere, K. Conrath, R. Loris, J. Kinne, S. Muyldermans, and L. Wyns. Molecular basis for the preferential cleft recognition by dromedary heavy-chain antibodies. *PNAS*, 103(12):4586–4591, March 2006. DOI: 10.1073/pnas.0505379103.

[135] M. Lauwereys, M.A. Ghahroudi, A. Desmyter, J. Kinne, W. Hölzer, E. De Genst, L. Wyns, and S. Muyldermans. Potent enzyme inhibitors derived from dromedary heavy-chain antibodies. *The EMBO Journal*, 17:3512–3520, July 1998. DOI: 10.1093/emboj/17.13.3512.

[136] Serge Muyldermans. Nanobodies: Natural Single-Domain Antibodies. *Annual Reviews of biochemistry*, 82:775–97, June 2013. DOI: 10.1146/annurev-biochem-063011-092449.

[137] J. Helma, M.C. Cardoso, S. Muyldermans, and H. Leonhardt. Nanobodies and recombinant binders in cell biology. *JCB*, 209(5):633–644, June 2015. DOI: 10.1083/jcb.201409074.

[138] Dirk Saerens, Mireille Pellis, Remy Loris, Els Pardon, Mireille Dumoulin, André Matagne, Lode Wyns, Serge Muyldermans, and Katja Conrath. Identification of a universal VHH framework to graft non-canonical antigen-binding loops of camel single-domain antibodies. *Journal of molecular biology*, 352(3):597–607, September 2005.

[139] U. Rothbauer, K. Zolghadr, S. Tillib, D. Nowak, L. Schermelleh, A. Gahl, N. Backmann, K. Conrath, S. Muyldermans, M.C. Cardoso, and H. Leonhardt. Targeting and tracing antigens in live cells with fluorescent nanobodies. *Nature Methods*, 3:887–889, October 2006. DOI: 10.1038/nmeth953.

[140] U. Rothbauer, K. Zolghadr, S. Muyldermans, A. Schepers, M.C. Cardoso, and H. Leonhardt. A Versatile Nanotrap for Biochemical and Functional Studies with Fluorescent Fusion Proteins. *Molecular and Cellular Proteomics*, 7(2):282–289, February 2008. DOI: 10.1074/mcp.M700342-MCP200.

[141] J. Helma, K. Schmidthals, V. Lux, S. Nüske, A.M. Scholz, H.G. Kräusslich, U. Rothbauer, and H. Leonhardt. Direct and Dynamic Detection of HIV-1 in Living Cells. *PlLOS one*, 7(11):e50026, November 2012. DOI: 10.1371/journal.pone.0050026.

[142] A. Burgess, T. Lorca, and A. Castro. Quantitative Live Imaging of Endogenous DNA Replication in Mammalian Cells. *PLOS one*, 7(9):e45726, September 2012. DOI: 10.1371/journal.pone.0045726.

[143] B. Traenkle, F. Emele, R. Anton, O. Poetz, R.S. Haeussler, J. Maier, P.D. Kaiser, A.M. Scholz, S. Nueske, A. Buchfellner, T. Romer, and U. Rothbauer. Monitoring Interactions and Dynamics of Endogenous Beta-catenin With Intracellular Nanobodies in Living Cells. *Molecular and Cellular Proteomics*, 14:707–723, January 2015. DOI: 10.1074/mcp.M114.044016.

[144] Emmanuel Caussinus, Oguz Kanca, and Markus Affolter. Fluorescent fusion protein knockout mediated by anti-GFP nanobody. *Nature structural & molecular biology*, 19(1):117–21, January 2012. DOI: 10.1038/nsmb.2180.

[145] Yeong Ju Shin, Seung Kyun Park, Yoo Jung Jung, Ye Na Kim, Ki Sung Kim, Ok Kyu Park, Seung-Hae Kwon, Sung Ho Jeon, Le A. Trinh, Scott E. Fraser, Yun Kee, and Byung Joon Hwang. Nanobody-targeted E3-ubiquitin ligase complex degrades nuclear proteins. *Scientific Reports*, 5:14269, September 2015. DOI: 10.1038/srep14269.

[146] Jonathan C.Y. Tang, Tamas Szikra, Yevgenia Kozorovitskiy, Miguel Teixiera, Bernardo L. Sabatini, Botond Roska, and Constance L. Cepko. A Nanobody-Based System Using Fluorescent Proteins as Scaffolds for Cell-Specific Gene Manipulation. *Cell*, 154(4):928–939, August 2013. DOI: 10.1016/j.cell.2013.07.021.

[147] J.C.Y. Tang, S. Rudolph, O.S. Dhande, V.E. Abraira, S. Choi, S.W. Lapan, Z.R. Drew, E. Drokhlyansky, A.D. Huberman, W.G. Regehr, and C.L. Cepko. Cell type-specific manipulation with GFP-dependent Cre recombinase. *Nature Neuroscience*, 18:1334–1341, August 2015. DOI: 10.1038/nn.4081.

[148] V.C. Twitty and J.L. Schwind. The growth of eyes and limbs transplanted heteroplastically between two species of *Amblystoma*. *Journal of Experimental Zoology*, 59(1):61–86, February 1931. DOI: 10.1002/jez.1400590105.

[149] Thomas P. Neufeld, A.F. De la Cruz, Laura A. Johnston, and Bruce A. Edgar. Coordination of Growth and Cell Division in the *Drosophila* Wing. *Cell*, 93(7):1183–1193, June 1998. DOI: 10.1016/S0092-8674(00)81462-2.

[150] R. Burke and K. Basler. Dpp receptors are autonomously required for cell proliferation in the entire developing *Drosophila* wing. *Development*, 122(7):2261–2269, December 1996.

[151] M. Peifer, C. Rauskolb, M. Williams, B. Riggleman, and E. Wieschaus. The segment polarity gene armadillo interacts with the wingless signaling pathway in both embryonic and adult pattern formation. *Development*, 111(4):1029–1043, April 1991.

[152] Stephen J. Day and Peter A. Lawrence. Measuring dimensions: the regulation of size and shape. *Development*, 127(14):2977–2987, July 2000.

[153] Dragana Rogulja and Kenneth D. Irvine. Regulation of Cell Proliferation by a Morphogen Gradient. *Cell*, 123(3):449–461, November 2005. DOI: 10.1016/j.cell.2005.08.030.

[154] Gerald Schwank and Konrad Basler. Regulation of Organ Growth by Morphogen Gradients. *Cold Spring Harbor Perspectives in Biology*, 2(1):a001669, January 2010. DOI: 10.1101/cshperspect.a001669.

[155] O Wartlick and M González-Gaitán. The missing link: implementation of morphogenetic growth control on the cellular and molecular level. *Current opinion in genetics & development*, 21(6):690–5, December 2011.

[156] Ortrud Wartlick, Peer Mumcu, Frank Jülicher, and Marcos Gonzalez-Gaitan. Understanding morphogenetic growth control – lessons from flies. *Nature Reviews Molecular Cell Biology*, 12(9):594–604, September 2011. DOI: 10.1038/nrm3169.

[157] A. Garcia-Bellido and J.R. Merriam. Parameters of the wing imaginal disc development of *Drosophila melanogaster*. *Dev. Biol.*, 24(1):61–87, January 1971.

[158] Laura A. Johnston and Angela L. Sanders. Wingless promotes cell survival but constrains growth during *Drosophila* wing development. *Nature Cell Biology*, 5:827–833, August 2003. DOI: 10.1038/ncb1041.

[159] Cristina Martín-Castellanos and Bruce A. Edgar. A characterization of the effects of Dpp signaling on cell growth and proliferation in the *Drosophila* wing. *Development (Cambridge, England)*, 129(4):1003–1013, February 2002.

[160] O. Wartlick, P. Mumcu, F. Jülicher, and M. Gonzalez-Gaitan. Response to Comment on "Dynamics of Dpp Signaling and Proliferation Control". *Science*, 335(6067):401, January 2012. DOI: 10.1126/science.1211373.

[161] Gerald Schwank, Gerardo Tauriello, Ryohei Yagi, Elizabeth Kranz, Petros Koumoutsakos, and Konrad Basler. Antagonistic growth regulation by Dpp and Fat drives uniform cell proliferation. *Developmental Cell*, 20(1):123–30, January 2011. DOI: http://dx.doi.org/10.1016/j.devcel.2010.11.007.

[162] I. Averbukh, D. Ben-Zvi, S. Mishra, and N. Barkai. Scaling morphogen gradients during tissue growth by a cell division rule. *Development*, 141(10):2150–2156, May 2014. DOI: 10.1242/dev.107011.

[163] P. Fried and D. Iber. Dynamic scaling of morphogen gradients on growing domains. *Nature Communications*, 5(5077), October 2014. DOI: 10.1038/ncomms6077.

[164] Fisun Hamaratoglu, Aitana Morton de Lachapelle, George Pyrowolakis, Sven Bergmann, and Markus Affolter. Dpp signaling activity requires Pentagone to scale with tissue size in the growing *Drosophila* wing imaginal disc. *PLoS biology*, 9(10):e1001182, October 2011. DOI: 10.1371/journal.pbio.1001182.

[165] Karen Tumaneng, Ryan C. Russell, and Kun-Liang Guan. Organ Size Control by Hippo and TOR Pathways. *Current Biology*, 22(9):R368–R379, May 2012. DOI: 10.1016/j.cub.2012.03.003.

[166] Yanlan Mao, Alexander L. Tournier, Andreas Hoppe, Lennart Kester, Barry J. Thompson, and Nicolas Tapon. Differential proliferation rates generate patterns of mechanical tension that orient tissue growth. *The EMBO journal*, 32(21):2790–2803, October 2013. DOI: 10.1038/emboj.2013.197.

[167] Thomas Schluck, Ulrike Nienhaus, Tinri Aegerter-Wilmsen, and Christof M. Aegerter. Mechanical control of organ size in the development of the *Drosophila* wing disc. *PloS one*, 8(10):e76171, January 2013. DOI: 10.1371/journal.pone.0076171.

[168] B.I. Shraiman. Mechanical feedback as a possible regulator of tissue growth. *PNAS*, 102(9):3318–3323, March 2005. DOI: 10.1073/pnas.0404782102.

[169] Lars Hufnagel, Aurelio A. Teleman, Hervé Rouault, Stephen M. Cohen, and Boris I. Shraiman. On the mechanism of wing size determination in fly development. *PNAS*, 104(10):3835–3840, March 2007. DOI: 10.1073/pnas.0607134104.

[170] Nikolaos Doumpas, Marina Ruiz-Romero, Enrique Blanco, Bruce Edgar, Montserrat Corominas, and Aurelio A. Teleman. Brk regulates wing disc growth in part via repression of Myc expression. *EMBO reports*, 14(3):261–8, March 2013. DOI: 10.1038/embor.2013.1.

[171] Thomas Lecuit and Stephen M. Cohen. Dpp receptor levels contribute to shaping the Dpp morphogen gradient in the *Drosophila* wing imaginal disc. *Development*, 125(24):4901–4907, December 1998.

[172] H. Tanimoto, S. Itoh, P. ten Dijke, and T. Tabata. Hedgehog creates a gradient of DPP activity in *Drosophila* wing imaginal discs. *Molecular Cell*, 5(1):59–71, January 2000. DOI: 10.1016/S1097-2765(00)80403-7.

[173] Myriam Zecca and Gary Struhl. Recruitment of cells into the *Drosophila* wing primordium by a feed-forward circuit of *vestigial* autoregulation. *Development*, 134(16):3001–3010, August 2007. DOI: http://dx.doi.org/10.1242/dev.006411.

[174] Myriam Zecca and Gary Struhl. A Feed-Forward Circuit Linking Wingless, Fat-Dachsous Signaling, and the Warts-Hippo Pathway to *Drosophila* Wing Growth. *PLOS Biology*, 8(6):e1000386, June 2010. DOI: 10.1371/journal.pbio.1000386.

[175] Fillip Port, Hui-Min Chen, Tzumin Lee, and Simon L. Bullock. Optimized CRISPR/Cas tools for efficient germline and somatic genome engineering in *Drosophila*. *Proceedings of the National Academy of Sciences of the United States of America*, 111(29):E2967–E2976, July 2014. DOI: 10.1073/pnas.1405500111.

[176] Oguz Kanca, Emmanuel Caussinus, Alexandru S. Denes, Anthony Percival-Smith, and Markus Affolter. Raeppli: a whole-tissue labeling tool for live

imaging of *Drosophila* development. *Development (Cambridge, England)*, 141(2):472–80, January 2014. DOI: 10.1242/dev.102913.

[177] Tzumin Lee and Liqun Luo. Mosaic Analysis with a Repressible Neurotechnique Cell Marker for Studies of Gene Function in Neuronal Morphogenesis. *Neuron*, 22(3):451–461, March 1999. DOI: 10.1016/S0896-6273(00)80701-1.

[178] M. Stornaiuolo, L.V. Lotti, N. Borgese, M. Torrisi, G. Mottola, G. Martire, and Bonatti S. KDEL and KKXX Retrieval Signals Appended to the Same Reporter Protein Determine Different Trafficking between Endoplasmic Reticulum, Intermediate Compartment, and Golgi Complex. *Molecular Biology of the Cell*, 14(3):889–902, November 2002. DOI: 10.1091/mbc.E02-08-0468.

[179] Johannes Bischof, Robert K. Maeda, Monika Hediger, and Konrad Basler. An optimized transgenesis system for *Drosophila* using germ-line-specific phiC31 integrases. *PNAS*, 104(9):3312–3317, February 2007. DOI: 10.1073/pnas.0611511104.

[180] Thomas Schaffter. *From genes to organisms: Bioinformatics System Models and Software*. PhD thesis, École polytechnique fédérale de Lausanne, 2014.

[181] David Foronda, Ainhoa Pérez-Garijo, and Francisco A. Martín. Dpp of posterior origin patterns the proximal region of the wing. *Mechanisms of development*, 126(3-4):99–106, March 2009. DOI: 10.1016/j.mod.2008.12.002.

[182] Robin Vuilleumier, Alexander Springhorn, Lucy Patterson, Stefanie Koidl, Matthias Hammerschmidt, Markus Affolter, and George Pyrowolakis. Control of Dpp morphogen signalling by a secreted feedback regulator. *Nature cell biology*, 12(6):611–617, June 2010. DOI: 10.1038/ncb2064.

[183] Jorge V. Beira, Alexander Springhorn, Stefan Gunther, Lars Hufnagel, Giorgos Pyrowolakis, and Jean-Paul Vincent. The Dpp/TGFbeta-Dependent Corepressor Schnurri Protects Epithelial Cells from JNK-Induced Apoptosis in *Drosophila* Embryos. *Developmental Cell*, 31(2):240–247, October 2014. DOI: 10.1016/j.devcel.2014.08.015.

[184] Dong Yan and Xinhua Lin. Shaping Morphogen Gradients by Proteoglycans. *CSH Perspectives*, 1(3):a002493, September 2009. DOI: 10.1101/cshperspect.a002493.

[185] Xavier Franch-Marro, Oriane Marchand, Eugenia Piddini, Sara Ricardo, Cyrille Alexandre, and Jean-Paul Vincent. Glypicans shunt the Wingless signal between local signalling and further transport. *Development (Cambridge, England)*, 132(4):659–666, February 2005. DOI: 10.1242/dev.01639.

[186] Armel Gallet, Laurence Staccini-Lavenant, and Pascal P. Thérond. Cellular trafficking of the glypican Dally-like is required for full-strength Hedgehog signaling and Wingless transcytosis. *Developmental Cell*, 14(5):712–25, May 2008. DOI: 10.1016/j.devcel.2008.03.001.

[187] Katie L. Ayers, Rana Mteirek, Alexandra Cervantes, Laurence Lavenant-Staccini, Pascal P. Thérond, and Armel Gallet. Dally and Notum regulate the switch between low and high level Hedgehog pathway signalling. *Development (Cambridge, England)*, 139(17):3168–79, September 2012. DOI: 10.1242/dev.078402.

[188] M. Zecca and G. Struhl. Control of *Drosophila* wing growth by the *vestigial* quadrant enhancer. *Development*, 134(16):3011–3020, August 2007. DOI: 10.1242/dev.006445.

[189] Ana-Citlali Gradilla and Isabel Guerrero. Hedgehog on the move: a precise spatial control of Hedgehog dispersion shapes the gradient. *Current Opinion in Genetics & Development*, 23(4):363–373, August 2013. DOI: 10.1016/j.gde.2013.04.011.

[190] S. Swarup and E.M. Verheyen. Wnt/Wingless signaling in *Drosophila*. *Cold Spring Harbor Perspectives in Biology*, 4(6):a007930, June 2012. DOI: 10.1101/cshperspect.a007930.

[191] P. Müller, K.W. Rogers, S.R. Yu, M. Brand, and A.F. Schier. Morphogen transport. *Development*, 140(8):1621–1638, April 2013. DOI: 10.1242/dev.083519.

[192] Kimberly D. McClure and Gerold Schubiger. Developmental analysis and squamous morphogenesis of the peripodial epithelium in *Drosophila* imaginal discs. *Development*, 132:5033–5042, November 2005. DOI: 10.1242/dev.02092.

[193] M.C. Gibson and G. Schubiger. *Drosophila* peripodial cells, more than meets the eye? *BioEssays*, 23(8):691–697, August 2001.

[194] S.K. Pallavi and L.S. Shashidhara. Signaling interactions between squamous and columnar epithelia of the *Drosophila* wing disc. *Journal of Cell Science*, 118:3363–3370, August 2005. DOI: 10.1242/jcs.02464.

[195] David M. Umulis and Hans G. Othmer. Mechanisms of scaling in pattern formation. *Development (Cambridge, England)*, 140(24):4830–43, December 2013. DOI: 10.1242/dev.100511.

[196] Y.H. Chang and Y.H. Sun. Carrier of Wingless (Cow), a secreted heparan sulfate proteoglycan, promotes extracellular transport of Wingless. *PLOS One*, 9(10):e111573, October 2014. DOI: 10.1371/journal.pone.0111573.

[197] Eric Marois, Ali Mahmoud, and Suzanne Eaton. The endocytic pathway and formation of the Wingless morphogen gradient. *Development (Cambridge, England)*, 133(2):307–17, January 2006. DOI: 10.1242/dev.02197.

[198] A. Gallet, L. Ruel, L. Staccini-Lavenant, and P.P. Therond. Cholesterol modification is necessary for controlled planar long-range activity of Hedgehog in *Drosophila* epithelia. *Development*, 133:407–418, January 2006. DOI: 10.1242/dev.02212.

[199] A. Callejo, C. Torroja, L. Quijada, and I. Guerrero. Hedgehog lipid modifications are required for Hedgehog stabilization in the extracellular matrix. *Development*, 133:471–483, January 2006. DOI: 10.1242/dev.02217.

[200] Ainhoa Callejo, Aphrodite Bilioni, Emanuela Mollica, Nicole Gorfinkiel, Germán Andrés, Carmen Ibáñez, Carlos Torroja, Laura Doglio, Javier Sierra, and Isabel Guerrero. Dispatched mediates Hedgehog basolateral release to form the long-range morphogenetic gradient in the *Drosophila* wing disk epithelium. *Proceedings of the National Academy of Sciences of the United States of America*, 108(31):12591–8, August 2011. DOI: 10.1073/pnas.1106881108.

[201] Gisela D Angelo, Tamas Matusek, Sandrine Pizette, and Pascal P. Therond. Endocytosis of Hedgehog through Dispatched Regulates Long-Range Signaling. *Developmental Cell*, 32(3):290–303, February 2015. DOI: 10.1016/j.devcel.2014.12.004.

[202] A.C. Gradilla, E. González, I. Seijo, G. Andrés, M. Bischoff, L. González-Mendez, V. Sánchez, A. Callejo, C. Ibáñez, M. Guerra, J.R. Ortigão-Farias, J.D. Sutherland, M. González, R. Barrio, J.M. Falcón-Pérez, and I. Guerrero. Exosomes as Hedgehog carriers in cytoneme-mediated transport and secretion. *Nature Communications*, 4(5):5649, December 2014. DOI: 10.1038/ncomms6649.

[203] Matthew C. Gibson, Dara A. Lehman, and Gerold Schubiger. Lumenal Transmission of Decapentaplegic in *Drosophila* Imaginal Discs. *Developmental Cell*, 3(3):451–460, September 2002. DOI:10.1016/S1534-5807(02)00264-2.

[204] M. Fujise, S. Takeo, K. Kamimura, T. Matsuo, T. Aigaki, S. Izumi, and H. Nakato. Dally regulates Dpp morphogen gradient formation in the *Drosophila* wing. *Development*, 130(8):1515–1522, April 2003. DOI: 10.1242/dev.00379.

[205] D.J. Bornemann, J.E. Duncan, W. Staatz, S. Selleck, and R. Warrior. Abrogation of heparan sulfate synthesis in *Drosophila* disrupts the Wingless, Hedgehog and Decapentaplegic signaling pathways. *Development*, 131(9):1927–1938, May 2004. DOI: 10.1242/dev.01061.

[206] C. Han, T.Y. Belenkaya, M. Khodoun, M. Tauchi, X. Lin, and X. Lin. Distinct and collaborative roles of *Drosophila* EXT family proteins in morphogen signalling and gradient formation. *Development*, 131(7):1563–1575, April 2004. DOI: 10.1242/dev.01051.

[207] M. Gonzáles-Gaitán and H. Jäckle. The range of spalt-activating Dpp signalling is reduced in endocytosis-defective *Drosophila* wing discs. *Mechanisms of Development*, 87(1-2):143–151, September 1999. DOI: 10.1016/S0925-4773(99)00156-2.

[208] M. Bischoff, A. Gradilla, I. Seijo, G. Andrés, C. Rodríguez-Navas, L. González-Méndez, and I. Guerrero. Cytonemes are required for the establishment of

a normal Hedgehog morphogen gradient in *Drosophila* epithelia. *Nature Cell Biology*, 15:1269–1281, October 2013. DOI: 10.1038/ncb2856.

[209] Katie L. Ayers, Armel Gallet, Laurence Staccini-Lavenant, and Pascal P. Thérond. The long-range activity of Hedgehog is regulated in the apical extracellular space by the glypican Dally and the hydrolase Notum. *Developmental Cell*, 18(4):605–20, April 2010. DOI: 10.1016/j.devcel.2010.02.015.

[210] N. Lowe, J.S. Rees, J. Roote, E. Ryder, I.M. Armean, G. Johnson, E. Drummond, H. Spriggs, J. Drummond, J.P. Magbanua, H. Naylor, B. Sanson, R. Bastock, S. Huelsmann, V. Trovisco, M. Landgraf, S. Knowles-Barley, J.D. Armstrong, H. White-Cooper, C. Hansen, R.G. Phillips, K.S. The UK Drosophila Protein Trap Screening Consortium, Lilley, S. Russell, and D. St Johnston. Analysis of the expression patterns, subcellular localisations and interaction partners of *Drosophila* proteins using a *pigP* protein trap library. *Development*, 141(20):3994–4005, October 2014. DOI: 10.1242/dev.111054.

[211] V. Kölsch, T. Seher, G.J. Fernandez-Ballester, L. Serrano, and M. Leptin. Control of *Drosophila* Gastrulation by Apical Localization of Adherens Junctions and RhoGEF2. *Science*, 315(5810):384–386, January 2007. DOI: 10.1126/science.1134833.

[212] M.P. Krahn, D.R. Klopfenstein, N. Fischer, and A. Wodarz. Membrane Targeting of Bazooka/PAR-3 Is Mediated by Direct Binding to Phosphoinositide Lipids. *Current Biology*, 20(7):636–642, April 2010. DOI: 10.1016/j.cub.2010.01.065.

[213] Xiaomeng Wang, Robin E. Harris, Laura J. Bayston, and Hilary L. Ashe. Type IV collagens regulate BMP signalling in *Drosophila*. *Nature*, 455(7209):72–7, September 2008. DOI: 10.1038/nature07214.

[214] . Morin, R. Daneman, M. Zavortink, and W. Chia. A protein trap strategy to detect GFP-tagged proteins expressed from their endogenous loci in *Drosophila*. *PNAS*, 98(26):15050–15055, December 2001. DOI: 10.1073/pnas.261408198.

[215] Stefan Harmansa, Fisun Hamaratoglu, Markus Affolter, and Emmanuel Caussinus. Dpp spreading is required for medial but not for lateral wing disc growth. *Nature*, 527(7578):317–322, November 2015. DOI: 10.1038/nature15712.

[216] B. Sun and P.M. Salvaterra. Two *Drosophila* nervous system antigens, Nervana 1 and 2, are homologous to the beta subunit of Na+,K(+)-ATPase. *PNAS*, 92(12):5396–5400, June 1995.

[217] P. Xu, B. Sun, and P.M. Salvaterra. Organization and transcriptional regulation of *Drosophila* Na(+), K(+)-ATPase beta subunit genes: *Nrv1* and *Nrv2*. *Gene*, 236(2):303–13, August 1999. DOI: 10.1016/S0378-1119(99)00269-3.

[218] Jennifer L. Genova and Richard G. Fehon. Neuroglian, Gliotactin, and the Na+/K+ ATPase are essential for septate junction function in *Drosophila*. *The Journal of Cell Biology*, 161(5):979–89, June 2003. DOI: 10.1083/jcb.200212054.

[219] Sarah M. Paul, Michael J. Palladino, and Greg J. Beitel. A pump-independent function of the Na,K-ATPase is required for epithelial junction function and tracheal tubesize control. *Development*, 134(1):147–155, January 2007. DOI: 10.1242/dev.02710.

[220] S. Yasothornsrikul, W.J. Davis, G. Cramer, D.A. Kimbrell, and C.A. Dearolf. *viking*: identification and characterization of a second type IV collagen in *Drosophila*. *Gene*, 198(1-2):17–25, October 1997. DOI: 10.1016/S0378-1119(97)00274-6.

[221] M. Saitoh, T. Shirakihara, A. Fukasawa, K. Horiguchi, K. Sakamoto, H. Sugiya, H. Beppu, Y. Fujita, I. Morita, K. Miyazono, and K. Miyazawa. Basolateral BMP Signaling in Polarized Epithelial Cells. *PLOS One*, May 2013. DOI: 10.1371/journal.pone.0062659.

[222] I. Fernandes, H. Chanut-Delalande, P. Ferrer, Y. Latapie, L. Waltzer, M. Affolter, F. Payre, and S. Plaza. Zona Pellucida Domain Proteins Remodel the Apical Compartment for Localized Cell Shape Changes. *Developmental Cell*, 18(1):64–76, January 2010. DOI: 10.1016/j.devcel.2009.11.009.